Massey University

DNA Replication Asynchrony in *Pseudomonas fluorescens* SBW25

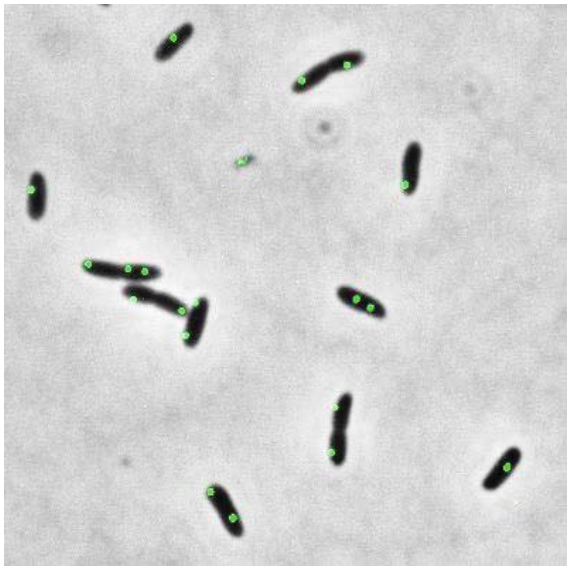

A thesis presented in partial fulfillment of the requirements

for the degree of

Master of Science (Genetics)

at Massey University, Albany,

New Zealand

Akarsh Mathrani

2015

Abstract

Bacterial growth rate is largely dependent on the availability of nutrients in the environment. Past studies have shown that bacterial species such as *E. coli* can significantly increase their growth rate in nutrient-rich environments by initiating multiple cycles of DNA replication simultaneously. As a result, offspring cells not only inherit the full chromosome, but also an additional, partially replicated chromosome. However, studies have found that this multi-fork replication does not occur in all organisms such as *Caulobacter crescentus*. Detailed investigations of replication fork dynamics have thus far been limited to only a small number of bacterial species.

In this study, the cell cycle and DNA replication dynamics of *Pseudomonas fluorescens* SBW25, a gram-negative, plant-associated bacterium, is investigated. The study involves incorporating arrays of repeated operator regions bound by their fluorescently-labelled cognate repressors. A single array appears as a fluorescent focus upon live-cell imaging. An origin proximal array can therefore be visualized to follow the chromosome replication and segregation process in single living cells. Nutrient concentrations were varied in order to learn if multi-fork replication occurs in the model organism.

Results from this study show evidence for concurrent DNA replication cycles in *P. fluorescens* SBW25. This process appears to be exacerbated in nutrient-rich media (LB) as opposed to cells grown in nutrient-poor media (M9-glycerol). Moreover, asynchronous DNA replication initiations were also observed. This more stochastic initiation appears to be a common phenomenon when cells are grown in nutrient-rich media but not in nutrient-poor media. This study sheds light on a key cellular process in the *Pseudomonads*, a genus where DNA replication has not been studied extensively.

Acknowledgements

There are many individuals who have contributed and made this research possible during the course of my study. I am delighted to acknowledge their contributions.

First and foremost, I would like to thank my supervisor Dr. Heather Hendrickson for her invaluable contribution at every stage of this research. I am grateful for her continuous support, guidance and encouragement throughout this study.

I am grateful to Massey University for providing the laboratory facility for the conduct of my experiments. I am also grateful to Massey University for the financial support, which has allowed me to attend a conference during my study.

I would like to thank Dr. Brenda Youngren for providing me with various genetic tools which have made this research possible, my laboratory colleagues for their generous giving of time and support during my experimentation phase.

Finally, and most importantly, I wish to thank my parents for their continuous encouragement and support.

Table of Contents

List of Tables

List of Figures

Chapter 1

Introduction

1.1 Introduction

Bacteria are the most abundant living organisms on the planet with an estimated 5x 10^{30} cells [1]. These small anucleated unicellular organisms inhabit a vast and diverse range of habitats and not only play vital roles in sustaining countless ecosystems, but can also cause serious illnesses. As a result, they form an essential component of earth's biota and are therefore important subjects for evolutionary, medical and other biological research.

Over the past few decades of bacterial research, it has become evident that there is an enormous amount of variability between bacterial species. Even now, researchers are only able to grow and cultivate a mere handful of bacterial species in the laboratory [2]. In addition to this, phylogenetic classifications have also been quite challenging to establish, since researchers have had to cope with analysis of over 3.5 billion years of horizontal gene transfer that is bacterial evolution [3].

For my research, I decided to investigate the cell cycle of *Pseudomonas fluorescens* SBW25, one of the few bacterial species that can be grown *in vitro*. No such investigations have been carried out on this organism before, and it is closely related to *Pseudomonas aeruginosa*, an opportunistic pathogen of cystic fibrosis patients [4]. *P. fluorescens* SBW25 was chosen as the model organism for this study because it is closely related to other wild organisms; unlike *Escherichia coli* and *Bacillus subtilis*, which are commonly studied but have been grown in the laboratory for many decades.

Before explaining my approach in carrying out this study, I will first provide an overview of the prokaryotic cell cycle, prokaryotic DNA replication and multi-fork DNA replication in the following sections of the chapter.

1.2 The Bacterial Cell Cycle

1.2.1 Overview

Key events that occur once per generation in the life cycle of a cell, such as cellular growth, replication of genetic material and cell division, define the cell cycle [5]. Although these key events occur in both prokaryotic and eukaryotic organisms, the cell cycle is quite different between the two biological systems. While eukaryotic cells go through several cell cycle checkpoints and controlled stages during continuous growth (i.e. exponential growth), most prokaryotic cells do not have such a well-defined cell cycle; rather they continuously replicate their DNA throughout the cell cycle as shown in Figure 1.

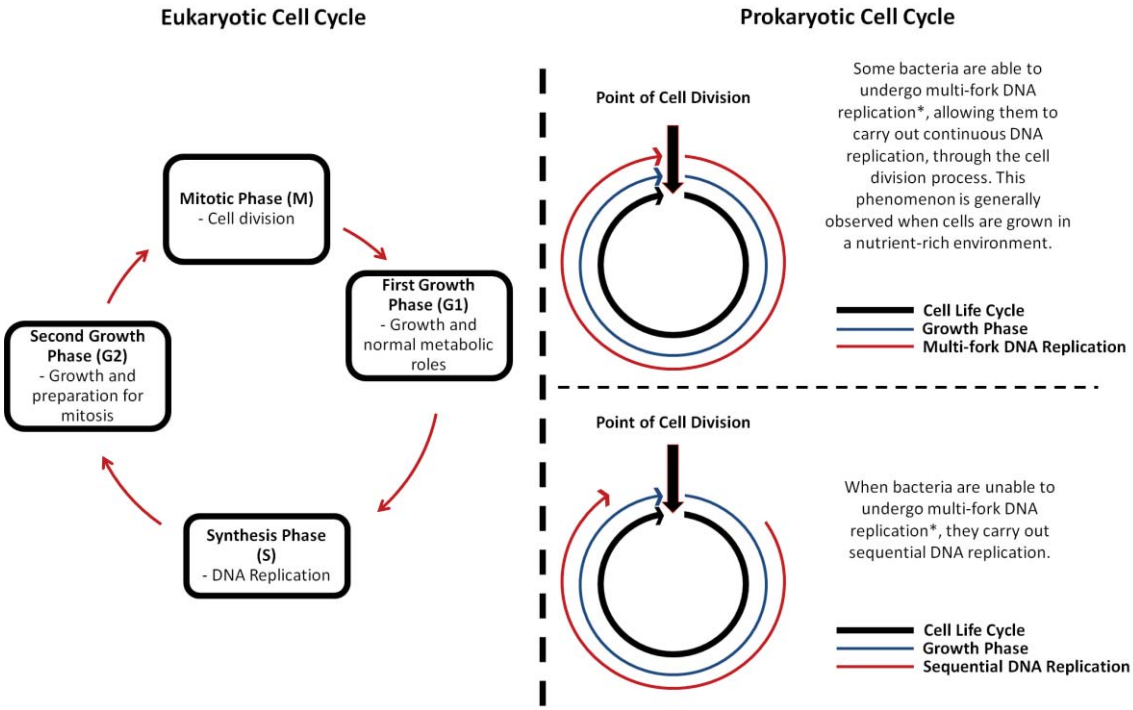

Figure 1: Diagrams showing standard eukaryotic and prokaryotic cell cycles during continuous growth. The length of arrows represent the duration of the phase being carried out. * Multi-fork DNA replication is explained in section 1.3.

While eukaryotic cell cycle has been comprehensively studied in a wide variety of organisms such as budding yeast, fission yeast and various plant and animal cell model systems, prokaryotic cell cycle studies have been mainly focused on *E. coli* and a small number of other organisms [6]. However, ever since the rise in genome sequencing technologies, there has been a rapid increase in full genome sequencing of prokaryotic organisms. This has greatly assisted in tracing and defining horizontal gene transfer events in bacterial genomes and has had tremendous implications on the phylogenetic classifications of bacterial strains [2]. The collection of this new data along with further advances in prokaryotic cell biology has led to the detection of the fundamental differences between eukaryotic and prokaryotic cell cycles [7].

1.2.2 Growth Phase

Unlike eukaryotic cells which increase their protein biomass at specific time points of their cycle (G1 and G2 phases respectively), bacterial cells maintain a steady ribosome production throughout the cell cycle. There is also a continuous increase of protein biomass production during continuous growth and therefore the synthesis of metabolites and other cellular machineries is also increased over time [8]. Since the main goal of a microorganism is to replicate its genetic material and divide, the end result is that DNA replication as a process occurs throughout the cell cycle, and the checkpoint system that is present in eukaryotes, does not seem to occur in most studied prokaryotes [8, 9].

1.2.3 DNA Replication

1.2.3.1 Background

As a process, DNA replication forms the foundation of heredity. By ensuring duplication of the cell's genome prior to cell division, it generates a new set of genetic material for the

offspring cell to inherit. In evolutionary terms, this allows preservation and enhancement of the genetic information over long periods of time.

When the double helix structure of the DNA molecule was discovered in 1953, scientists immediately noticed that the structure could act as a template which could be used in some mechanism for replicating the DNA. It took several years of rigorous investigations in *E. coli* and other bacteria, before semi-conservative replication was confirmed over conservative or dispersive DNA replication [10]. In 1961, the theta replication model was finally developed for *E. coli* and other bacteria with circular genomes, which is the fundamental blueprint for DNA replication in prokaryotes [11].

As shown in Figure 2, the theta replication model states that the DNA replication process is always initiated at a particular region of the circular bacterial chromosome termed the 'origin of replication', *oriC* locus. From this locus, replication proceeds bi-directionally until completion at the 'deletion induced filamentation', *dif* locus, which lies within the terminus region on the opposite end of the chromosome. Once a new copy of the chromosome is produced, it can be segregated into the daughter cell during cell division [5, 11-13].

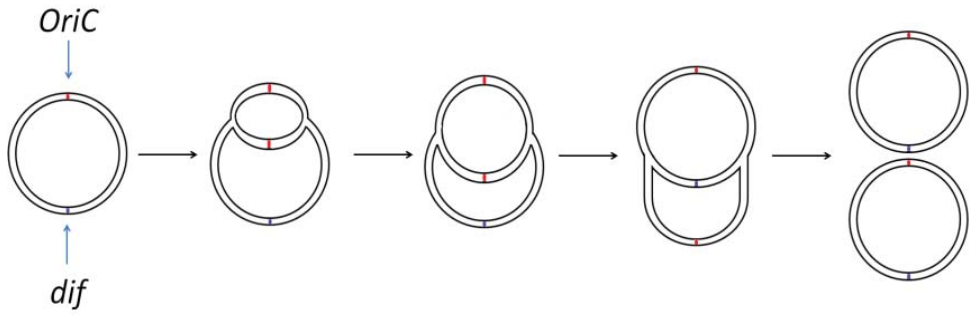

Figure 2: Diagram showing the theta replication model for DNA replication in bacteria (adapted from John Cairns, 1961 [11]).

1.2.3.2 DNA Replication: The Process

DNA replication is a very important process and must be exact, although mutations do occur. Even small errors in copying the genetic information can have disastrous results for the offspring cell. Because of this fragility, the process must be carried out carefully through three main stages; initiation, elongation and termination:

i. Initiation

In order to begin the replication process, the initiator protein DnaA locates the *oriC* site in the circular genome, and recruits the replication machinery or 'replisome' to it (Figure 3). The replisome is a protein complex containing various enzymes required for the replication process. The replisome then opens up the double stranded DNA helix, stabilizes the resulting ssDNA that will be used as a template, and allows the DNA polymerase III holoenzyme to begin copying the DNA [14, 15].

Bacterial *oriC* sites are often characterized by the DnaA proteins' binding locations and the presence of the typical AT-rich regions which are used to form an open complex for recruitment of DNA polymerase III holoenzyme [16-18]. In fact, many of the bacterial *oriC* sites that have so far been identified have been found to be located in close proximity of the *dnaA* gene [16, 19, 20]. Even the *oriC* site in *E. coli*, which is flanked by *gidA* and *gidB* genes is thought to have originally been near the *dnaA* gene and was translocated away at some point in its evolutionary history [21]. This is not always the case however; the *oriC* sites of bacterial species such as *Coxiella burnetii*, *Caulobacter crescentus* and *Rickettsia prowazekii* have been mapped at locations non-proximal to their respective *dnaA* genes [22-25].

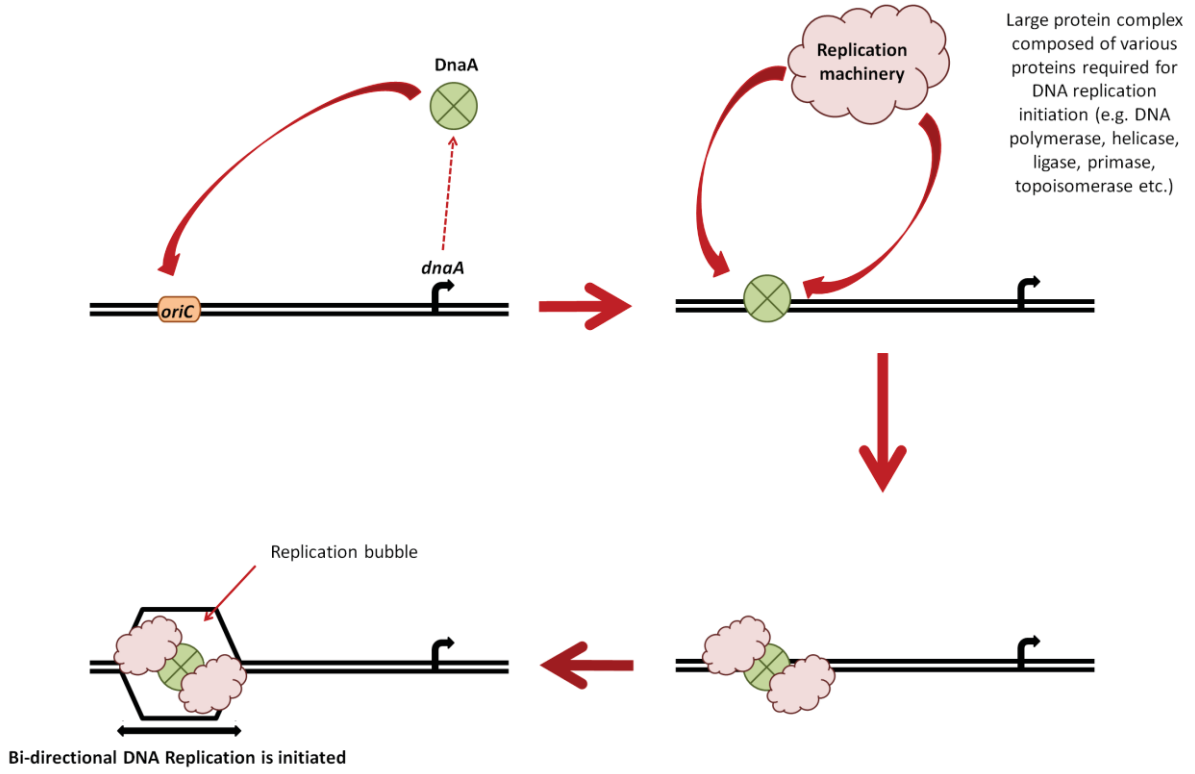

Figure 3: A schematic diagram illustrating the recruitment of replisomes onto *oriC* locus by DnaA.

ii. Elongation

Once the replisomes have been recruited to the *oriC* sequence, bi-directional replication is initiated as enzyme primase adds short RNA primers with a free 3' OH groups on the template strand for the DNA polymerase III holoenzyme to attach to and begin the elongation process in the 5' to 3' direction. The leading strand receives a single primer due to the DNA polymerase III holoenzyme being able to extend it with high processivity, and the lagging strand receives numerous primers as it is extended discontinuously, producing okazaki fragments (see Figure 4). Enzyme RNase then removes the RNA fragments and a lower processivity DNA polymerase I and enzyme Ligase fill in the remaining gaps. While DNA polymerase III holoenzyme has 3' to 5' exonuclease activity, which it uses for proof-reading purposes by replacing any replication mistakes, DNA polymerase I has 5' to 3' exonuclease activity which it uses

to remove the primers in front of it. This process continues until both the replication forks meet in the terminus region for replication termination [13, 26].

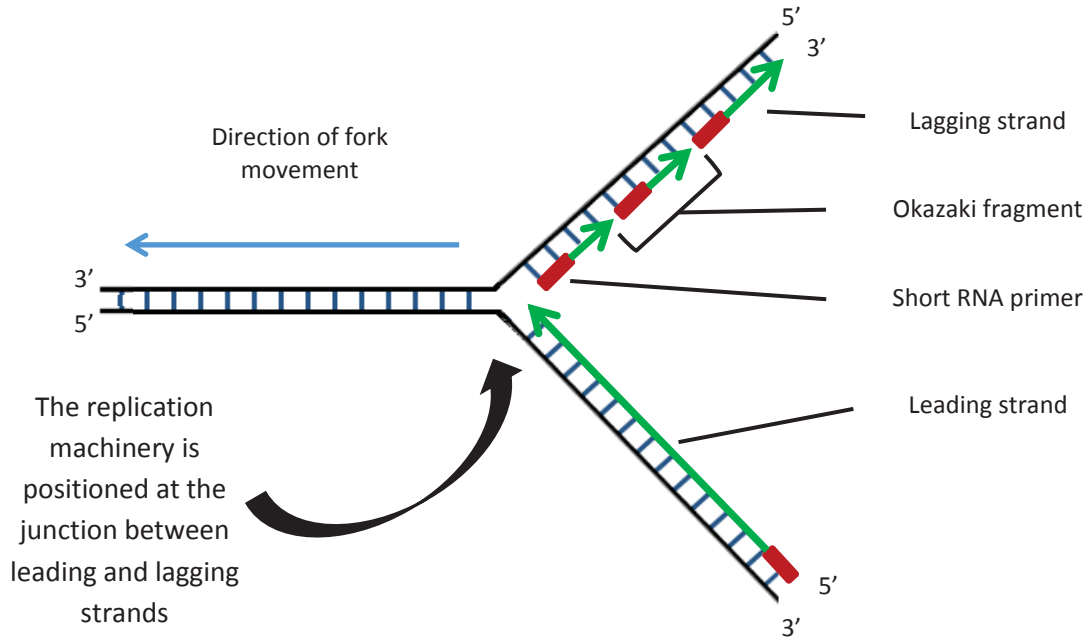

Figure 4: Diagram showing a replication fork and its components.

iii. Termination

When DNA replication is approaching completion, the replication forks finally encounter each other at specific sequences called replication termini, on the opposite side of the circular chromosome from the *oriC* locus [27].

In this region of the chromosome, there are DNA-binding proteins called replication terminator proteins (Terminus Utilization Substance or Tus proteins in *Escherichia coli* and Replication Terminus Protein or RTP in *Bacillus subtilis*), which associate and bind with the replication termini sequence and only allow the replication forks to pass through them from single direction [28, 29]. Once the replication forks pass through each other, they are arrested by the terminator protein – replication termini association as the terminator protein interacts with DnaB, the helicase protein used for opening up the replication forks [26]. After the replication forks have been halted, enzyme

topoisomerase IV is utilized for separating the two replicated chromosomes, and termination is finally completed [30].

1.2.3.3 DNA Replication: Regulation

In eukaryotic cells the initiation of DNA replication is tightly regulated to occur only once per cell cycle and is typically characterized by the utilization of several origins of replication sites. The origin recognition complex (ORC) proteins locate the various origin of replication sites across the chromosome(s) and direct the replication machinery to these locations [14]. This presence of multiple replication origin sites has not yet been observed in any of the bacterial species studied; however some archaeal species have been shown to initiate DNA replication from multiple origins [14].

Eukaryotes can prevent reinitiation of replication from occurring by increasing intracellular cyclin levels during the S, G2 and M phases of the cell cycle. When this happens, cyclin-dependent kinases (CDKs) become activated and prevent formation of the replication complex. Bacteria such as *Escherichia coli* have also been observed to inhibit reinitiation of DNA replication under nutrient-poor conditions; however the strategies they employ are quite different to that of eukaryotic cells. By converting the active DnaA-ATP form to the inactive DnaA-ADP form, the initiator proteins are inhibited from any further recruitment of the replisome complex to the origin of replication site [7]. Another strategy involves stochastically decreasing intracellular DnaA levels by allowing the proteins to bind to the large number of binding sites at the origin region during initiation which leaves very few initiator proteins for reinitiation [14]. Alternatively temporary inactivation of the origin of replication locus itself can also be utilized to inhibit reinitiation. This can be done by utilizing SeqA, a protein that specifically binds to the GATC sequences adjacent to the DnaA-binding sites and methylating the adenines in the GATC sequences using Dam methylases. The result

is that the newly replicated strand of DNA is unmethylated and is unable to initiate another round of replication until methylation at the same sites occur. The exact mechanism of how this inhibition process works is however, still poorly understood [31-33].

Therefore prevention of replication reinitiation seems to be quite different in eukaryotic cells and prokaryotic cells. It is also noteworthy that these *E. coli* strategies discussed are unlikely to be representative for all prokaryotes, however it does give us some insight into how a typical prokaryotic cell such as *E. coli* carries out such regulatory functions.

1.2.4 Chromosome Segregation

In order for the cell to pass on a duplicated chromosome to the offspring cell, chromosome segregation must occur. Since the septum will form at the mid-cell location during cell division, the two copies of the genetic material must be separated and moved to each of the cell halves.

In eukaryotic cells, everything happens in a defined series of stages. The DNA replication process and the cell division process are separated by a G2 phase. Here the cell prepares for mitosis by aligning the multiple chromosomes to the appropriate locations at mid-cell and utilizing the microtubules to assemble a mitotic spindle to ensure successful segregation [34]. In stark contrast, bacterial chromosome segregation occurs in parallel with DNA replication [35]. Prokaryotic investigations of chromosome segregation using fluorescently labelled *oriC* sites have shown that as the DNA is replicated, the *oriC* sites move towards the opposite cell poles. One theory explaining this phenomenon suggests that the force driving the replicating DNA out of the fixed mid-cell replication factory is enough to provide the momentum and directionality required for separating the two chromosomes into either halves of the cell [7, 35]. Another suggests that since the length of the chromosome is so large in comparison to

the small proteins supposedly carrying out the segregation process, that the dominant driving force for the segregation mechanism may be entropic forces [36].

Many bacterial species also utilize the ParABS partitioning system to assist in plasmid and chromosomal segregation. Employing two *trans*-acting proteins that form a nucleoprotein partition complex (ParAB) and a *cis*-acting centromere-like locus (ParS), this system is able to actively separate chromosomes apart into their respective cell halves [37]. This system is discussed in more detail in Chapter 3.

Studies in *E. coli* have also found evidence suggesting that prokaryotic chromosome segregation may be a more dynamic process, coordinated by an actin-like MreB cytoskeletal protein [7, 38]. MreB is an actin-homolog found in some bacterial species that forms a helical structure from one cell pole to the other. While complete deletion of MreB results in severe defects in cell shape, partial inhibition of the gene results in chromosome missegregation [7, 38]. However, since numerous species of prokaryotes do not have these actin-like cytoskeletons, other underlying mechanisms must also play a role in carrying out chromosome segregation.

1.2.5 Cell Division

As DNA replication is nearing termination and the resulting two chromosomes are separated and segregated into their respective cell halves, the bacterial cell undergoes binary fission and begins splitting in two. Unlike eukaryotic cells which utilize actin-myosin ring contractions to carry out the mechanical process, and only begin doing so once DNA replication is completely over; prokaryotes coordinate cytokinesis with a tubulin-like ring of FtsZ [7, 39]. The FtsZ ring is analogous to septin ring found in most eukaryotes (not in plants) as they both assemble along the mid-cell site of cytokinesis.

Once the FtsZ ring is in place, it recruits a diverse array of regulatory proteins involved in maintaining the ring's stability and begins contraction, forming a septum. The closing of the septum and DNA replication termination is tightly regulated so that both the processes finish at about the same time. This regulation is not yet well understood [7, 40].

Formation of the FtsZ ring at the correct mid-cell location is assisted by the MinC and MinD proteins. The MinCD proteins are FtsZ inhibitors and are found near the cell poles, therefore reducing chances of FtsZ ring formation at locations outside of the mid-cell region [41, 42].

Recruitment of the MinCD proteins to cell poles is carried out by a curvature sensitive membrane binding protein, such as MinE or DivIVA, depending on the bacterial species. These proteins are especially useful in guiding the MinCD proteins away from mid-cell region in spherical cells, where locating the polar regions can be especially unclear [43-45].

1.3 Multi-fork DNA Replication in Prokaryotes

Development of our current understanding of the bacterial DNA replication has been a long process with contributions from many important studies and experiments done over the past six decades. Initially observed in *E. coli*, one of the most significant discoveries in the field has proven to be the multi-fork replication model [35, 46, 47].

Unlike Figure 2, which depicts sequential replication (*i.e.* only one DNA replication process is carried out in the cell at any one point in time), multi-fork replication occurs in rapidly growing cells when the newly replicated *OriC* site produced during the early stages of DNA replication, initiates a new replication bubble before the initial one has resolved itself. This therefore results in replication bubbles occurring within older replication bubbles, as shown in Figure 5.

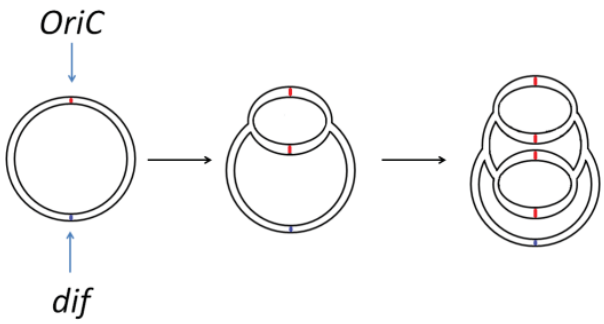

Figure 5: Diagram showing the multi-fork replication model for DNA replication in prokaryotic organisms (adapted from Skarstad, *et al.*, 1986 [48]).

1.4 DNA Replication and Bacterial Growth Rate

Under optimal nutrient conditions, DNA replication is also an important factor in determining the growth rate of different bacterial strains. Since DNA replication is one of the slowest phases of the bacterial cell cycle (Figure 1), it has a major influence on the rate of cell division. A review done in 2011 simulated the typical prokaryotic cell cycle using the Cell Cycle Simulation program (CCSim) [49] , and observed that if replication time is increased by limiting thymine availability in the cell environment, then cell division rate is also significantly reduced [50].

A fast growth rate allows the bacterial cells to reproduce faster and thus produce more offspring per generation when compared to a slow growth rate. While producing more offspring every generation does not increase the inherent mutation rate of the bacterial genome, it does lead to production of more mutants every generation through sheer numbers [51, 52]. This results in an increased likelihood for the bacterial population as a whole to develop immunity to any antibiotics or antimicrobial agents in the environment. Pathogenic bacterial populations with a fast growth rate can therefore be more infectious than pathogenic bacterial populations with a slower growth rate.

1.5 Previous Studies on *E. coli*

Escherichia coli is a gram-negative bacteria and is commonly used as a model organism to work with in molecular and cell biology studies. It is inexpensive and easy to grow in a laboratory environment and has been extensively studied since 1946 [6]. Over the past few decades, there has been a great deal of research done on *E. coli* regarding its cell cycle and DNA replication initiation regulation. In this section I will present an overview of some of the key investigations carried out in *E. coli* regarding its multi-fork replication.

It was a study in 1958 that found DNA content in *Salmonella typhimurium* cells to be increasing with faster cell-culture growth rates [53] which inspired Cooper and Helmstetter's well-known investigations in *E. coli* in 1968; setting up the initial framework for future multi-fork replication studies. Their study showed that while the time period required for complete chromosomal replication (C phase of cell cycle) in *E. coli* is usually approximately 40 minutes, the overall generation time (*i.e.* all the phases in the cell cycle combined) can range from as little as 20 minutes to longer than 180 minutes at 37ºC, depending on the nutrients present in the growth medium [46, 54]. Their results supported the observations of Yoshikawa and Sullivan (1964), who reported the presence of multiple replication origin points in rapidly growing bacteria only four years prior, and the hypotheses of Maaloe and Kjeldgaard (1966), who were the first to suggest that multiple replication forks are introduced by the cells when the rate of carrying out a single DNA replication process becomes limiting [55, 56].

The reason this multi-fork replication phenomenon is able to assist bacteria in reducing generation time is because it allows the offspring cell to not only inherit a new copy of the genome during cell division, but also additional partly-replicated copies of the genome, *i.e.* there are active replication forks at the time of DNA segregation into daughter cells during

cell division. The offspring cell therefore requires considerably less time to replicate a complete copy of the genome and thus has a significantly shorter DNA replication phase in its cell cycle.

Computer simulation and flow cytometry studies by Skarstad *et al.*, in 1985 and 1986 have also shown that new DNA replication initiations in *E. coli* cells with multiple o*riC* sites occur in a synchronous fashion, with a small fraction of the population (~2-7%) carrying out asynchronous initiations [48, 57]. This means that rapidly growing *E. coli* cells will typically have an even number of *oriC* sites (e.g. 2, 4, 6 or 8) rather than odd. By adding rifampicin and chloramphenicol in *E. coli* cultures to inhibit cell division and initiation of new DNA replication bubbles, flow cytometry was then used to measure the numbers of completely replicated chromosomes in the cells after completion of the already ongoing replication bubbles. The results indicated concurrent initiation of the replication process at all *oriC* sites in the cell, suggesting a very tightly regulated timing system. Furthermore, they also found their *E. coli* cultures to have a doubling time of around 27 minutes while the duration of DNA replication as a process lasted around 43 minutes which supports the model proposed by Cooper and Helmstetter (1968) [48, 57]. Investigations by Kitagawa *et al.* in 1998 support these conclusions of Skarstad *et al.* (1986) as they discovered a 1Kb DNA segment in the *E. coli* chromosome called *datA*. This region was found to finely control intracellular DnaA concentrations in the cells by sequestering and titrating the proteins through separate mechanisms to ensure synchronized DNA replication initiation events. Strains lacking this 1Kb *datA* segment grew normally but demonstrated an asynchronous DNA replication initiation phenotype [15].

This phenomenon of overlapping replication cycles has been found to be more apparent in rich media than in minimal media. However, this is expected since rich media is more abundant in nutrients, and provides the cells with an optimum environment for rapid growth.

Minimal media on the contrary, contains significantly fewer nutrients and forces the cells to adapt to a humble lifestyle where rapid growth is limited [35, 47, 54, 58, 59]. Studies investigating the regulation of the DNA replication initiator protein, DnaA, support this idea and propose that cellular DnaA protein concentrations are down-regulated when the cell growth rates are low, causing the DNA replication processes to stay at a minimum, which would be the case in nutrient-poor environments [60, 61].

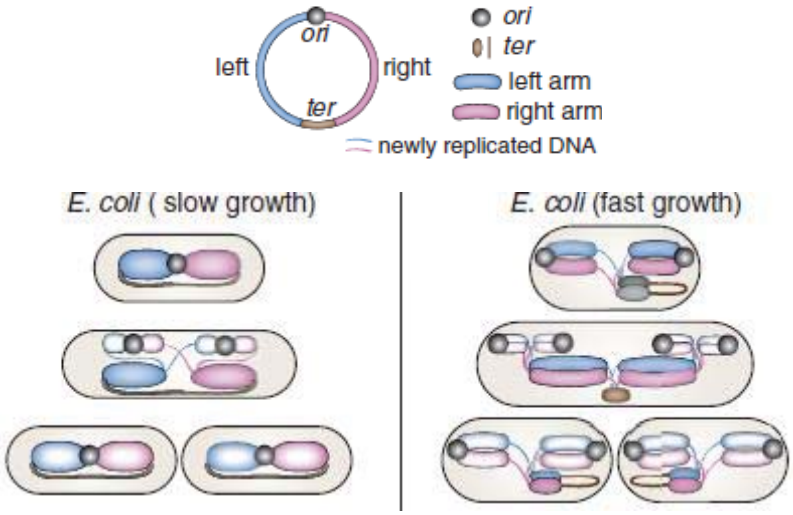

Figure 6: Illustration of chromosomal organization inside an *E. coli* cell at various stages of its cell cycle during slow and fast growth (source: Wang & Rudner, 2014 [62]).

1.6 Multi-fork Replication Studies on Other Model Organisms

Although DNA replication initiation and the bacterial cell cycle has been studied most extensively in *E. coli*, studies on this topic have also been extended to other bacterial species such as *Vibrio cholerae*, *Caulobacter crescentus*, *Bacillus subtilis*, *Neisseria gonorrhoeae* and some others. From the investigations which have examined their respective model species under both nutrient-rich and nutrient-poor conditions, the studies have shown that not all bacteria are capable of undergoing multi-fork replication like *E. coli*. While some gram-

negative bacteria like *V. cholerae* can in fact maintain multiple DNA replication processes simultaneously [63], other gram-negative species like *C. crescentus* and *N. gonorrhoeae* cannot [64-66]. Certain strains of gram-positive bacteria like *B. subtilis* have also been found to be capable of maintaining concurrent replication cycles [67, 68]. In the following sub-sections I will outline some of the major findings in these organisms.

Our current knowledge of multi-fork replication, therefore, stems from only a handful of bacterial species studied. Since these detailed investigations of replication fork dynamics have been limited to a rather small number of species to date, investigating fresh and different types of prokaryotes is essential for establishing a bigger picture of how these replication mechanisms are conserved and for developing a deeper understanding of the process in general. Since DNA replication as a process plays a predominant role in the prokaryotic cell cycle, gaining insight into this process should help us better understand the bacterial cell cycle as a whole.

1.6.1 Studies on *V. cholerae*

Not all bacteria have a single circular genome. *V. cholerae* is a prime example of such an organism; consisting of two circular chromosomes. The larger of the two, chromosome I (ChrI) is ~3Mbp in size, whereas chromosome II (ChrII) is ~1Mbp in size. Both the chromosomes also have their own unique *oriC* sites; *oriI* and *oriII* respectively. There have been many studies done on *V. cholerae* in the past, with some debate occurring on whether replication initiation of the two chromosomes is synchronous or asynchronous in slow growing cells [69, 70]. But perhaps the most relevant study for determination of multi-fork replication and resolving the opposing conclusions of past investigations, is the flow cytometry and fluorescent microscopy experiments carried out by Stokke, Waldminghaus and Skarstad in 2010 [63]. In this study, wild type *V. cholerae* cells were grown in four different

media (AB minimal media supplemented with fructose, glycerol or glucose + casamino acids and LB media) and analyzed for their timing of replication initiation of the two chromosomes at exponential phase.

By conducting replication run-out in minimal media (slow growing cells) through simultaneous inhibition of DNA replication reinitiation and cell division (similar to the method used by Skarstad *et al.* (1986) in *E. coli* [48]) and analyzing the cells under a flow cytometer, it was observed that replication of ChrI occurs first and replication of ChrII occurs much later. The termination of replication of both the chromosomes however, is synchronous. Furthermore, it was observed that in rich media, the cell cycles do overlap and multi-fork replication does occur in *V. cholerae.*

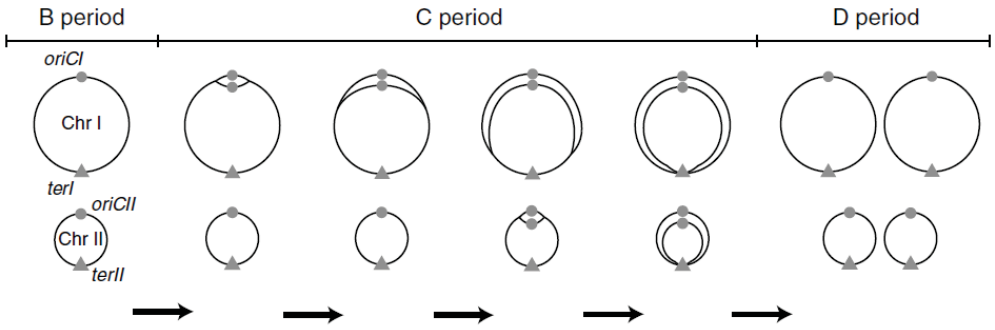

Figure 7: Diagram showing the cell cycle of *V. cholerae* (source: Rasmussen, *et al.* 2007 [70]).

1.6.2 Studies on *B. subtilis*

B. subtilis is a well-studied model organism like *E. coli*. The multi-fork replication in strain W168 was observed first in 1964 by Yoshikawa, O'Sullivan and Sueoka, four years before Cooper and Helmstetter's famous multi-fork replication investigations in *E. coli* began. After

introducing markers at various sites across the *B. subtilis* genome, the frequency of markers observed were compared in cells at exponential growth phase (where active DNA replication was expected to be occurring) with cells at stationary growth phase (where only a single complete chromosome was expected to be observed). These expectations were based on previous investigations on the *B. subtilis* strain W23. It was observed however, that the regulation of DNA replication initiation was significantly different in strain W168, when compared to the previously studied strain W23. While W23 was found to be carrying out only sequential replication and only during exponential growth, W168 was observed to be carrying out DNA replication even during stationary phase and multi-fork replication during exponential phase [55].

Since then, there have been several studies on the cell cycle of *B. subtilis*, and it has often been compared with *E. coli*. Parameters such as growth rate, cell size and DNA content have been measured at different stages of the cell cycle and in a number of different media [68].

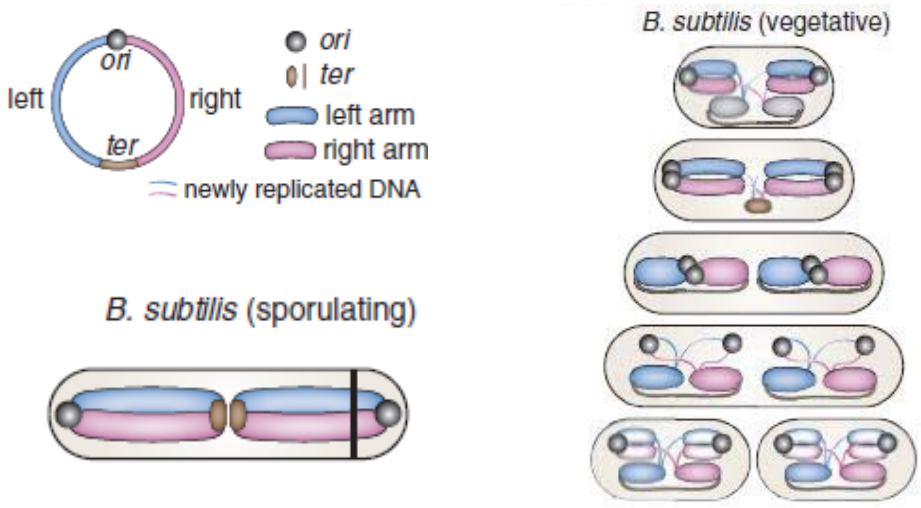

Figure 8: Illustration of chromosomal organization inside a *B. subtilis* cell during various stages of its cell cycle (source: Wang & Rudner, 2014 [62]).

1.6.3 Studies on *N. gonorrhoeae*

Unlike *E. coli*, which has been extensively studied, not much is known about the DNA replication dynamics of *N. gonorrhoeae* [71]. Gonococci are spherical cells which can exist as a mixture of diplococcal and monococcal cells during infection [72]. Even though the genome of this organism has been sequenced (strain FA1090) and was found to consist of only one chromosome, the location of the *oriC* site remains elusive [66].

When Tobiason and Seifert (2006) analyzed an exponentially growing population of gonococcal cells through a flow cytometer, there was a broad distribution of DNA content per cell observed, with the highest proportion of cells containing four to six genome equivalents [66]. Since the gonococcal genome is approximately half the size of the *E. coli* genome, it was hypothesized that the majority of gonococcal cells growing at exponential phase would be containing two to six chromosomes, which would suggest multi-fork replication at play [66].

Testing this hypothesis proved difficult however, since growing gonococcal cells to stationary phase leads to autolysis and due to the organisms being fastidious, with a very complex nutritional requirement, they are unable to grow in minimal media [66, 68, 69, 73, 74]. Therefore in order to slow down their growth rate, the researchers decided to grow the cultures at lower temperatures.

Their results showed that cultures grown at 30ºC expressed a generation time of ~90 minutes whereas cultures grown at 37ºC expressed a generation time of ~60 minutes. However even with a 1.5 fold slower growth rate, there was no significant change in DNA content per cell. As a control, when *E. coli* cells were run through the same procedure, reduced DNA content in cells growing at the lower temperatures was observed. Therefore their conclusions based

on these results were that *N. gonorrhoeae* cell cycles do not overlap, suggesting the possible occurrence of polyploidy [66].

1.6.4 Studies on *C. crescentus*

C. crescentus is a unique case as it is the only known prokaryotic organism that has been observed to have a cell cycle which is similar to that of eukaryotes. The life cycle of *C. crescentus* begins as a swarmer cell which has a single polar flagellum allowing it to be motile. Since the swarmer cell is unable to replicate its DNA, this phase of the life cycle can be directly compared to the G1 phase of the eukaryotic cell cycle. Then a transition occurs where the cell loses its flagellum and grows a stalk (flagellum biogenesis) [7]. This new stalked cell is able to carry out sequential DNA replication and this phase is analogous to the S phase of the eukaryotic cell cycle. Next a distinct DNA segregation phase occurs where DNA is partitioned into the 2 halves of the cell, similar to the eukaryotic G2 phase, which is followed by asymmetric cell division which yields a new swarmer cell and the old stalked cell (M phase of the eukaryotic cell cycle) [7, 64, 65]. Because of this tight regulation of the cell cycle, it is ensured that DNA replication only occurs once per generation [75].

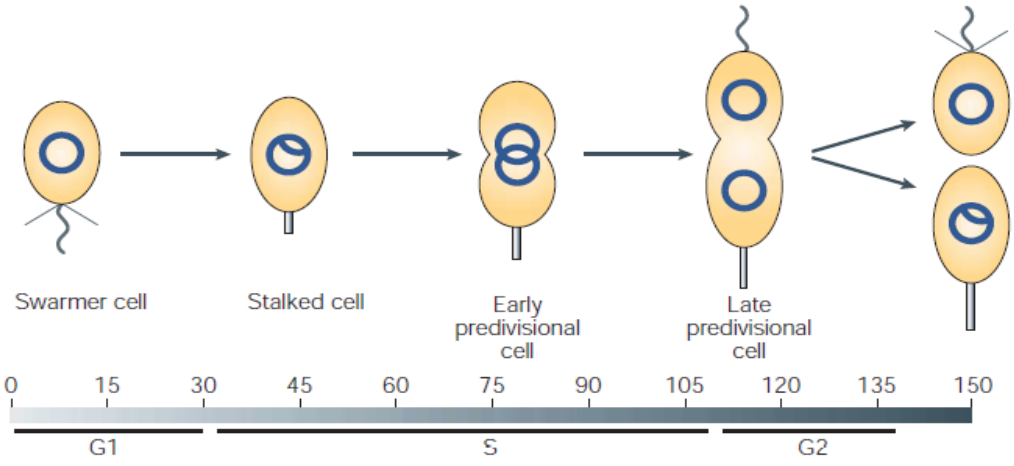

Figure 9: Diagram showing the current understanding of the *C. crescentus* cell cycle (source: Skerker & Laub, 2004 [65]).

1.6.5 Studies on *P. aeruginosa*

Recently in 2013, the cell cycle of *P. aeruginosa* PAO1 was investigated by Vallet-Gely and Boccard [76]. As the only member of the pseudomonas genus that has had its cell cycle studied thus far, even if it has only been investigated in minimal media, it is worth mentioning and is a very important example for my study due to its close relation to *P. fluorescens*, my model organism.

Vallet-Gely and Boccard managed to fluorescently label several sites in the *P. aeruginosa* genome as well as some components of the replication machinery. The labelled cells were subsequently analyzed under a fluorescent microscope and the localizations of the fluorescent foci were analyzed. Their observations indicate that at cell birth there is usually partial DNA replication occurring and each partially replicated chromosome is globally orientated from either pole to mid-cell region (where the future septum will form) along the *oriC-dif* axis. The replication machinery is positioned at mid-cell where replication continues as the cell grows. As the cell becomes longer, the two *oriC* sites move further apart along with the cell poles, which suggests an active role for DNA segregation machinery, the ParABS system. As DNA replication is completed, and the two chromosomes move apart to opposite cell halves, septum formation is initiated. Finally, as cell division is carried out, the *oriC* sites near the poles recoil back towards the center of the daughter cells to initiate a new round of replication [76].

Even though this derived model for the *P. aeruginosa* cell cycle depicts partially replicated chromosomes at cell birth, it does not appear that the cell cycles overlap. However, this investigation was carried out with cells grown in minimal media and whether the PAO1 strain is able to carry out multi-fork replication in nutrient-rich media is yet to be seen.

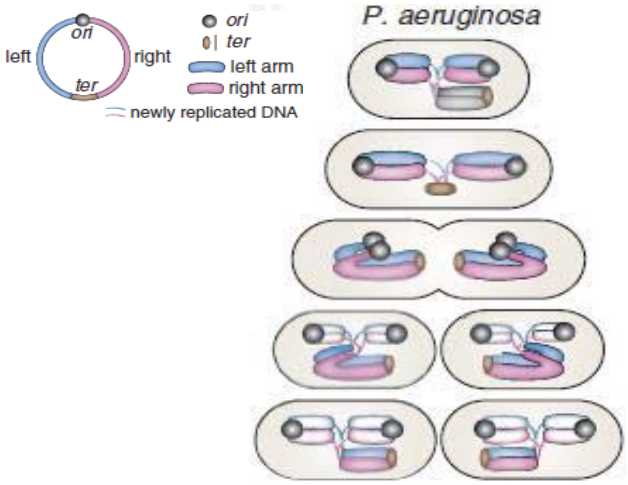

Figure 10: An Illustration of the chromosomal organization inside a *P. aeruginosa* PAO1 cell during various stages of its cell cycle (source: Wang & Rudner, 2014 [62]).

1.7 Aims

I have initiated an investigation on the DNA replication dynamics of the pseudomonas genus, a group which boasts phenomenal diversity and adaptability. Many members of the genus are disease causing agents in plants as well as animals and have many uses in biotechnological applications [77]. To carry out this investigation, I have used a non-pathogenic member of the genus as the model organism, *Pseudomonas fluorescens* SBW25; a gram-negative, plant associated saprophytic bacterium that appears to play a protective or beneficial role on its host plant [78]. *P. fluorescens* is also closely related to the more opportunistic and dangerous pathogen, *Pseudomonas aeruginosa*. *P. fluorescens* has not previously been studied for its cell cycle and DNA replication dynamics, making it an ideal candidate for such an investigation. My study involves insertion of arrays of engineered DNA sequence motifs repeated near the origin or replication site of the *P. fluorescens* genome, and then marking these sites with their fluorescently-labelled cognate repressors. By doing this, the origin-proximal regions of the genome become visible and fluorescent foci can be observed upon

live-cell imaging. This method has been used quite effectively in labelling genomic sites in other bacterial species in previous such studies [12, 76, 79].

By following these visualized foci under a fluorescent microscope the DNA replication and segregation processes have been studied in single living cells. Furthermore, since various studies have indicated that cellular growth rates are a key factor in determining regulation of dnaA proteins and thus DNA replication initiation, cells have also been analyzed under varying nutrient concentrations in order to learn if multi-fork replication occurs in this model organism [59-61].

1.8 Summary

Although our understanding of bacterial DNA replication as a process has improved a lot since 1958, there is still a lot that we do not yet know [53]. In order to develop insight into how bacteria manage their key cell cycle events, many different types of bacterial species must be investigated. *P. fluorescens* is a species that has not yet been studied for its DNA replication. Since these bacteria are known to colonize plant roots and provide protection for the host plant against various plant pathogens, it is a useful organism to study [80]. Additionally, due to the *Pseudomonas* genus having several pathogenic members, and with *P. fluorescens* being closely related to the pathogen *P. aerigunosa* in particular, exploring the inner processes of *P. fluorescens* may prove useful in finding new means to control its pathogenic siblings in the future [77].

Furthermore, by observing the replication processes of *P. fluorescens* in both nutrient-rich and minimal (nutrient-poor) media, potentially further evidence will be made available to the idea that cellular growth rates are a key factor in regulation of DnaA proteins and therefore DNA replication initiation, as claimed by several studies [59-61].

Chapter 2
Materials and Methods

2.1 Media Used for Bacterial Growth

2.1.1 Liquid Media: LB and M9 Glycerol 0.4%

LB Media (600 ml):

- NaCl 6 g
- Tryptone 6 g
- Yeast Extract 3 g

All ingredients were dissolved in distilled H_2O to a final volume of 600 ml and sterilized via autoclaving.

M9 Glycerol 0.4% Media (600 ml):

- M9 Salt (5X) 120 ml
- 1 M $MgSO_4$ 1.2 ml
- 0.1 M $CaCl_2$ 0.6 ml
- Glycerol (20%) 24 ml
- NH_4Cl (100 mg/ml) 6 ml
- Distilled H_2O 448.2 ml

All reagents were combined together in a flask and filter sterilized through a 0.22 µm disposable filter.

M9 Salt (5X) (500 ml):

- Na_2HPO_4 16.95 g
- KH_2PO_4 7.5 g
- NaCl 1.25 g
- NH_4Cl 2.5 g

All reagents were dissolved in distilled H_2O to a final volume of 500 ml and sterilized via autoclaving.

2.1.2 Solid Media: LB Agar

LB Agar (600 ml):

- NaCl 6 g
- Tryptone 6 g
- Yeast extract 3 g
- Agar 9 g

All ingredients were dissolved in distilled H_2O to a final volume of 600 ml and sterilized via autoclaving.

2.2 Plasmid Design

2.2.1 Designing the ParB-GFP and parS-GMR Plasmids

The ParB-GFP plasmid has 2 main components:

1. A ~5.8 Kb linearized pALA2705 plasmid (insert) [81]:

    i. BamHI restriction digested pALA2705 plasmid

ii. Encodes ParB-GFP fluorescent fusion protein under control of a Lac promoter

iii. Contains Ampicillin^R antibiotic selective gene

2. An ~8.3 Kb linearized pME6010 plasmid (backbone) [82]:

i. BamHI restriction digested pME6010 plasmid

ii. Contains an *oriV* origin of replication site for both *P. fluorescens* and *E. coli* (originally from plasmids pVS1 and p15A respectively) [82]

iii. Contains Tetracycline^R and Ampicillin^R antibiotic selective genes

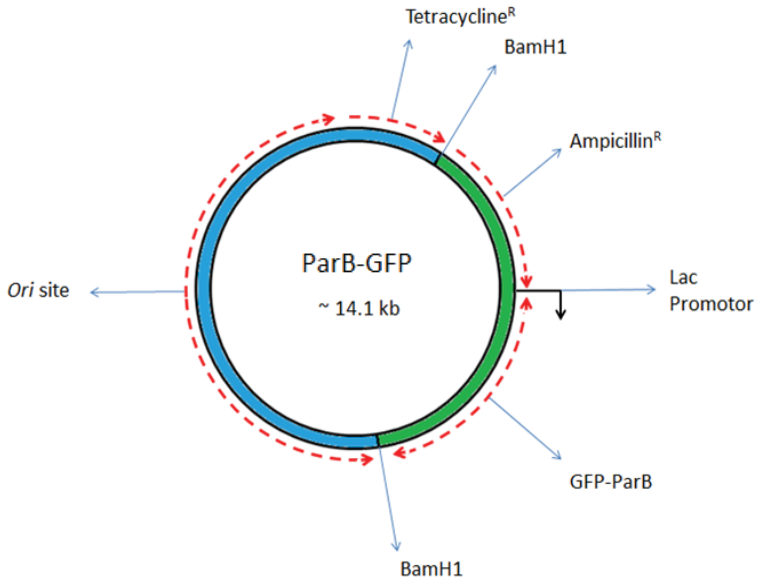

Figure 11: Plasmid map of the ParB-GFP plasmid.

Both, pALA2705 and pME6010 plasmids were linearized through restriction digestion with BamHI. Alkaline phosphatase was used for this process in order to avoid self-ligation of the plasmids. The linearized plasmids were ligated together and transformed into chemically competent DH5α (*E. coli*) for storage.

The transformants were plated on selective LB + Tetracycline plates and incubated at 37^{o}C. The resulting single colonies were isolated and analyzed under a fluorescent microscope to look for GFP expression. The candidate colonies expressing fluorescence were then mini-

prepped (Omega Bio-Tek E.Z.N.A® plasmid DNA isolation kit) and the extracted plasmids were linearized and run on a gel to make sure the plasmid size was correct (~14.1 kb).

The *parS*-GMR plasmid has 2 main components:

1. A *parS* sequence (insert):

    i. Flanked by XhoI and SpeI restriction sites

    ii. Sequence:

SpeI_*parS*_XhoI_F	ACCACTAGT_TTTCAAGGTGAAATCGCCACGATTTCACCTTGGATT_CTCGAGCC
XhoI_*parS*_SpeI_R	GGGCTCGAG_AATCCAAGGTGAAATCGTGGCGATTTCACCTTGAAA_ACTAGTGGT

2. The remainder of the plasmid (backbone):

    i. Derived from pUC18R6KminiTn7

    ii. Contains a mini-Tn7 transposon island consisting of Gentamycin^{R} antibiotic selective gene and SpeI and XhoI restriction sites. The mini-Tn7 transposon chromosome insertion system is a commonly used cloning tool for inserting DNA fragments of interest into bacterial chromosomes at specific *att*Tn7 sites. The system is compatible in a large range of bacterial hosts and is known to be able to transpose over 20 bacterial species [83]. The target *att*Tn7 insertion sites are normally located downstream of the highly conserved *glmS* genes, which expresses the glucosamine-6-phosphate synthetase protein. In *P. fluorescens* SBW25, the *glmS* gene and the target *att*Tn7 site is in close proximity to the *oriC* site [84, 85].

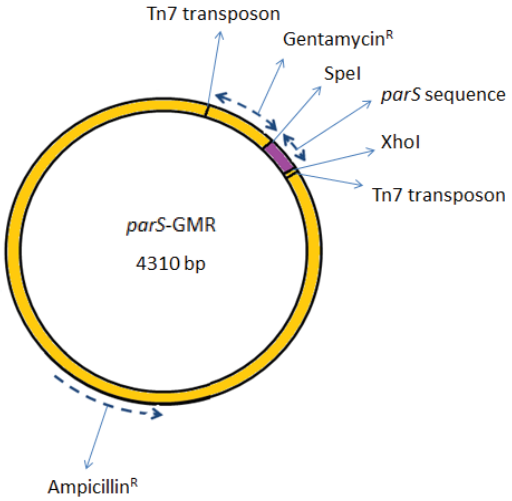

Figure 12: Plasmid map of the *parS*-GMR plasmid.

The *parS* sequence and the pUC18R6KminiTn7 plasmid were both restriction digested with SpeI and XhoI and subsequently ligated together. The ligation product was then transformed into WT SBW25 cells with the aid of a pUX-BF13, a helper plasmid. The transformants were plated on selective LB + Gentamycin plates and incubated at 28^{o}C.

The resulting colonies were Gentamycin resistant and were therefore considered to have the transposon island inserted into the SBW25 genomes (since the *parS-GMR* plasmid does not contain an *Ori* site for *P. fluorescens*, the plasmid cannot be segregated to offspring cells during cell division. Thus, the transposon island must have been inserted into the genome for offspring cells to express Gentamycin resistance). A colony PCR protocol was also carried out to ensure the array was inserted at the correct location in the *P. fluorescens* genome.

2.2.2 Designing the pLICTRY, *LacO*-GMR and *TetO*-GMR Plasmids

The pLICTRY plasmid has 2 main components:

1. A LacI-CFP + TetR-YFP region (insert):

    i. Derived from pLau53 plasmid [79]

ii. Encodes the fluorescent DNA-binding fusion proteins

2. The remainder of the plasmid (backbone):

i. Derived from pME6010 plasmid.

ii. Contains an *oriV* origin of replication site for both *P. fluorescens* and *E. coli* (originally from plasmids pVS1 and p15A respectively) [82].

iii. Contains Tetracycline^R and Ampicillin^R antibiotic selective genes

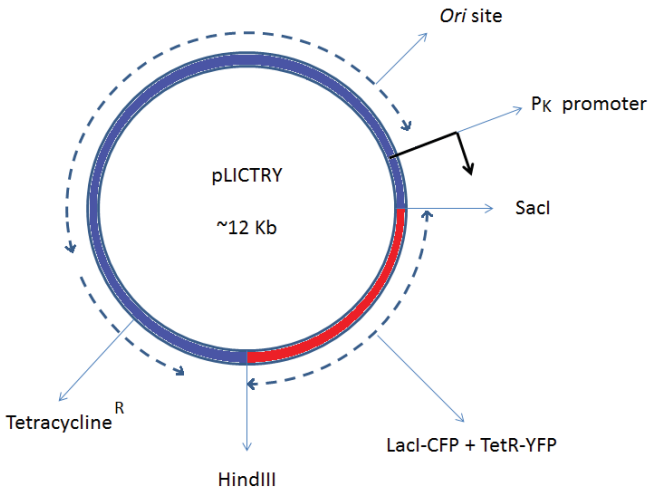

Figure 13: Plasmid map of the pLICTRY plasmid.

In order to extract the insert from pLau53, special primers were designed in order to attach SacI and HindIII restriction sites on either end of the PCR product:

F. Primer	5' GAGCTCGGATCCTACCTGAC 3'
R. Primer	5' CCAAGCTTTTATCTAGACTT 3'

The ~3.3Kb PCR product and the ~8.7Kb pME6010 plasmid were both restriction digested with SacI and HindIII and subsequently gel purified. Finally, the purified DNA fragments were ligated together and transformed into chemically competent DH5α (*E.* coli) for storage. The transformants were plated on selective LB + Tetracycline plates and incubated at 37°C.

The resulting single colonies were isolated and analyzed under a fluorescent microscope to look for CFP and YFP expression. The candidate colonies expressing the fluorescent proteins were then mini-prepped and the extracted plasmids were restriction digested with PstI (restriction site only present in the insert region of pLICTRY) and AhdI (restriction site only present in the backbone region of pLICTRY) and analyzed on the gel to make sure the plasmid was correct.

The *lacO*-GMR plasmid has 2 main components:

1. *lacO* array (insert):
    i. BamHI and KpnI restriction digested pLau43 plasmid [79]
    ii. Contains a ~7Kb array of repeated *lacO* sequences
    iii. Contains Kanamycin^R antibiotic selective gene
2. The remainder of the plasmid (backbone):
    i. Derived from pUC18R6KminiTn7
    ii. Contains a Tn7 transposon island consisting of Gentamycin^R antibiotic selective gene and BamHI and KpnI restriction sites. The Tn7 transposons are specific to the target *att*Tn7 site in close proximity to the *oriC* site of *P. fluorescens*.

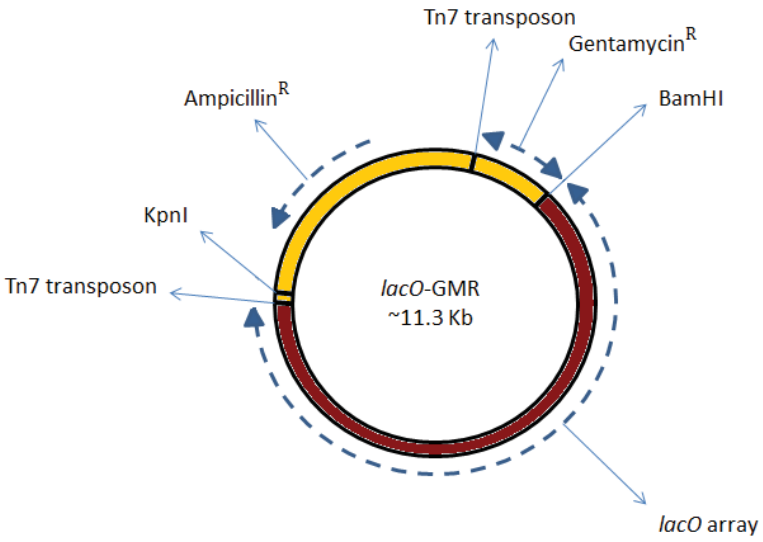

Figure 14: Plasmid map of the *lacO*-GMR plasmid.

The pLau43 plasmid and the pUC18R6KminiTn7 plasmid were both restriction digested with BamHI and KpnI and the resulting ~7Kb *lacO* array and "open" pUC18R6KminiTn7 plasmid were subsequently gel purified and ligated together. The ligation product was then transformed into WT SBW25 cells with the aid of a pUX-BF13, a helper plasmid. The transformants were plated on selective LB + Gentamycin plates and incubated at 28^{o}C.

The resulting colonies were Gentamycin resistant and were therefore considered to have the transposon island inserted into the SBW25 genomes (since the *lacO-GMR* plasmid does not contain an *Ori* site for *P. fluorescens*, the plasmid cannot be segregated to offspring cells during cell division. Thus, the transposon island must have been inserted into the genome for offspring cells to express Gentamycin resistance). A colony PCR protocol was also carried out to ensure the array was inserted at the correct location in the *P. fluorescens* genome.

The *tetO*-GMR plasmid has 2 main components:

1. *tetO* array (insert):
    i. XhoI and SmaI restriction digested pLau44 plasmid [79]
    ii. Contains a ~7Kb array of repeated *tetO* sequences
    iii. Contains Gentamycin^{R} antibiotic selective gene
2. The remainder of the plasmid (backbone):
    i. Derived from pUC18R6KminiTn7
    ii. Contains a Tn7 transposon island consisting of Gentamycin^{R} antibiotic selective gene and XhoI and SmaI restriction sites. The Tn7 transposons are specific to the target *att*Tn7 site in close proximity to the *oriC* site of *P. fluorescens*.

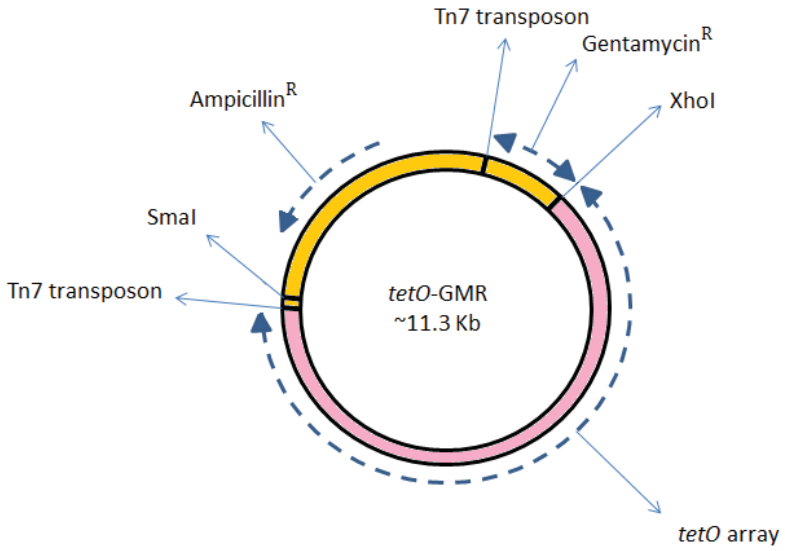

Figure 15: Plasmid map of the *tetO*-GMR plasmid.

The pLau44 plasmid and the pUC18R6KminiTn7 plasmid were both restriction digested with XhoI and SmaI and the resulting ~7Kb *tetO* array and "open" pUC18R6KminiTn7 plasmid were subsequently gel purified and ligated together. The ligation product was then transformed into WT SBW25 cells with the aid of a pUX-BF13, a helper plasmid. The transformants were plated on selective LB + Gentamycin plates and incubated at 28^{o}C.

The resulting colonies were Gentamycin resistant and were therefore considered to have the transposon island inserted into the SBW25 genomes (since the *tetO-GMR* plasmid does not contain an *Ori* site for *P. fluorescens*, the plasmid cannot be segregated to offspring cells during cell division. Thus, the transposon island must have been inserted into the genome for offspring cells to express Gentamycin resistance). A colony PCR protocol was also carried out to ensure the array was inserted at the correct location in the *P. fluorescens* genome.

2.3 Transformation Protocols

2.3.1 Making Chemically Competent *E. coli* DH5α

E. coli DH5α was grown in liquid LB culture overnight in a 37ºC shaking incubator. The following day, the culture was diluted 1:20 into SOB broth (recipe below). This resulting culture was then incubated at 37ºC until the cells reached an OD_{600} of 0.6, followed by incubation on ice for 15 minutes. The cells were then pelleted via centrifugation at 4000x g for 15 minutes at 4ºC and subsequently resuspended in cold Transformation Buffer I (recipe below) at a new volume 1/6 of the original culture with SOB broth. The resuspended cells were again incubated on ice for 15 minutes, followed again by centrifugation at 4000x g for 15 minutes at 4ºC. Finally, the cell pellet was resuspended in cold Transformation Buffer II (recipe below) at a new volume 1/24 of the original culture with SOB broth; and subsequently distributed into 1.5 ml Eppendorf tubes. The cells were kept cold throughout the process and finally stored in -80ºC.

Media and buffers used:

i. SOB Broth (1 L):

- Bacto tryptone (casein peptone) 20.0 g
- Bacto yeast extract 5.0 g
- NaCl 0.6 g
- KCl 0.5 g

All reagents were dissolved in distilled H_2O to a final volume of 990 ml and sterilized by autoclaving. Prior to use, 10 ml of 2 M Mg^{2+} stock solution was added to the SOB broth to make the media 20 mM with respect to magnesium.

ii. 1 M CH_3CO_2K (Potassium Acetate) (100 ml):

9.8 g of potassium acetate was dissolved in distilled H_2O. The pH was adjusted to 7.5 with the addition of 0.2 M glacial (anhydrous) acetic acid and the solution was brought to a final volume of 100 ml. The buffer was then sterilized by autoclaving.

iii. 0.5 M MOPS (100 ml):

10.5 g of MOPS was dissolved in distilled H_2O. The pH was adjusted to 6.8 with addition of 10 M NaOH and the solution was brought to a final volume of 100 ml. The buffer was filter sterilized through a 0.22 μm disposable filter and the final result was a clear and colorless liquid.

iv. Transformation Buffer I (500 ml):

- RbCl 6.0 g
- $MnCl_2.4H_2O$ 5.0 g
- 1M CH_3CO_2K 15 ml
- $CaCl_2.2H_2O$ 0.8 g
- Glycerol 75 ml

All reagents were dissolved in distilled H_2O. The pH was adjusted to 5.8 with the addition of 0.2 M glacial (anhydrous) acetic acid and the solution was brought to a final volume of 500 ml. The buffer was then filter sterilized through a 0.22 μm disposable filter and stored at 4ºC until use.

v. Transformation Buffer II (500 ml):

- 0.5 M MOPS 10 ml
- RbCl 0.6 g
- $CaCl_2.2H_2O$ 5.5 g

- Glycerol 75 ml

All reagents were dissolved in distilled H_2O to a final volume of 500 ml and filter sterilized through a 0.22 μm disposable filter. The buffer was then stored at 4ºC until use.

2.3.2 Transformation of Chemically Competent *E. coli* DH5α

The cells were removed from the -80ºC freezer and thawed on ice for 20 minutes. Plasmid DNA was then introduced into the vial of chemically competent cells and gently mixed. The samples were then incubated on ice for another 30 minutes. The cells were then heat-shocked at 42ºC for 30 seconds and immediately transferred back on ice. 1ml of pre-warmed SOC broth was added to each tube and the cells were subsequently incubated at 37ºC for 1 hour to allow for plasmid antibiotic resistance protein expression. Cells were then plated onto solid LB agar media supplemented with the appropriate antibiotics to maintain selection pressure.

2.3.3 Making Electrocompetent *P. fluorescens* SBW25

P. fluorescens SBW25 was grown in a 6 ml liquid LB culture overnight in a 28ºC shaking incubator. The following day, the culture was equally distributed into 4 pre-chilled (on ice) 1.5 ml Eppendorf tubes and pelleted via centrifugation at 16000x g for 2 minutes at room temperature. Each cell pellet was then washed twice with 1ml of room temperature 300 mM sucrose solution, with centrifugation at 16000x g for 1 minute between the washes. The cells were kept cool on ice whenever outside of the centrifuge throughout this process. The cells were then pooled into a single tube and resuspended in a combined total of 100 μl of 300 mM sucrose solution. This resulting cell suspension could now be electroporated.

2.3.4 Electroporation of Electrocompetent *P. fluorescens* SBW25

Keeping the electrocompetent *P. fluorescens* SBW25 cell suspension cool on ice, 250 ng of the respective plasmid DNA was introduced into the sample tube. The plasmid DNA was gently mixed into the cell suspension and the combined mixture was subsequently transferred into a 0.1 cm gap-width electroporation cuvette. The cuvette was placed appropriately into the electroporator and an electric field* was applied to the cuvette. 1 ml of pre-warmed SOC broth was immediately added to the cuvette and the resulting cell suspension was then incubated at 28ºC for 1 hour to allow for plasmid antibiotic resistance protein expression. Cells were then plated onto solid LB agar media supplemented with the appropriate antibiotics to maintain selection pressure.

* The electroporator was set to the following parameters: 1800 V, 200 Ω and 25 µF.

2.4 Colony PCR

Colony PCR was carried out on all *P. fluorescens* SBW25 candidate transformants of *parS*-GMR, *lacO*-GMR or *tetO*-GMR Tn7 transposon insertion plasmids to test if the sequences were inserted at the target site or not:

F. Primer	5’ CACCAAAGCTTTCACCACCCAA 3’
R. Primer	5’ CAGCATAACTGGACTGATTTCAG 3’

A standard 50 µl reaction contained: 5 µl 10X Std. Taq buffer, 1 µl 10 mM dNTP mix, 2.5 µl DMSO or BSA, 1 µl 10 µM Forward Primer, 1 µl 10 µM Reverse Primer, 5 µl Template DNA, 0.5 µl Taq DNA Polymerase, made up to 50 µl with deionized water. Fresh colonies were mixed in 600 µl of deionized water to be used as template DNA.

PCR protocol:

Step 1: 95ºC, 15.00 minutes

Step 2: 95ºC, 00:15 seconds

Step 3: 56ºC, 00:45 seconds

Step 4: 72ºC, 1:00 minute

Step 5: Go To Step 2, 30X

Step 6: 72ºC, 0:10 seconds

Step 7: 4ºC, ∞

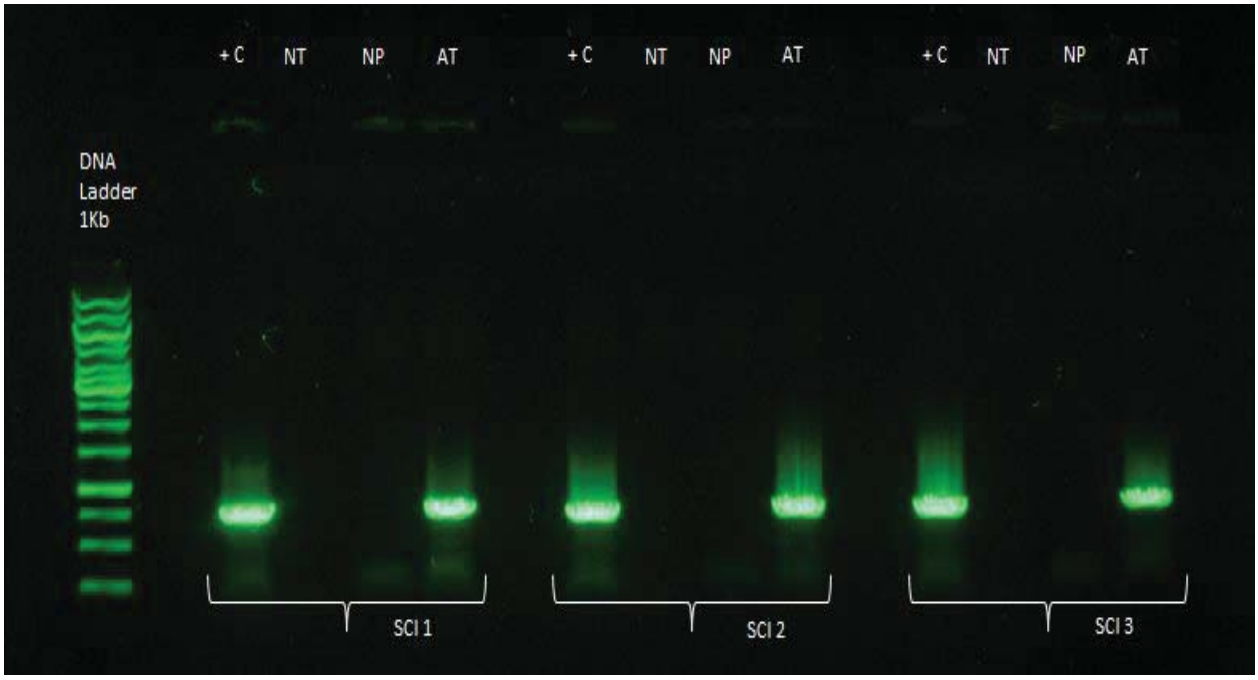

Figure 16: Picture of a gel depicting the results from a typical colony PCR reaction.

+C: Cells known to have a successful insertion at the target site (Positive Control)

- For testing insertion site of the *parS* sequence, another strain previously constructed by a colleague was used as a positive control. Once a strain with successful insertion of the *parS* sequence at the target site was established, this new strain was used as a

positive control for the following insertion site tests for the *lacO* and *tetO* arrays. The expected PCR product for successful insertion sites are ~700 b.p.

NT: No Template (Negative Control)

- All components for a successful PCR reaction were added into the mix except for the cells containing the template DNA. The purpose of this negative control was to check whether residual proteins were producing the bands or not.

NP: No Primers (Negative Control)

- All components for a successful PCR reaction were added into the mix except for the primers. The purpose of this negative control was to check if the primers were doing their job or not.

WT: Wild type cells without any insertion at the target site (Negative Control)

- Since WT cells do not have any insert at the target site in their genome, no amplification should occur when all the components required for a successful PCR reaction are added into the mix. This negative control was done to make sure the primers were attaching at the correct location in the genome and amplification was only occurring when an insert was present.

AT: Actual Test

- All the components required for a successful PCR reaction were added into the mix along with the untested transformants in order to check if the location of the insertion was correct or not.

2.5 Agarose Gel Electrophoresis

All gels were made using TBE buffer with 0.5% agarose. Gels were stained with ethidium bromide and the DNA bands were observed using a UV transilluminator with a camera. Gels were always run at 130 V however the duration was varied depending on the length of DNA fragments being run. A 1 kb DNA ladder was always used as a standard for sample length measurement. When gel purifying, the DNA bands of interest were always excised under a bright blue light illuminator with sterile blades.

2.6 Fluorescent Microscopy

2.6.1 Conditioning the Cells to M9 Glycerol 0.4% Media

SBW25_*parS*_ParB-GFP cells:

In order to compare the foci of cells grown in LB media and M9 glycerol media, SBW25_*parS*_ParB-GFP cells were grown at 28ºC in liquid LB culture (+ Tetracycline) overnight, followed by sub-culturing at 1:1000 dilution into liquid LB culture (+ Tetracycline) and liquid M9 0.4% glycerol culture (+ Tetracycline) overnight. Finally, on the third day, the cells were sub-cultured again at 1:50 dilution into liquid LB and M9 0.4% glycerol cultures without any antibiotics and induced them with IPTG at 28ºC for a few hours until an OD of ~ 0.2 - ~ 0.6 was reached. At this stage, the cells were analyzed under the microscope. This three day process was carried out to ensure that the ParB-GFP plasmid was not lost as the cells were under constant antibiotic selective pressure and to make sure that the cells were acclimated to their respective nutrient-rich and nutrient-poor media. The cells were grown to an OD of ~ 0.2 - ~ 0.6 to make sure that they were in exponential growth during the fluorescent microscopy analysis.

SBW25_*lacO*_pLICTRY and SBW25_*tetO*_pLICTRY cells:

In order to compare the foci of cells grown in LB media and M9 glycerol media, SBW25_*lacO*_pLICTRY cells and SBW25_*tetO*_pLICTRY cells were grown at 28ºC in liquid LB culture (+ Gentamycin + Tetracycline) overnight, followed by sub-culturing at 1:1000 dilution into liquid LB culture (+ Gentamycin + Tetracycline) and liquid M9 0.4% glycerol culture (+ Gentamycin + Tetracycline) overnight. Finally, on the third day, the cells were sub-cultured again at 1:50 dilution into liquid LB and M9 0.4% glycerol cultures without any antibiotics and incubated them at 28°C for a few hours until an OD of ~ 0.2 - ~ 0.6 was reached. At this stage, the cells were analyzed under the microscope. This three day process was carried out to ensure that the pLICTRY plasmids and operator arrays were not lost as the cells were under constant antibiotic selective pressure and to make sure that the cells were acclimated to their respective nutrient-rich and nutrient-poor media. The cells were grown to an OD of ~ 0.2 - ~ 0.6 to make sure that they were in exponential growth during the fluorescent microscopy analysis.

2.6.2 Image Analysis

Images of cells containing fluorescent foci obtained from the fluorescent microscope were analyzed on a software called, "ImageJ", a software developed especially for this purpose (http://imagej.nih.gov/ij/index.html). The fluorescent images were filtered with a plugin called 'Hatrick filter' to reduce background noise and the phase contrast image was subsequently merged with the filtered fluorescent image. The 'Analysis' feature was then used on the resulting image composite for measuring distances between cell poles and foci within individual bacterial cells.

2.7 Growth Assays

To measure growth rates of strains of interest, the respective strains were grown in liquid LB or M9 glycerol 0.4% media overnight with the addition of any selective agents required for the maintenance of genetic elements. The following day, a 96-well plate was prepared with 200 ml aliquots of the respective media in which the growth rates of the strains of interest were measured. The cultures were inoculated into the appropriate wells of the 96-well plate at a dilution of 1:1000 and the 96-well plate was subsequently placed into a microplate reader.

Every sample was always measured in triplicates and blank wells of sterile media were always included for every type of media the samples were being measured in. The optical density was always measured at 600 nm (OD_{600}) at 5 minute intervals for 40+ hours.

Chapter 3

Integration of Non-native Fluorescently-labeled parB-*parS* system into *P. fluorescens* SBW25 Indicates Incompatibility

My goal for this part of the project was to utilize the ParB-*parS* system to fluorescently label the *oriC* region in the *P. fluorescens* SBW25 genome. Before explaining my approach in carrying out this goal, I will first provide an overview of what the ParABS system is, and how bacteria utilize it to assist in chromosome and plasmid segregation.

3.1 Introduction to the ParABS System

Investigating DNA segregation in prokaryotes has been a long process and yet it is still not very well understood. A lot of our current understanding of how chromosomes are partitioned in to their respective cell halves prior to cell division is derived from studies analyzing segregation of low-copy number plasmids [86]. Unlike high-copy number plasmids which typically utilize passive diffusion to segregate, most low-copy number plasmids tend to carry partitioning (*par*) systems, which actively assist in segregation during cell division [37, 87-95].

The discovery of these plasmid partitioning systems was first identified in the *E. coli* P1 and F plasmids over 30 years ago [93, 96, 97]. Since then, several variants of the system have been discovered in plasmids from many different bacteria. Even though there are certain functional differences in the individual components of the systems between these variants;

the majority of the partitioning systems are very similar in their genetic make-up (Figure 17) and are composed of three main components:

1. A *cis*-acting centromere-like DNA sequence (typically called the *parS* locus).
2. A *trans*-acting DNA binding protein that specifically binds to the centromere-like DNA sequence (typically called the ParB protein).
3. A *trans*-acting ATPase enzyme required to generate the force necessary for the partitioning of the plasmids (typically called the ParA protein).

An in-depth review by Gerdes *et al.*, in 2000 [37] subjected all known partitioning systems to phylogenetic analyses and classified them into two main categories depending on the type of ATPase proteins present in the system. Most partitioning systems utilize ATPase proteins with deviant Walker-type motifs (Type I), but some others utilize ATPase proteins with actin-like folds (Type II). Since the centromere-like sequences and the DNA binding proteins display considerable sequence diversity, they could not be used to categorize the systems.

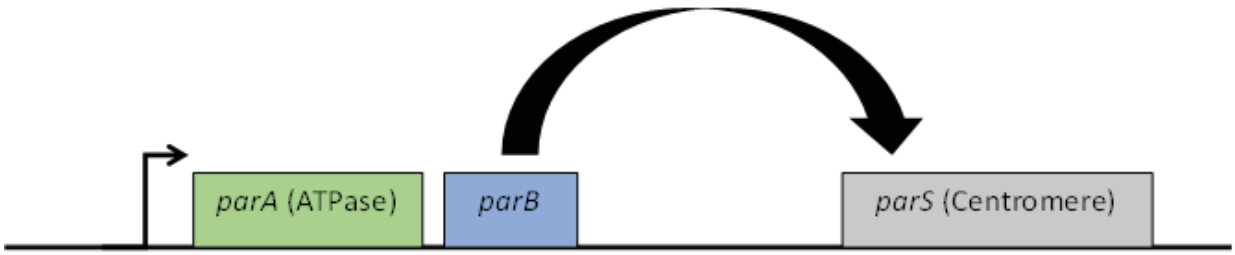

Figure 17: An illustration of the genetic organization of a *par* operon (Adapted from Gerdes, Howard & Szardenings 2010 [98]).

To begin segregation of the plasmids, first, the DNA binding ParB proteins must localize at and bind to the centromere-like *parS* locus, forming a protein complex called a segrosome [37, 87, 90, 99, 100]. As seen in Figure 17, the centromere-like *parS* site is usually found in close proximity to the *par* operon [37, 88, 90-93]. Next, the accumulation of associations

between the ParB proteins and the *parS* sites facilitates plasmid pairing [91, 101], after which, the segrosomes are recognized by the ParA ATPases. The ParA ATPases then initiates and drives plasmid separation to completion [88]. This whole partitioning process must be tightly regulated as too low or too high concentration of either *trans*-acting protein can lead to segregation failure [86].

These partitioning systems are not exclusive to only plasmids. A homologue for the ParB protein was inadvertently discovered during genetic investigations in *B. subtilis* in 1994 [102]. Since then, homologues of the partitioning systems have been found in several other bacterial species including *C. crescentus*, *V. cholerae*, *Pseudomonas putida* and *Pseudomonas aeruginosa* [103-107]. Not all bacteria contain such a partitioning system in their chromosome however; the model organism *E. coli* and other closely related species are the only handful of bacterial species found not to possess a partitioning system homolog. While the mechanism for bacterial chromosome segregation can be defined through this partitioning system, by and large the process is still a mystery for the majority of bacterial species studied. This is because, with the exception of *C. crescentus* and chromosome II of *V. cholerae*, these par protein homologues are not essential for chromosome segregation under normal growth conditions [64, 106-109]; which suggests that another underlying mechanism for successful chromosome segregation is at play.

3.2 The ParB-*parS* System

In order to fluorescently tag the *oriC* sites of the *P. fluorescens* SBW25 cells, I used fluorescent labelling techniques similar to those used in previous studies conducted on *E. coli*. Using previously established techniques is advantageous as it provides me with a

reference and allows for comparison between my results and those obtained in the previous studies.

The main concept of the procedure incorporates two main components:

1. A DNA-binding protein fused with a fluorescent protein.

2. A DNA sequence that the DNA-binding protein will bind to specifically.

The fluorescent proteins can therefore be localized at the target site, *oriC*, by (1) transforming the cells with a plasmid encoding the DNA-binding protein transcriptionally fused with a fluorescent protein, and (2) inserting the specific DNA segment respective to the DNA-binding protein at a location proximal to the *oriC* target site. This method has been used quite effectively by previous studies conducted in organisms such as *E. coli* and *P. aeruginosa* [12, 76, 79].

To carry out this technique, a non-native fluorescently labeled ParB-*parS* sysrem was utilized where the ParB protein would function as the DNA-binding protein and its respective *parS* locus as the DNA sequence to be inserted. Due to the strong interaction between ParB and the partitioning site *parS*, it is a widely used mechanism for fluorescent labeling.

3.3 Results

To initiate the investigation, I designed and developed a plasmid encoding ParB-GFP fusion proteins under control of a Lac promoter and also inserted the *parS* DNA sequence in close proximity to the *oriC* site in the *P. fluorescens* SBW25 genome using Tn7 transposons. Next, I transformed the SBW25_*parS* transformants with the ParB-GFP plasmid and analyzed the resulting transformants under a fluorescent microscope. Table 1 summarizes all the strains mentioned in this chapter and their genetic elements with respect to the Par system.

Table 1: Summary of all the strains with their genetic features in relation with the ParB-*parS* system.

Strain	***parS* sequence**	**ParB-GFP plasmid**	**Fluorescence**	**Foci Expected**	**Foci Observed**
WT SBW25	No	No	No	No	No
SBW25_*parS*	Yes	No	No	No	No
SBW25_ParB-GFP	No	Yes	Yes	No	No
SBW25_*parS*_ ParB-GFP	Yes	Yes	Yes	Yes	No

At first, no significant difference in fluorescent protein expression was observed between WT SBW25 cells and the SBW25_*parS*_ParB-GFP cells. After analysis of the cells under a flow cytometer it was evident that these cells were not expressing any GFP (Figure 18A). After further analysis it was discovered that the ParB-GFP plasmid was also expressing LacI (a lac repressor protein), which could be repressing the expression of the Lac promoter controlling GFP expression. To test this hypothesis, I decided to induce the SBW25_*parS*_ParB-GFP cells with IPTG, since IPTG acts as a molecular mimic of allolactose (a lactose metabolite), and thus activates the lac operon by repressing LacI proteins. As expected, after IPTG induction of the cells, the problem was resolved (Figure 18B).

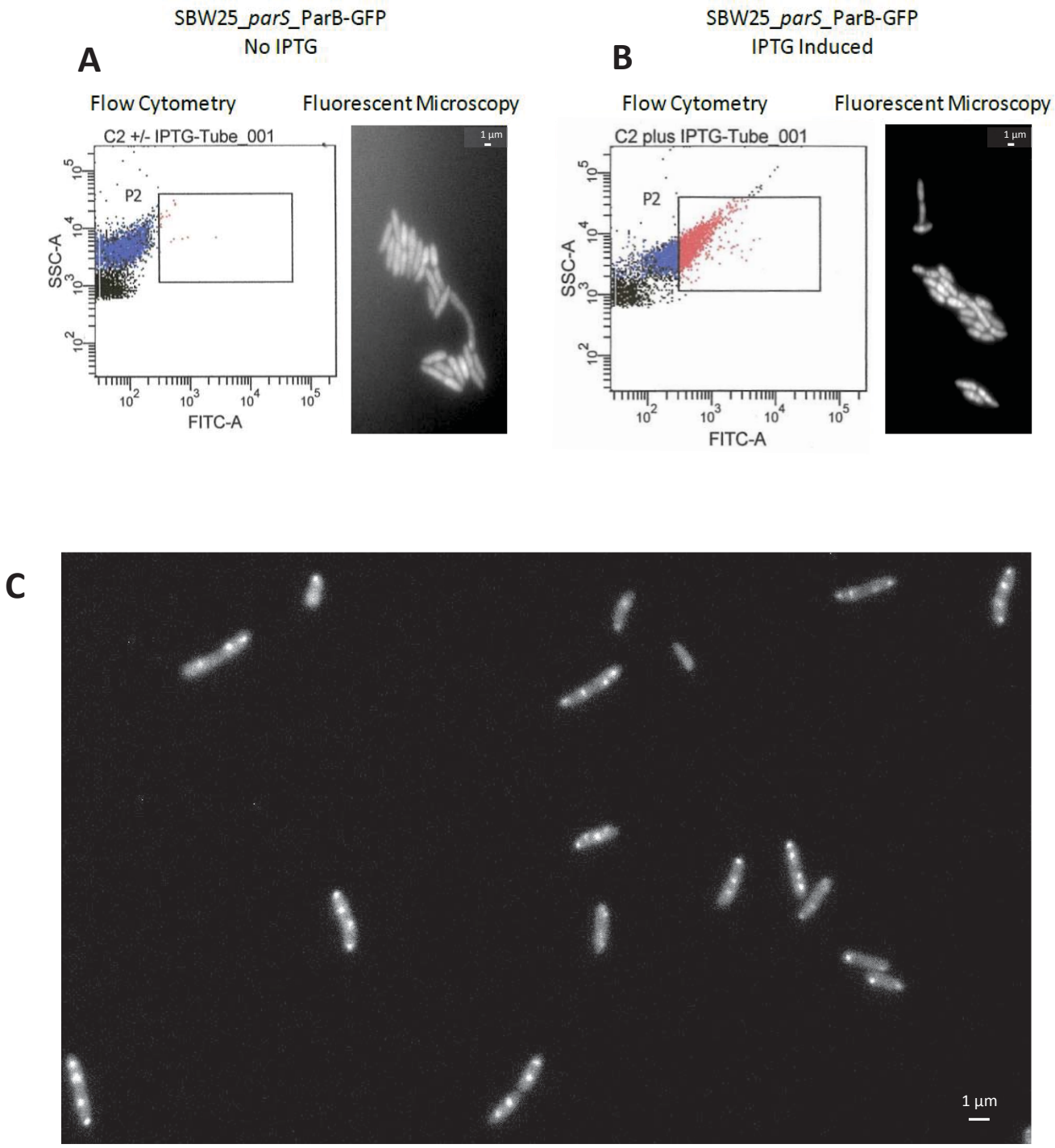

Figure 18: (A) Measuring GFP expression of SBW25_*parS*-GFP cells without IPTG induction using flow cytometry and fluorescent microscopy. (B) Measuring GFP expression of SBW25_*parS*_ParB-GFP cells with IPTG induction using flow cytometry and fluorescent microscopy. (C) *P. fluorescens* SBW25 with suitable foci.

However, even after IPTG induction, the fluorescence in SBW25_*parS*_ParB-GFP did not appear to be real foci (Figure 18B). For comparison, Figure 18C demonstrates what real foci should look like. It was not clear if the fluorescence from the pyoverdin production by the bacteria was resulting in too much background noise, and was therefore making it difficult to visualize the foci clearly. Since pyoverdin is produced by fluorescent pseudomonads to chelate and accumulate iron from the environment [110-112], I tried adding $FeCl_3$ into the SBW25_*parS*_ParB-GFP cultures so that the bacteria have a sufficient supply of iron and reduce pyoverdin production. In doing so, I measured the average background brightness levels and the average 'foci' brightness levels in the cells (Figure 19). I then compared the average difference in these brightness levels between cells grown in cultures supplemented with and without $FeCl_3$. A statistical t-test of this comparison showed that this difference was not significant however, suggesting that pyoverdin production may not be responsible for the excessive background noise as illustrated in Table 2.

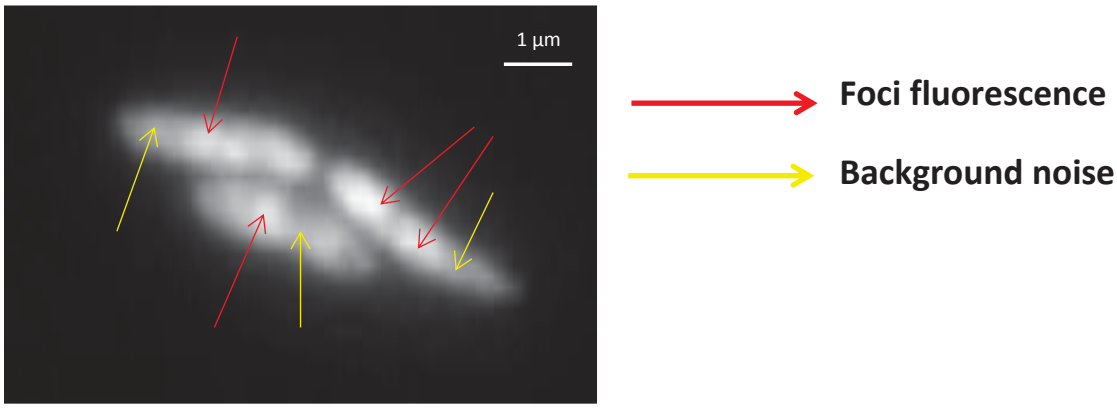

Figure 19: Image depicting which regions of the SBW25_*parS*_ParB-GFP cells were considered to be 'background noise' and 'foci fluorescence". Red arrows point to locations considered as "foci fluorescence" and yellow arrows point to locations considered as "background noise".

Table 2: Quantification of $FeCl_3$ induced fluorescent background noise reduction in WT SBW25 and SBW25_*parS*_ParB-GFP cells.

Sample	No. of cells tested	Average Difference in brightness*	t-test value
WT SBW25: No $FeCl_3$	35	70.77	0.98
WT SBW25: $FeCl_3$ Added	30	70.63	
SBW25_*parS*_ParB-GFP: No $FeCl_3$	47	554.49	0.97
SBW25_*parS*_ParB-GFP: $FeCl_3$ Added	67	551.79	

***Average difference in brightness levels was calculated by subtracting the average background brightness levels from average foci brightness levels**

Since the addition of $FeCl_3$ in my samples was ineffective in reducing the background noise, I decided to grow the cells in nutrient-poor media (M9 0.4% glycerol) instead of nutrient-rich (LB), in consideration of the possibility that the auto-fluorescence from LB media was responsible for the excess background noise. To do this, the cells were conditioned for three days to become accustomed to the M9 0.4% glycerol media (refer section 2.6.1), followed by IPTG induction and fluorescent microscopy analysis. The results however, displayed very similar fluorescence patterns in cells from both media as shown in Figure 20A.

In light of observing very similar fluorescence patterns in cells grown in LB and M9 glycerol media and due to the excessive background noise the cells were displaying, foci comparison of SBW25_*parS*_ParB-GFP cells with SBW25_ParB-GFP cells in M9 glycerol media was carried out. It was considered, that by comparing these two samples in nutrient-poor media, I would most likely only observe one or two foci per cell in the SBW25_*parS*_ParB-GFP sample and no foci at all in the SBW25_ParB-GFP sample. If this is true then I would be able to establish a differentiation between real foci from background noise, and use it to distinguish real foci in my other comparisons. To do this, WT SBW25 cells were transformed

with the ParB-GFP plasmid and compared with the SBW25_*parS*_ParB-GFP strain under a fluorescent microscope. Prior to microscope analysis, the cells were again conditioned for three days to become accustomed to M9 0.4% glycerol media and were induced with IPTG on the final day. The results were inconclusive since the fluorescence patterns appeared to be very similar between the two samples as shown in Figure 20B. Possible reasons for the poor performance of the Par system in the strains are discussed further in section 3.4.

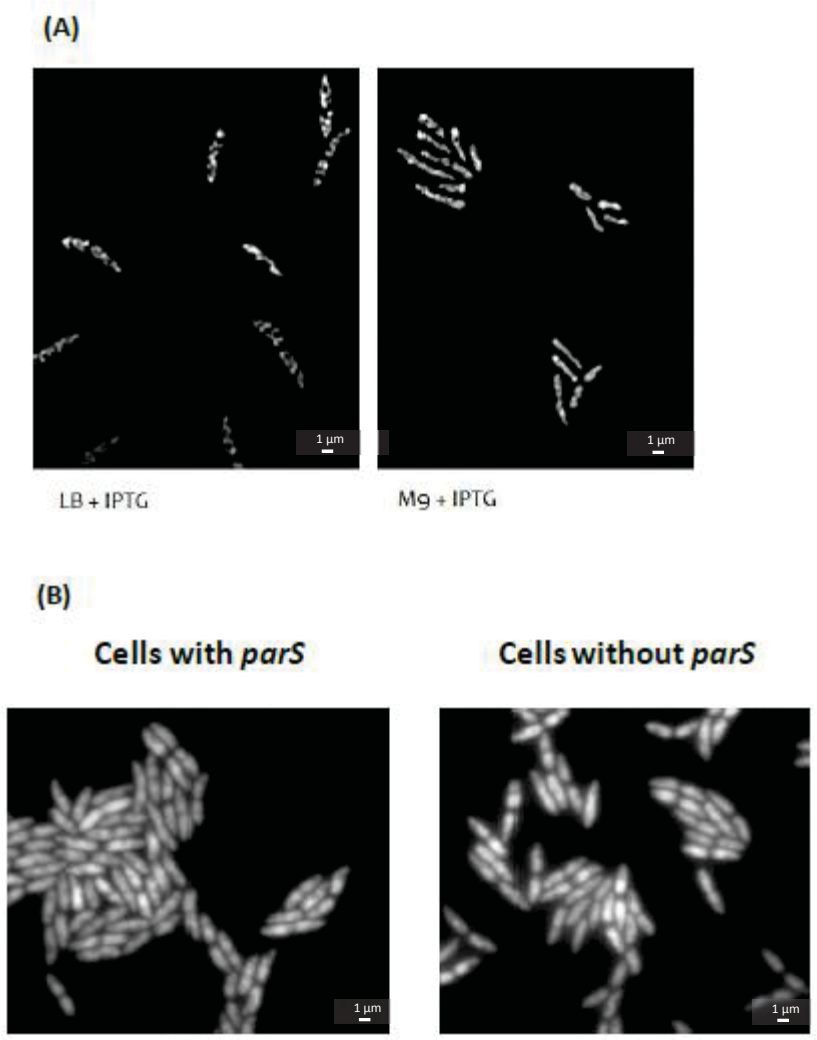

Figure 20: (A) Foci comparison between SBW25_*parS*_ParB-GFP cells grown in nutrient-rich media (LB) and SBW25_*parS*_ParB-GFP cells grown in nutrient-poor media (M9 0.4% glycerol). The images have been treated with 'Hatrick Filter', a plugin for ImageJ, the image analysis software used. Hatrick Filter is used to decrease background noise. **(B) Foci comparison between SBW25_*parS*_ParB-GFP cells and SBW25_ParB-GFP cells. Both of the samples were grown in nutrient-poor media (M9 0.4% glycerol).**

3.4 Discussion

Despite trying various methods to get the ParB-*parS* system to work in my model organism *P. fluorescens* SBW25, the system remained ineffective.

There are a couple of possible explanations for the Par system failing in producing foci:

1. As evident in STRING database, *P. fluorescens* SBW25 utilizes the ParABS system for assistance in chromosomal segregation [113]. Therefore, since there are already *parB* genes present in the *P. fluorescens* genome. It is possible that these non-fluorescent ParB proteins may have been binding with the inserted *parS* sequence and therefore interfering with the *parS*-ParB-GFP interaction. As a result, the majority of the unbound fluorescent fusion proteins may have been dispersed around the cell, generating background noise.

2. There could be another unknown protein interfering with the ParB-*parS* interaction by binding to either the ParB-GFP fusion protein or the *parS* sequence.

In light of the fact that a lot of the time was invested into a system that did not seem to be compatible with my organism, I decided to move on from the ParB-*parS* system and start fresh with some of the other tools available to me; the Lac and Tet systems, which is explained in the next chapter.

Chapter 4

Integration of LacI-*lacO* and TetR-*tetO* Systems Show Different Replication Patterns

4.1 The LacI-*lacO* and TetR-*tetO* Systems

Since the ParB-*parS* system remained ineffective at fluorescent labelling the *P. fluorescens* SBW25 genome, two different labelling systems developed by Lau, *et al.* (2003) [79] were used as a second option. Unlike the parB-*parS* system, which is derived from the bacterial chromosome segregation mechanism; the components of these new LacI-*lacO* and TetR-*tetO* systems were derived from *E. coli* transcription regulation mechanisms [79]. The LacI-*lacO* system, first developed by Straight et al. (1996) [114], is derived from the lac operon, which is utilized for regulating lactose transport and metabolism. The TetR-*tetO* system, first developed by Michaelis et al. (1997) [115], is derived from the tetracycline resistance operon, which is utilized for regulating the activation of a neighboring promoter in the presence or absence of tetracycline.

Since being developed, these two systems have been used quite effectively to visualize genomes in a variety of eukaryotic organisms such as yeast cells [114-116], Chinese hamster ovary [116], and higher plants (e.g., *Arabidopsis thaliana* [117, 118] and tobacco chloroplast [119], as well as prokaryotic organisms such as *E. coli* [12, 79] and *B. subtilis* [120].

Although the components of the LacI-*lacO* and TetR-*tetO* systems are different and originate from different metabolic pathways, the mechanism through which they are used for fluorescent labelling is analogous to that of the ParB-*parS* system. Similar to the ParB-*parS* system, the LacI-*lacO* and TetR-*tetO* systems also incorporate a DNA-binding protein that is

transcriptionally fused with a fluorescent marker protein; and a DNA sequence to which the fluorescent DNA-binding fusion protein specifically binds to (refer section 3.1). However, since the LacI and TetR proteins cannot spread along the DNA from their respective *lacO* and *tetO* sequences like ParB proteins can with the *parS* sequence [121]; insertion of 240 repeats of the respective DNA sequences was required to allow enough room for effective interaction with fluorescent proteins for production of clear and distinct foci.

4.2 Results

4.2.1 Building the SBW25_*lacO*_pLICTRY and SBW25_*tetO*_pLICTRY Strains

I designed and developed a plasmid encoding LacI-CFP and TetR-YFP fusion proteins under control of a constitutive pK promoter (plasmid pLICTRY), and inserted the *lacO* and *tetO* repetitive sequence arrays in close proximity to the *oriC* site in the *P. fluorescens* SBW25 genome using Tn7 transposons. Both of these newly prepared SBW25_*lacO* and SBW25_*tetO* strains were then transformed with the pLICTRY plasmid, resulting in two final mutant strains of *P. fluorescens* SBW25; SBW25_*lacO*_pLICTRY and SBW25_*tetO*_pLICTRY. Table 3 below shows all the strains mentioned in this section and their genetic elements with respect to the LacI-*lacO* and TetR-*tetO* systems.

Table 3: Summary of all the strains with their genetic features in relation with the LacI-*lacO* and TetR-*tetO* systems.

Strain	Sequence array inserted	pLICTRY plasmid	Fluorescence	Foci Expected	Foci Observed
WT SBW25	None	No	No	No	No
SBW25_*lacO*	*lacO* array	No	No	No	No
SBW25_*lacO*_ pLICTRY	*lacO* array	Yes	Yes	Yes	Yes
SBW25_*tetO*	*tetO* array	No	No	No	No
SBW25_*tetO*_ pLICTRY	*tetO* array	Yes	Yes	Yes	Yes

Both of the new strains, SBW25_*lacO*_pLICTRY and SBW25_*tetO*_pLICTRY were grown to exponential phase (OD = ~ 0.25) in nutrient-rich (LB) and nutrient-poor media (M9 0.4% glycerol) and analyzed under the fluorescent microscope. Finally, strong and distinct foci were observed (Figure 20). From the initial fluorescent images taken, it was immediately clear that *P. fluorescens* SBW25 does indeed perform multi-fork replication. Furthermore, as expected, the number of foci observed in cells grown in LB media considerably out-numbered the number of foci observed in the cells grown in M9 0.4% glycerol media. However, the sizes of the foci were generally larger in the cells grown in M9 0.4% glycerol media, than in the cells grown in LB media.

SBW25_*lacO*_pLICTRY Cells Grown in LB Media (OD_{600} = ~ 0.25)

SBW25_*tetO*_pLICTRY Cells Grown in LB Media (OD_{600} = ~ 0.25)

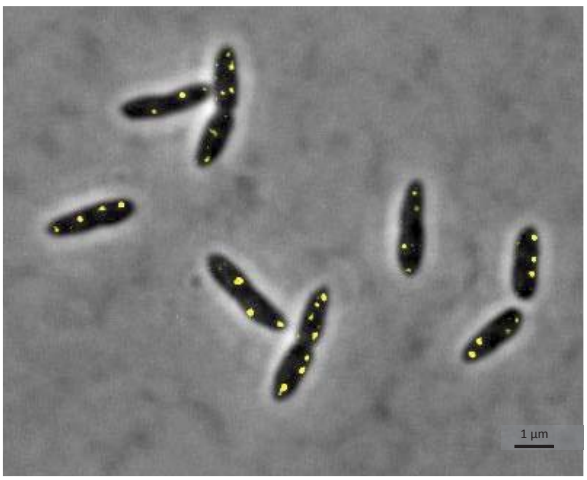

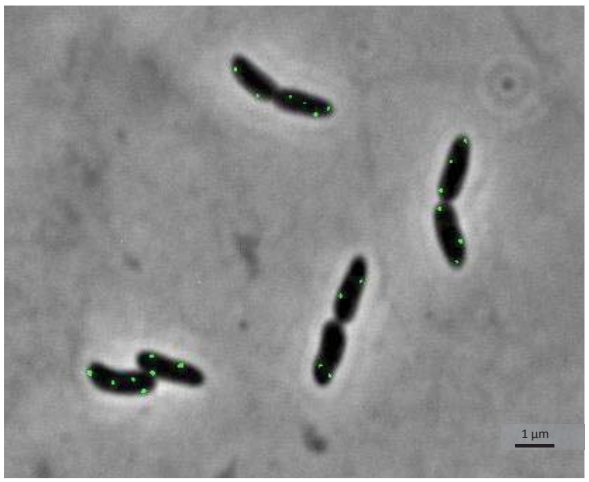

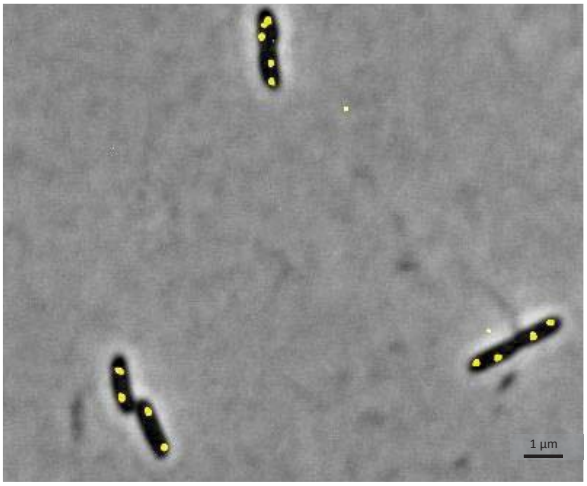

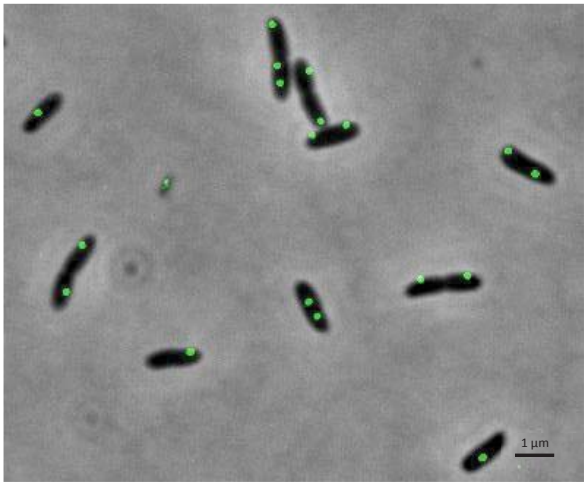

SBW25_*lacO*_pLICTRY Cells Grown in M9 0.4% Glycerol Media (OD_{600} = ~ 0.25)

SBW25_*tetO*_pLICTRY Cells Grown in M9 0.4% Glycerol Media (OD_{600} = ~ 0.25)

Figure 21: Typical field of view of SBW25_*lacO*_pLICTRY cells and SBW25_*tetO*_pLICTRY cells when grown in both LB media and M9 0.4% Glycerol media. The raw images have been treated with 'Hatrick Filter', a plugin for ImageJ, the image analysis software used. Hatrick Filter is used to decrease background noise.

In order to ensure that the genetic modifications applied to the strains did not significantly hinder their fitness levels, a growth assay was carried out for WT SBW25 and both the fluorescently tagged strains in LB and M9 glycerol 0.4% media, with and without the presence of antibiotics. Antibiotics were added in order to maintain selection for the

repetitive arrays (Gentamycin) and pLICTRY plasmid (Tetracycline). Additionally, the strains were also grown in antibiotic deficient media as controls, for the purpose of comparing growth rate of the strains in absence of selection pressures as shown in Figure 22.

A

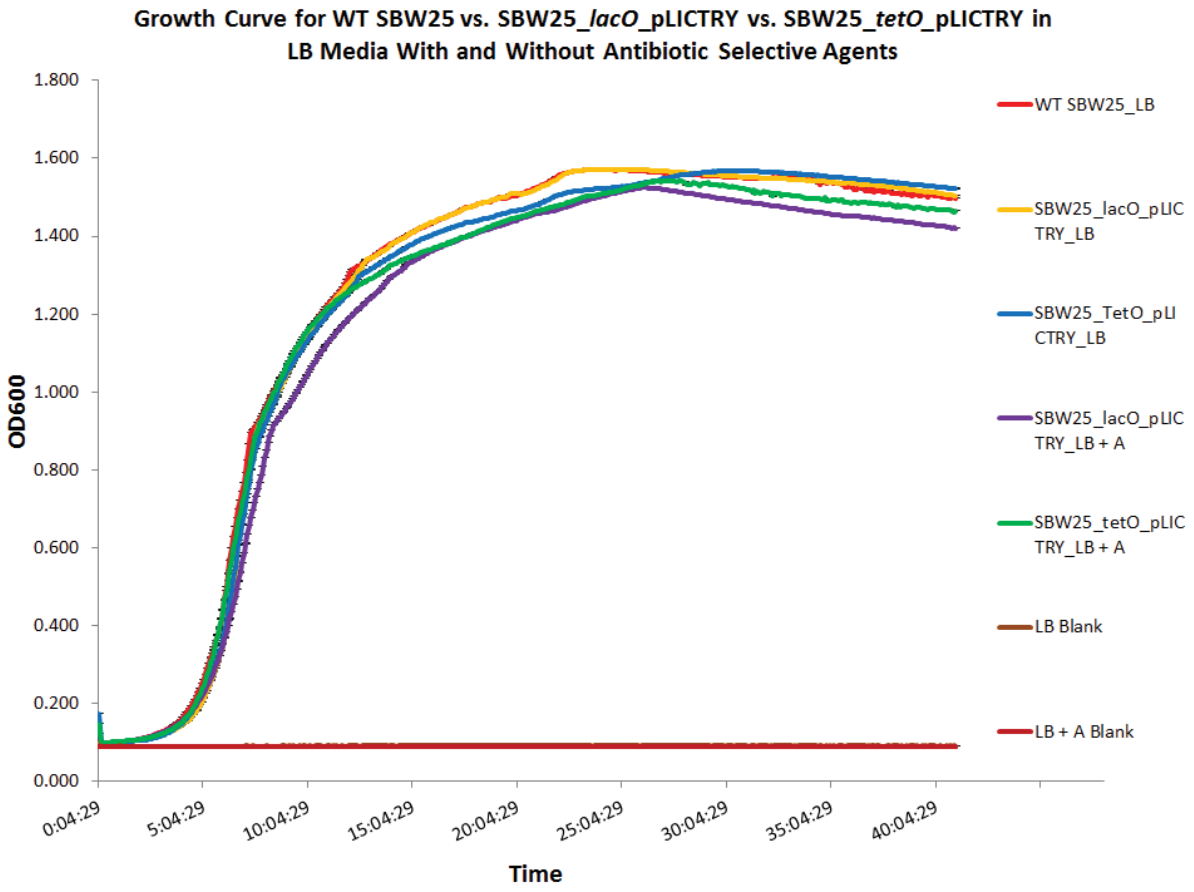

B

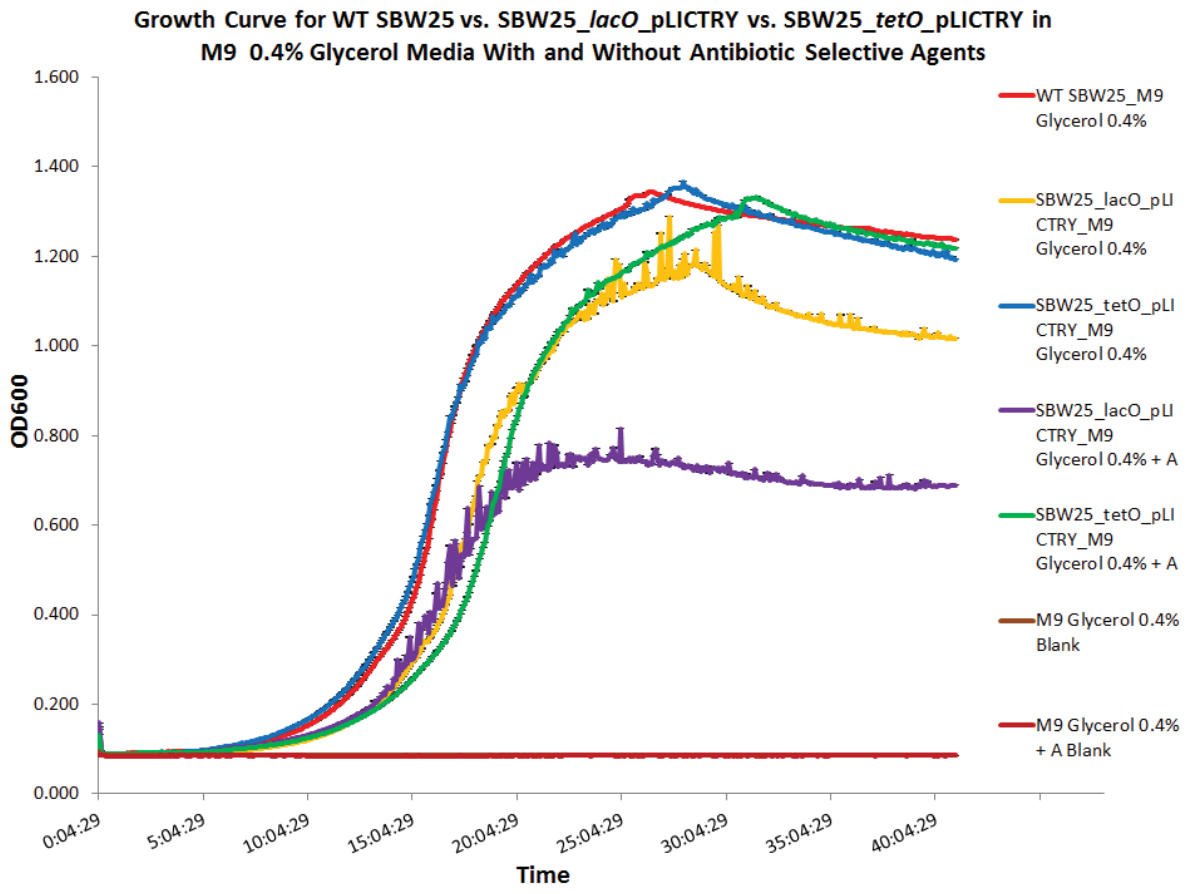

Figure 22: Growth Assay of WT SBW25, SBW25_*lacO*_pLICTRY and SBW25_*tetO*_pLICTRY strains in LB and M9 0.4% Glycerol media, with and without the presence of antibiotics. All the values presented are the averages of sample triplicates. The error bars denote standard error. (A) Growth curves of all the strains in nutrient-rich media (LB). (B) Growth curves of all the strains in nutrient-poor-media (M9 0.4% Glycerol). The fluctuating growth of the SBW25_*lacO*_pLICTRY strains in M9 0.4% Glycerol media indicates unstable growth.

Table 4: Doubling time of WT SBW25, SBW25_*lacO*_pLICTRY and SBW25_*tetO*_pLICTRY strains in LB and M9 0.4% Glycerol media, during exponential growth. The doubling times were calculated from the growth curves between 0.4 and 0.6 OD_{600} from Figure 22.

Strain	**Doubling time in LB**	**Doubling time in LB + Antibiotics**	**Doubling time in M9 0.4% Glycerol**	**Doubling time in M9 0.4% Glycerol + Antibiotics**
WT SBW25	~ 60 min	-	~ 120 min	-
SBW25_*tetO*_pLICTRY	~ 60 min	~ 68 min	~ 136 min	~ 145 min
SBW25_*lacO*_pLICTRY	~ 60 min	~ 85 min	~ 128 min	~ 180 min

These results indicate that when the mutant strains are growing in the presence of antibiotics, their growth rate is decreased in both LB and M9 0.4% glycerol media. In M9 0.4% Glycerol media, there even appears to be an increase in the duration of lag phase when SBW25_*tetO*_pLICTRY was grown in the presence of antibiotic selective agents. This brought up the possibility that the mutants are losing the added genetic elements in absence of the antibiotics; and thus increasing their growth rate. Since this effect is more pronounced in the SBW25_*lacO*_pLICTRY strain, this strain was used to test the hypothesis.

The strain was grown in liquid cultures overnight with and without antibiotics, and subsequently diluted and plated on various antibiotic plates the following morning. After growing the cells on these plates for approximately two days, colony forming units (CFU) were counted from each plate and antibiotic resistance of cells from either culture was analyzed (Figure 23).

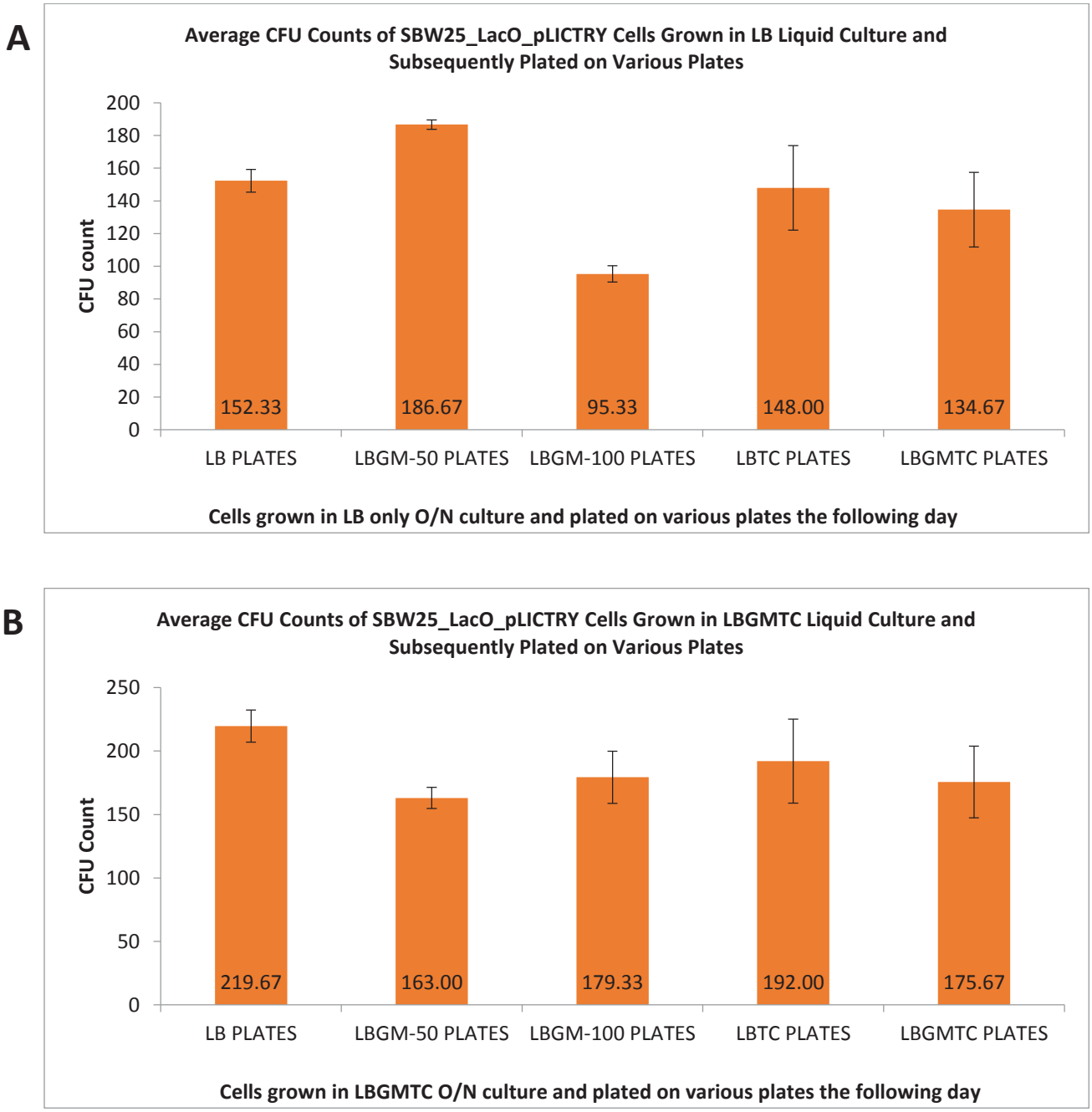

Figure 23: Charts showing the average CFU counts of SBW25_*lacO*_pLICTRY cells when plated on LB only and various LB + antibiotic plates, following overnight incubation in a liquid LB culture with and without the presence of antibiotic selection pressures. The error bars denote standard error. (A) Average CFU counts of cells plated on various plates following overnight incubation in liquid LB culture without the presence of antibiotic selection pressures. (B) Average CFU counts of cells plated on various plates following overnight incubation in liquid LB culture with the presence of antibiotic selection pressures.

From the CFU counts, we can see that when cells are grown without antibiotics overnight, generally the CFU count on LB + Antibiotics plates is not significantly lower than the CFU count on LB only plates. This suggests that the added genetic elements are maintained stably in our cells even after overnight growth in a liquid medium without antibiotic selection. Furthermore, microscope analysis of the cells that were grown overnight without antibiotics showed that the cells still displayed clear and distinct foci, which supports the conclusion that these mutant cells do not lose their genetic elements when grown in absence of selection pressure, overnight.

It was therefore inferred that the restricted growth observed in our growth assay when in presence of antibiotics, was due to the accepted strain on cellular metabolism resulting from the cells' need of manufacturing antibiotic resistance proteins.

4.2.2 Interpretation and Analysis of Foci

Next, it was decided that investigation of chromosome organization and segregation in *P. fluorescens* SBW25 should be conducted by studying the relationship between cell ages (*i.e.* cell lengths) and the foci locations in my mutant strains. To instigate such an attempt, exponentially growing cell populations (Optical Density = ~0.2 – 0.4) from nutrient-rich and nutrient-poor cultures were first isolated, and samples were examined under the fluorescent microscope. Images taken from the fluorescent microscope were then analyzed to calculate the proportions of cells in these populations that had varying numbers of foci, and the average cell lengths within these sub-populations (Figure 24).

A

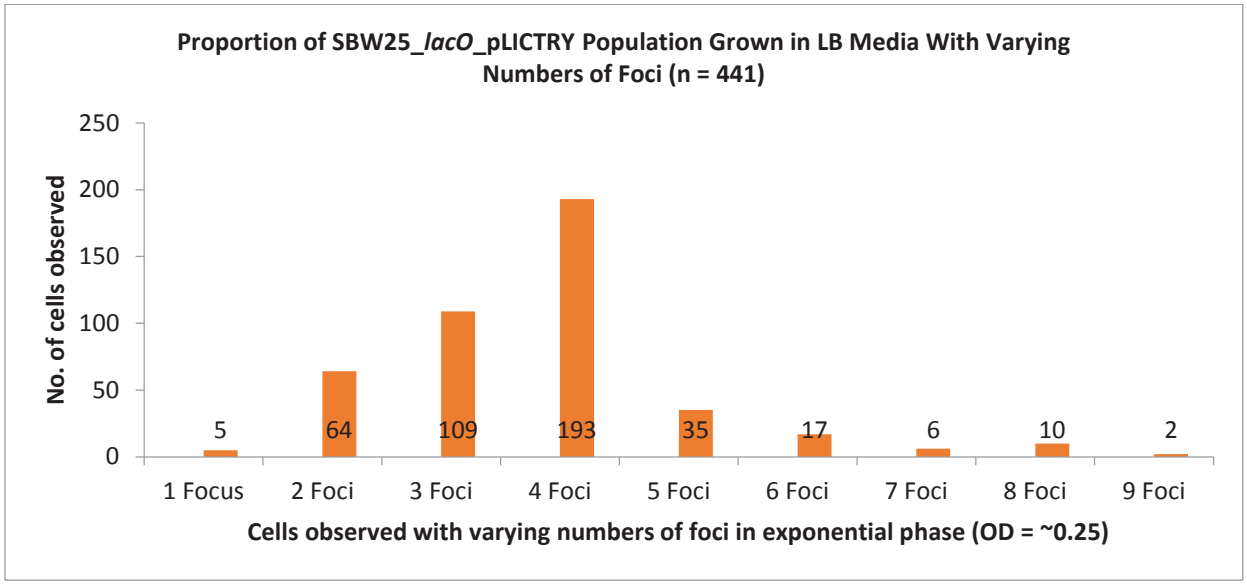
Proportion of SBW25_lacO_pLICTRY Population Grown in LB Media With Varying Numbers of Foci (n = 441)
No. of cells observed
250
200
150
100
50
0
5
64
109
193
35
17
6
10
2
1 Focus
2 Foci
3 Foci
4 Foci
5 Foci
6 Foci
7 Foci
8 Foci
9 Foci
Cells observed with varying numbers of foci in exponential phase (OD = ~0.25)

B

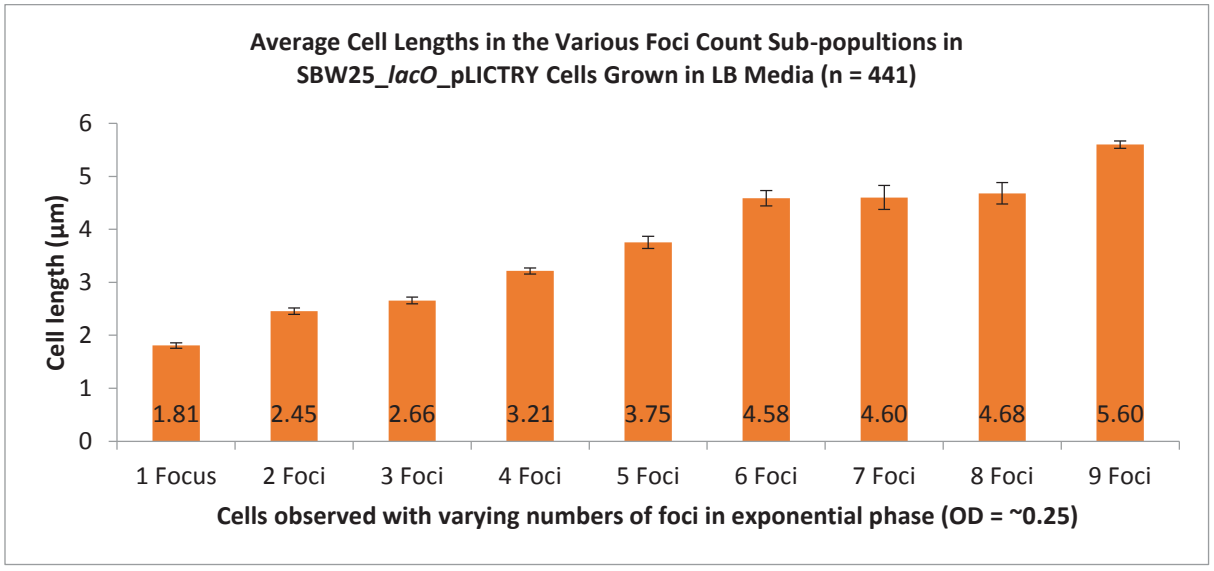
Average Cell Lengths in the Various Foci Count Sub-popultions in SBW25_lacO_pLICTRY Cells Grown in LB Media (n = 441)
Cell length (µm)
6
5
4
3
2
1
0
1.81
2.45
2.66
3.21
3.75
4.58
4.60
4.68
5.60
1 Focus
2 Foci
3 Foci
4 Foci
5 Foci
6 Foci
7 Foci
8 Foci
9 Foci
Cells observed with varying numbers of foci in exponential phase (OD = ~0.25)

C

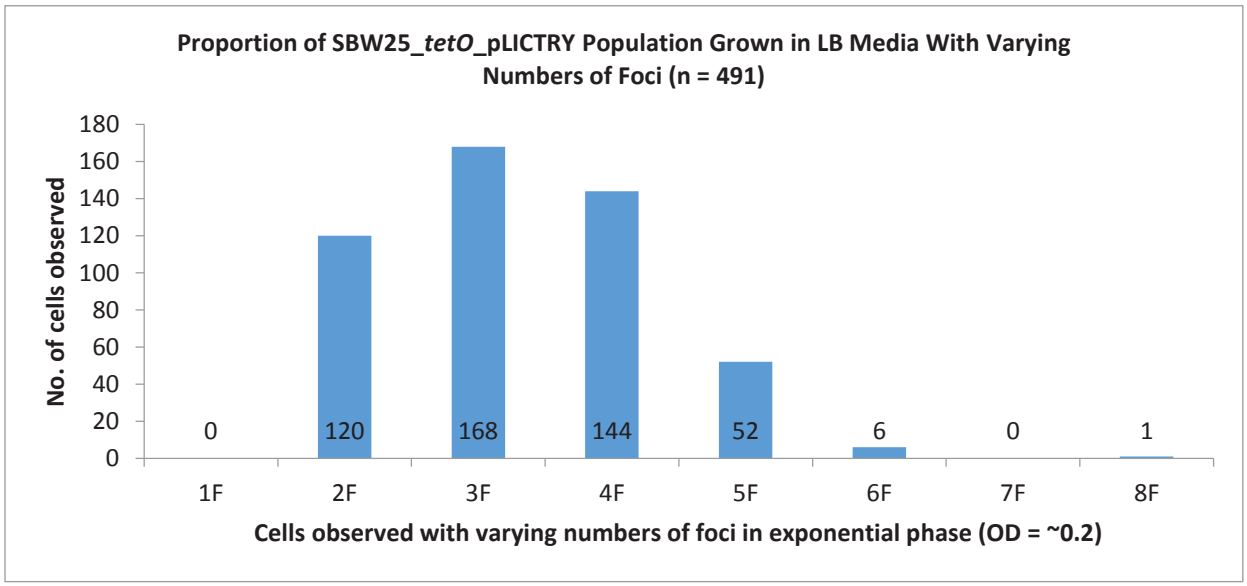
Proportion of SBW25_tetO_pLICTRY Population Grown in LB Media With Varying Numbers of Foci (n = 491)
No. of cells observed
180
160
140
120
100
80
60
40
20
0
0
120
168
144
52
6
0
1
1F
2F
3F
4F
5F
6F
7F
8F
Cells observed with varying numbers of foci in exponential phase (OD = ~0.2)

D

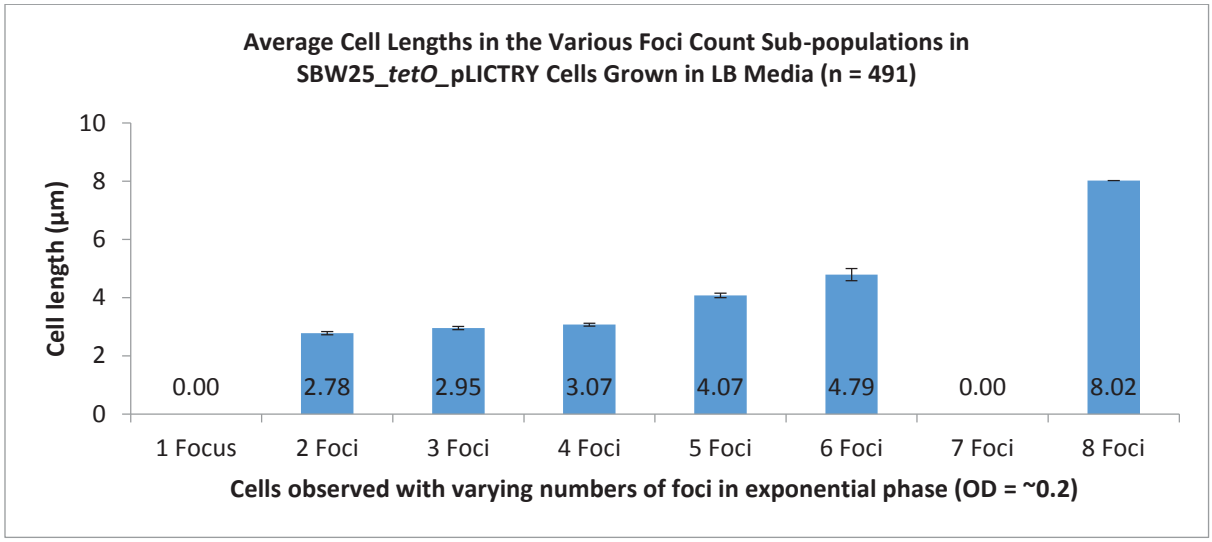
Average Cell Lengths in the Various Foci Count Sub-populations in SBW25_tetO_pLICTRY Cells Grown in LB Media (n = 491)
Cell length (µm)
10
8
6
4
2
0
0.00
2.78
2.95
3.07
4.07
4.79
0.00
8.02
1 Focus
2 Foci
3 Foci
4 Foci
5 Foci
6 Foci
7 Foci
8 Foci
Cells observed with varying numbers of foci in exponential phase (OD = ~0.2)

E

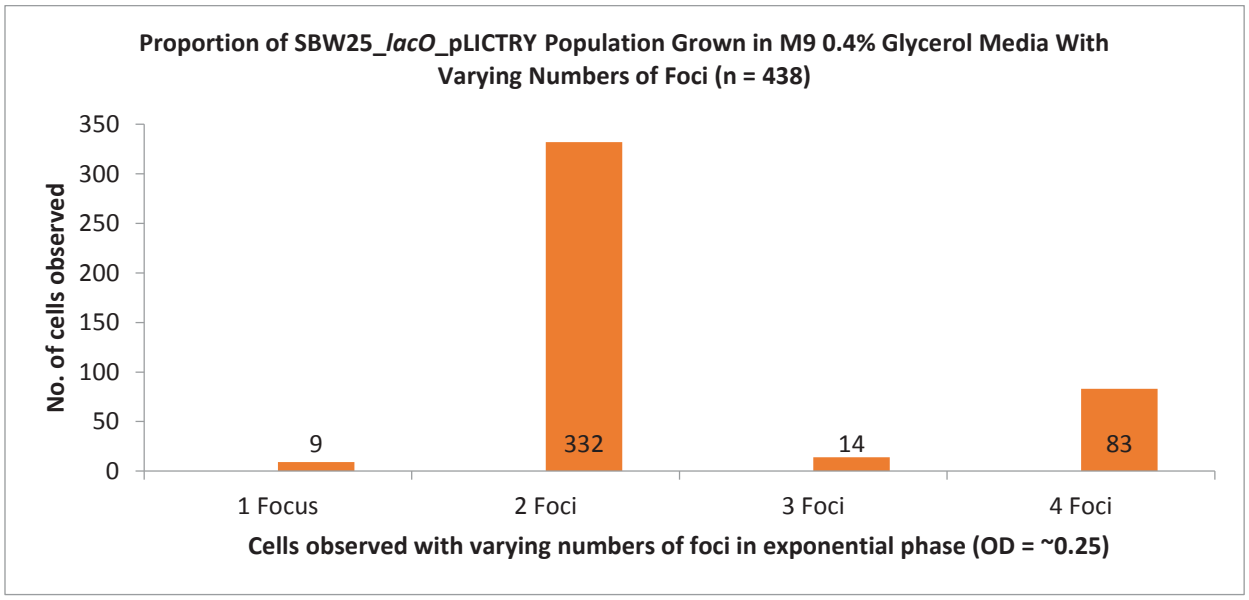
Proportion of SBW25_lacO_pLICTRY Population Grown in M9 0.4% Glycerol Media With Varying Numbers of Foci (n = 438)
No. of cells observed
350
300
250
200
150
100
50
0
9
332
14
83
1 Focus
2 Foci
3 Foci
4 Foci
Cells observed with varying numbers of foci in exponential phase (OD = ~0.25)

F

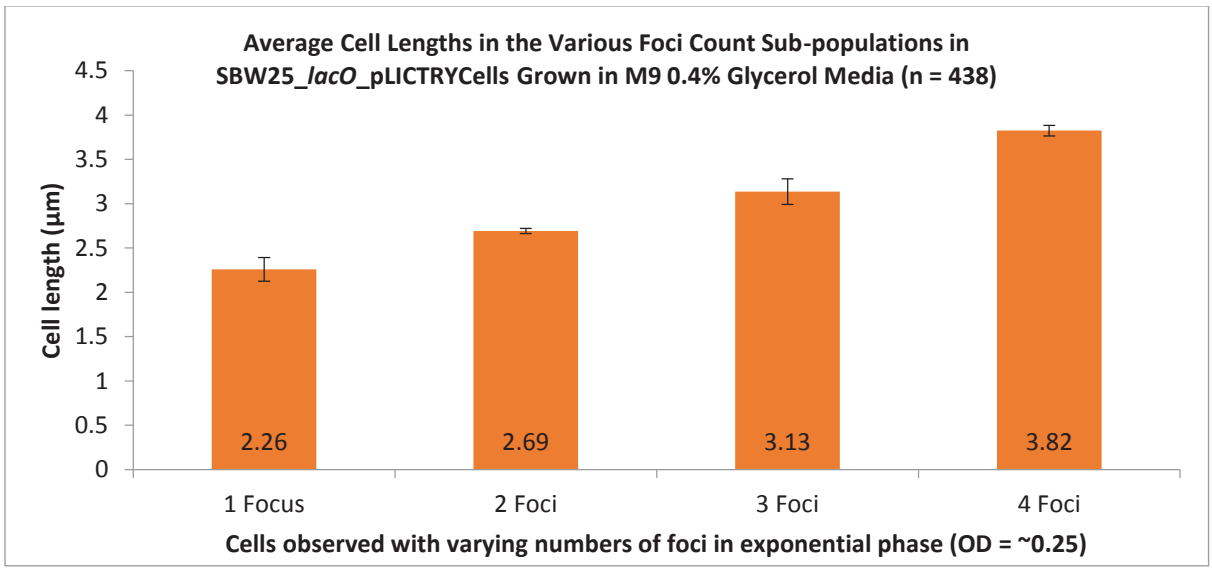
Average Cell Lengths in the Various Foci Count Sub-populations in SBW25_lacO_pLICTRYCells Grown in M9 0.4% Glycerol Media (n = 438)
Cell length (µm)
4.5
4
3.5
3
2.5
2
1.5
1
0.5
0
2.26
2.69
3.13
3.82
1 Focus
2 Foci
3 Foci
4 Foci
Cells observed with varying numbers of foci in exponential phase (OD = ~0.25)

G

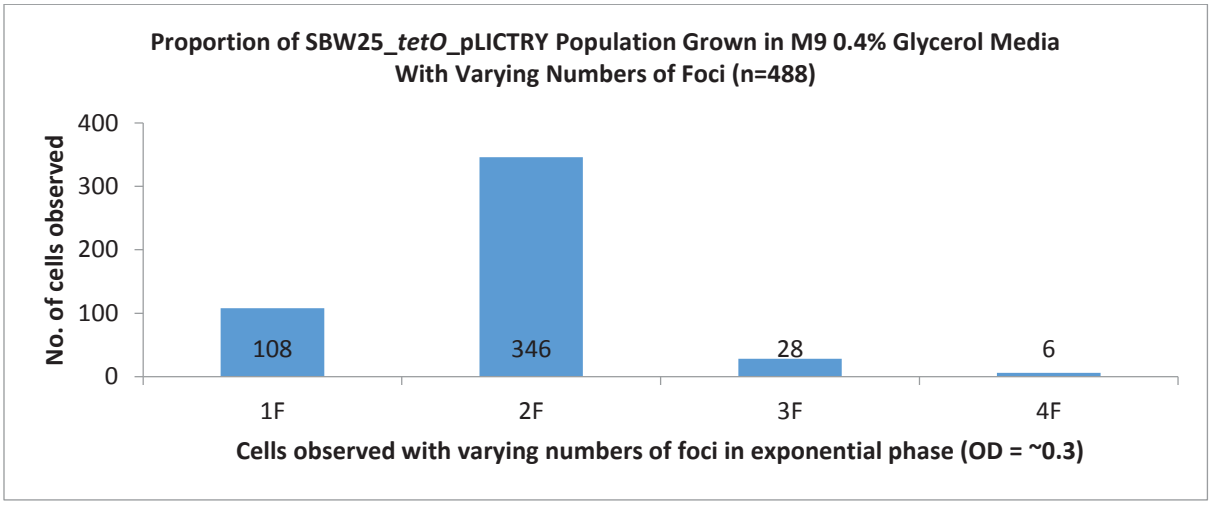

H

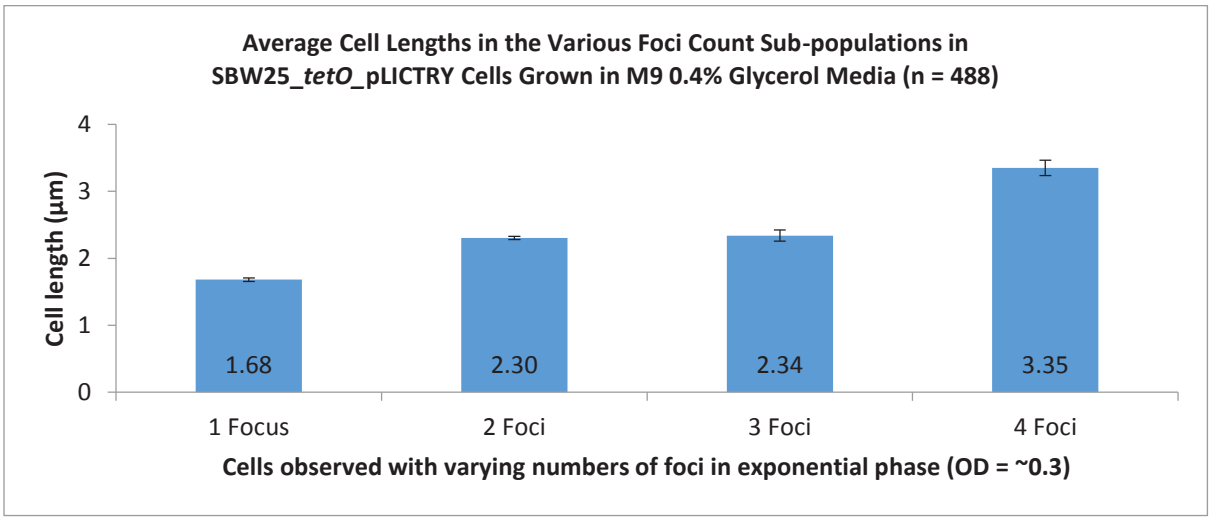

Figure 24: Charts showing results of fluorescent microscopy analysis of both SBW25_*lacO*_pLICTRY and SBW25_*tetO*_pLICTRY strains grown in LB and M9 0.4% Glycerol media. The error bars denote standard error. (A) Shows the proportions of cells containing varying numbers of foci, in the SBW25_*lacO*_pLICTRY population grown in LB media. (B). Shows the average cell lengths within the sub-populations presented in A. (C). Shows the proportions of cells containing varying numbers of foci, in the SBW25_*tetO*_pLICTRY population grown in LB media. (D). Shows the average cell lengths within the sub-populations presented in C. (E). Shows the proportions of cells containing varying numbers of foci, in the SBW25_*lacO*_pLICTRY population grown in M9 0.4% Glycerol media. (F). Shows the average cell lengths within the sub-populations presented in E. (G). Shows the proportions of cells containing varying numbers of foci, in the SBW25_*lacO*_pLICTRY population grown in M9 0.4% Glycerol media. (H). Shows the average cell lengths within the sub-populations presented in G.

This data immediately highlights that the proportions of populations consisting of varying numbers of foci are different between the SBW25_*lacO*_pLICTRY strain and the SBW25_*tetO*_pLICTRY strain. While in LB media, the largest sub-population in the SBW25_*lacO*_pLICTRY strain appears to be that of the 4 foci cells; in the SBW25_*tetO*_pLICTRY strain, it is the 3 foci cells. Moreover, in M9 0.4% Glycerol media, while the second largest sub-population in the SBW25_*lacO*_pLICTRY strain appears to be the 4 foci cells; in the SBW25_*tetO*_pLICTRY strain it is the 1 focus cells.

The majority of this inconsistency between the two strains may be explained by the limits of the fluorescent labelling technique employed. During image analysis, it is possible to come across cells where 2 foci are overlapping each other. On such occasions, it is difficult to determine whether the 'point of light' should be counted as a single focus or 2 foci, and the human has to make an educated guess. Because of this, it is possible that a significant portion of the 3 foci cells from the SBW25_*tetO*_pLICTRY population growing in LB media, are in actuality 4 foci cells. The section of cells highlighted in a red circle in Figure 25 C shows such an example where the foci displayed are counted as '1st focus', but in reality could be the 2nd focus, which would make the cells containing them 4 focus cells instead of 3 focus cells. This explanation can also be extended to the inconsistency seen in M9 0.4% Glycerol media, where the SBW25_*tetO*_pLICTRY strain appears to have very few 4 foci cells in comparison to the SBW25_*lacO*_pLICTRY strain. Since differentiating between 2 foci cells and 4 foci cells in M9 0.4% Glycerol media during image analysis is often dependent on whether the septum in between the two pairs of foci is completely closed or not, a cell with 4 foci can often be considered to instead be two cells with 2 foci each. In cases where it is difficult to determine if the septum is completely closed or not, again the human has to make an educated guess. Additionally, LacI and TetR proteins are different from each other, and as such, may dimerize differently.

The findings show that while SBW25_*tetO*_pLICTRY strain produces single focus cells under nutrient-poor conditions, the SBW25_*lacO*_pLICTRY strain produces 2 foci and 4 foci cells. These results from the SBW25_*tetO*_pLICTRY strain are consistent with the previous study conducted by Vallet-Gely and Boccard (2013) [76], who found *P. aeruginosa*, a closely related organism, to also only be producing single focus and 2 foci cells under nutrient-poor conditions. However, the results from the SBW25_*lacO*_pLICTRY strain oppose these findings and instead suggest multi-fork replication to be occurring in *P. fluorescens* SBW25 even under nutrient-poor conditions. This inconsistency is evaluated further in the Discussion section.

In order to see if the SBW25_*lacO*_pLICTRY cells would produce single focus cells at stationary phase, the cells were grown in M9 0.4% glycerol media until an OD_{600} of 1.5 was reached and subsequently analyzed again under the fluorescent microscope. Once again hardly any single focus cells were observed and almost all the cells seemed to display either 2 or 4 foci (Figure 25).

SBW25_*lacO*_pLICTRY Cells Grown in M9 0.4% Glycerol Media (OD_{600} = ~ 1.5)

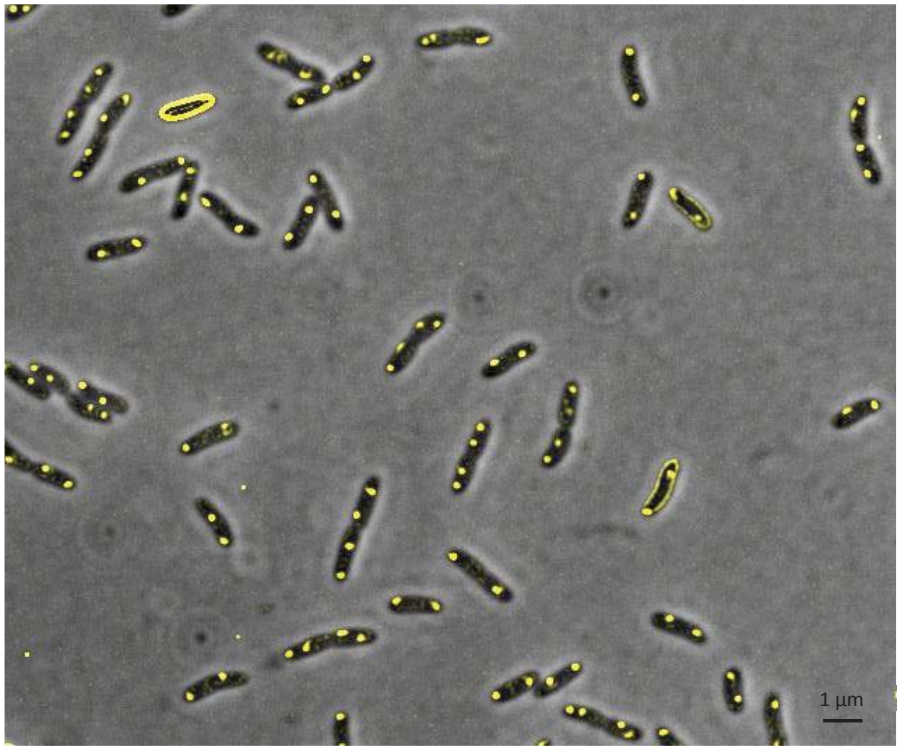

Figure 25: Image showing SBW25_*lacO*_pLICTRY cells when viewed under the fluorescent microscope after growth in nutrient-poor media until stationary phase was reached (OD = ~ 1.5). Cells displaying a yellow outline are likely a product of the interaction between Hatrick Filter and cells overexpressing the fluorescent proteins.

From the data in Figure 24, it was calculated that the majority of SBW25_*lacO*_pLICTRY cells in both LB and M9 0.4% Glycerol media are at an average of ~2.91 µm in length (in LB media, the 'majority' of cells were considered to be the cells in sub-populations of 2, 3, 4 and 5 foci; whereas in M9 0.4% Glycerol media, the majority of cells were considered to be the cells in sub-populations of 2 and 4 foci). However, the cells in nutrient-rich media are typically performing either 1, 2 or 3 cycles of DNA replication simultaneously (2, 3 or 4 visible *oriC* sites), whereas the cells in nutrient-poor media are typically performing either 1 or 3 cycles of DNA replication simultaneously (2 or 4 visible *oriC* sites). Unlike the SBW25_*lacO*_pLICTRY cells however, the average cell lengths of the majority in the SBW25_*tetO*_pLICTRY strain are different between the population growing in LB (~3.06

μm) in comparison with the population growing in M9 0.4% Glycerol media (~2.15 μm) (in LB media, the majority of cells were considered to be cells in the sub-populations of 2, 3, 4 and 5 foci; whereas in M9 0.4% Glycerol media, the majority of cells were considered to be in sub-populations of 1 and 2 foci). The SBW25_*tetO*_pLICTRY cells growing in nutrient-rich media appear to typically be performing either 1, 2, 3 or 4 cycles of DNA replication simultaneously (2, 3, 4 or 5 visible *oriC* sites), whereas the cells in nutrient-poor media are typically performing either no DNA replication or a single cycle of DNA replication (1 or 2 visible *oriC* sites).

It is also interesting that there are cells present which are performing 2, 4, 6 and 8 cycles of DNA replication simultaneously, as that implies asynchrony in DNA replication initiation occurring. The proportion of the populations carrying out asynchronous DNA replication initiation are presented in Table 5 for both strains.

Table 5: Table showing the proportions of SBW25_*lacO*_pLICTRY and SBW25_*tetO*_pLICTRY populations that undergo asynchronous DNA replication initiation when grown in LB or M9 0.4% Glycerol media.

Strain	**Asynchrony in LB Media**	**Asynchrony in M9 0.4% Glycerol Media**
SBW25_*lacO*_pLICTRY	34.46 %	3.19 %
SBW25_*tetO*_pLICTRY	44.8 %	5.74 %

Although these results address DNA replication initiation and the presence of multi-fork replication in *P. fluorescens* SBW25, chromosome segregation was still not confronted. Therefore, in order to learn more about the segregation process, cell length and the foci location values within those lengths were measured from individual cells in exponential

growth, using the earlier images accumulated during the fluorescent microscopy analysis (Figure 24). Using the resulting data, a series of plots were produced (Figures 26, 27 and 28), which are analyzed in the discussion section.

A

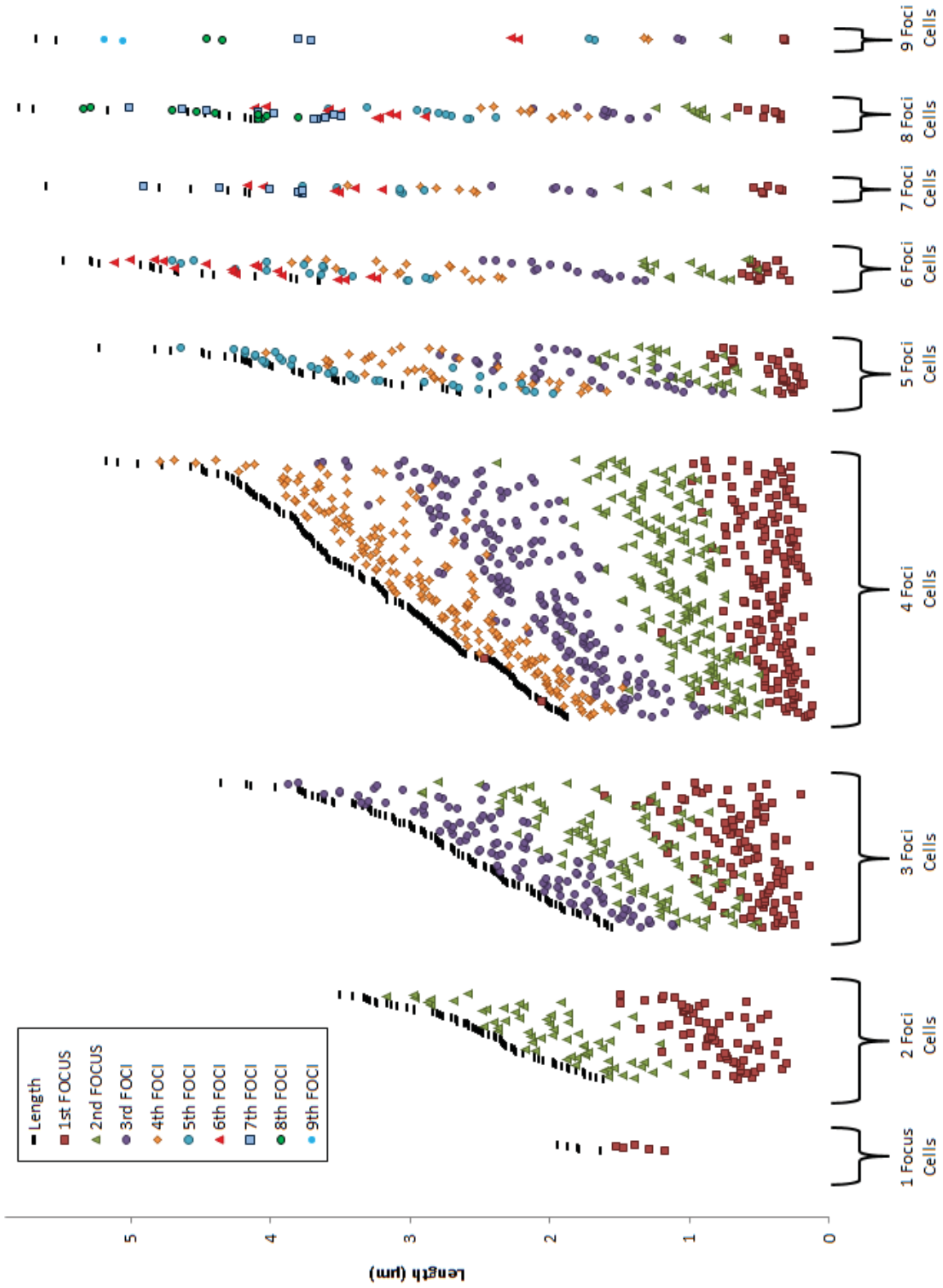
Cell Age (µm) Vs. Foci Location of SBW25_lacO_pLICTRY Cells Grown in LB [n = 441]
Length
1st FOCUS
2nd FOCUS
3rd FOCI
4th FOCI
5th FOCI
6th FOCI
7th FOCI
8th FOCI
9th FOCI
Length (µm)
0
1
2
3
4
5
1 Focus Cells
2 Foci Cells
3 Foci Cells
4 Foci Cells
5 Foci Cells
6 Foci Cells
7 Foci Cells
8 Foci Cells
9 Foci Cells

B

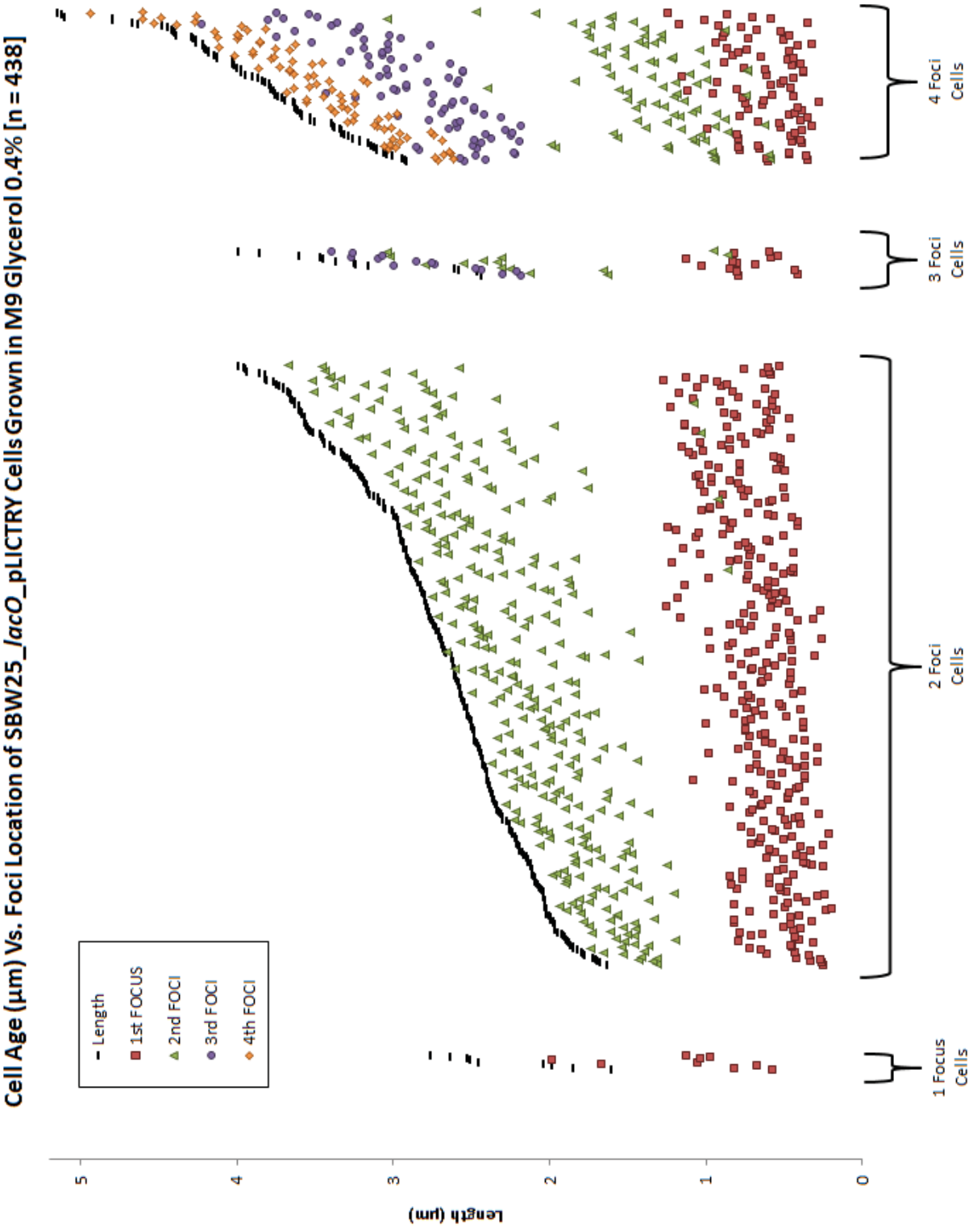
Cell Age (µm) Vs. Foci Location of SBW25_lacO_pLICTRY Cells Grown in M9 Glycerol 0.4% [n = 438]
Length
1st FOCUS
2nd FOCI
3rd FOCI
4th FOCI
Length (µm)
0
1
2
3
4
5
1 Focus Cells
2 Foci Cells
3 Foci Cells
4 Foci Cells

C

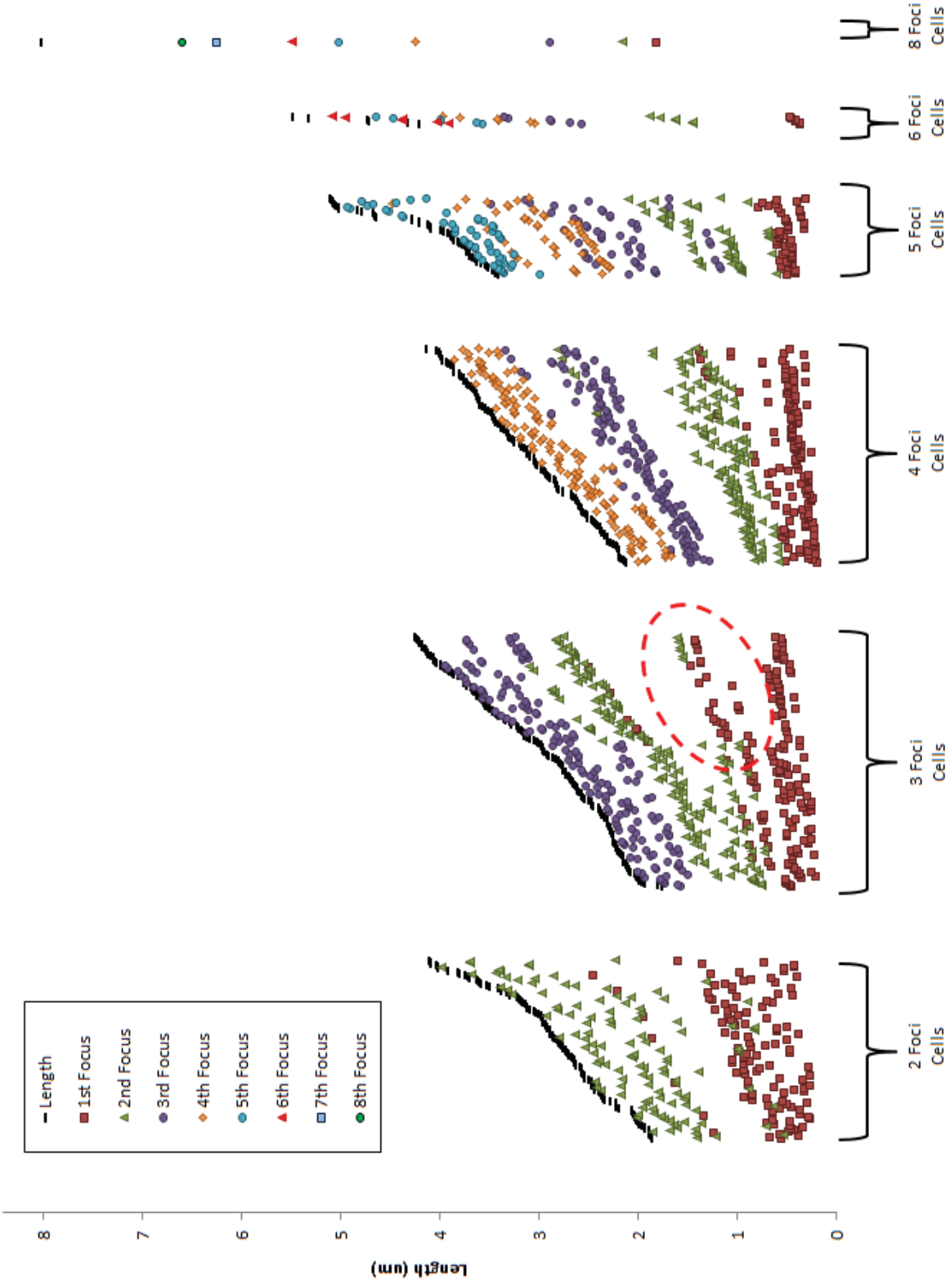
Cell Age (um) Vs. Foci Location of SBW25_tetO_pLICTRY Cells Grown in LB (n = 491)
Length (um)
0
1
2
3
4
5
6
7
8
Length
1st Focus
2nd Focus
3rd Focus
4th Focus
5th Focus
6th Focus
7th Focus
8th Focus
2 Foci Cells
3 Foci Cells
4 Foci Cells
5 Foci Cells
6 Foci Cells
8 Foci Cells

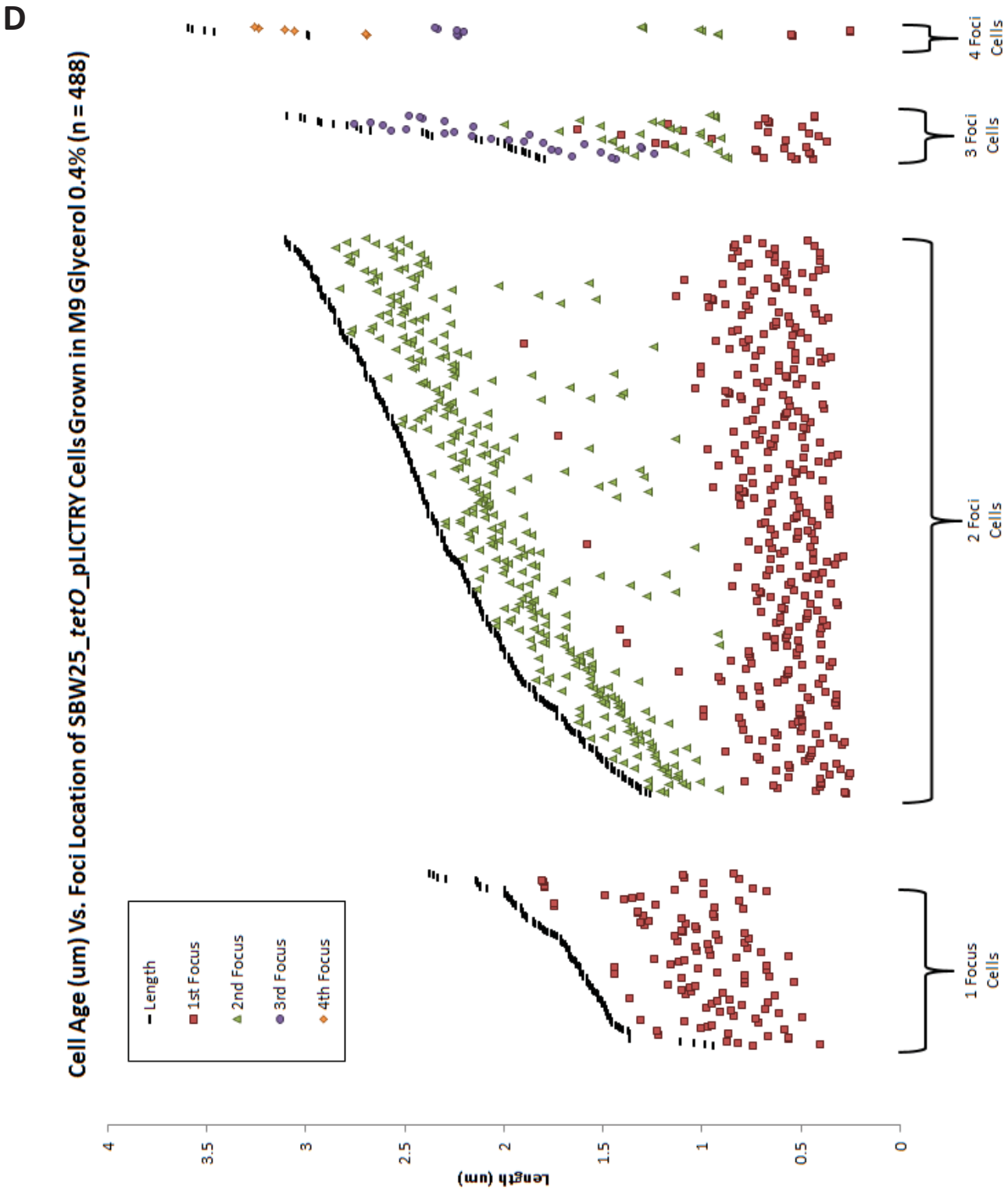

Figure 26: Plots showing lengths and foci locations within those lengths, of individual cells in exponential growth, from populations of SBW25_*lacO*_pLICTRY and SBW25_*tetO*_pLICTRY strains grown in LB & M9 0.4% Glycerol media. A. Shows data from SBW25_*lacO*_pLICTRY cells when grown in LB. B. Shows data from SBW25_*lacO*_pLICTRY cells when grown in M9 0.4% Glycerol. C. Shows data from SBW25_*tetO*_pLICTRY cells when grown in LB. The dotted red circle represents a group of foci which may have been counted as 'first focus', although they could potentially be 'second focus' instead. If this is true, then the cells containing those foci will be 4 foci cells instead of 3 foci cells as categorized. **D. Shows data from SBW25_*tetO*_pLICTRY cells when grown in M9 0.4% Glycerol.** (Note: It is worth noting that when measuring the cell pole to foci distance, the focus that was more distant from the pole was always considered to be the first focus).

A

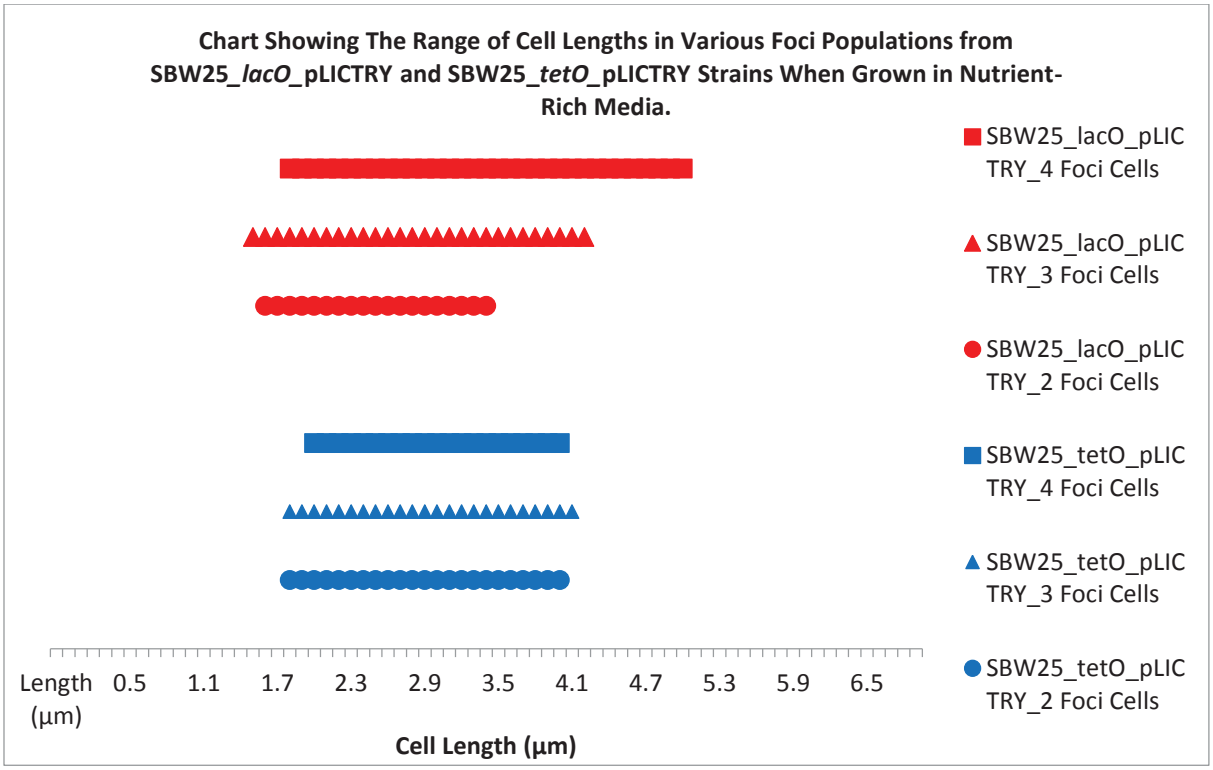

B

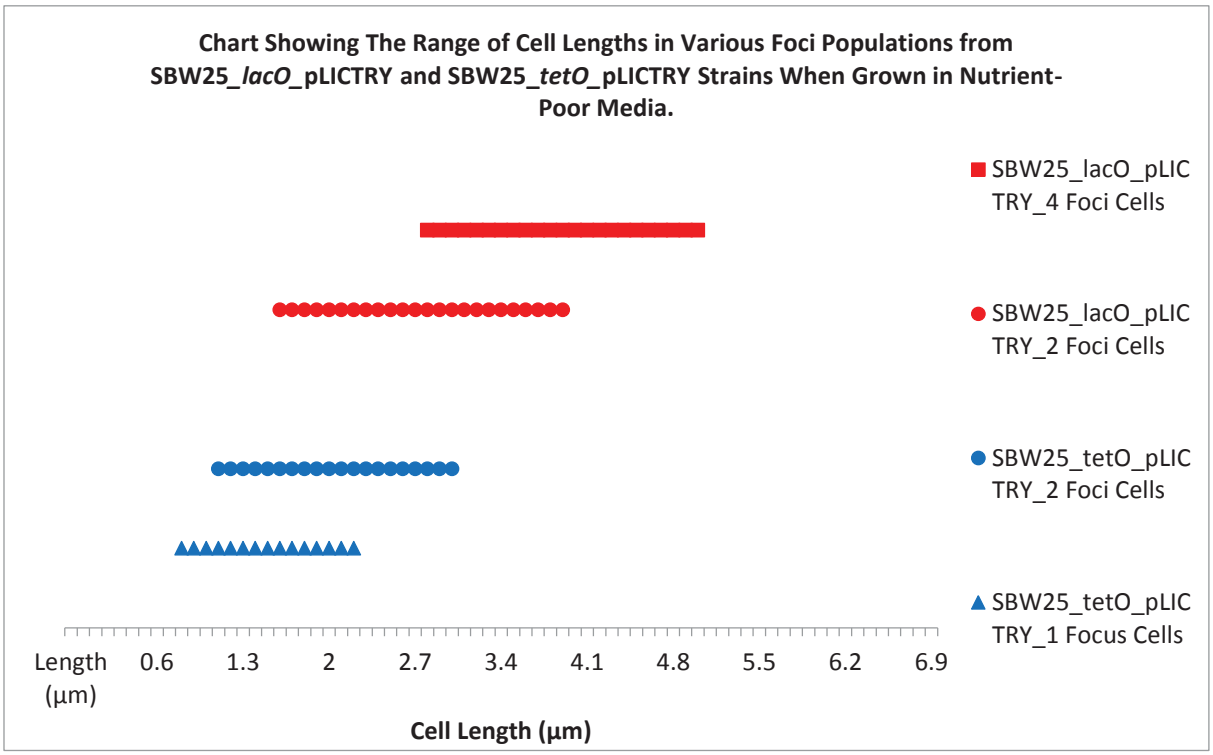

Figure 27: Charts showing the overlap between cell length ranges of cell populations from SBW25_*lacO*_pLICTRY and SBW25_*tetO*_pLICTRY strains consisting varying numbers of foci, when grown in nutrient-rich (A) and nutrient-poor (B) conditions.

A

Cell Age	Populations of SBW25_*lacO*_pLICTRY Cells With Various Numbers of Foci When Grown in LB Media.				
0.0 - 1.5 µm	1st Focus (n=0)	2nd Focus (n=0)	3rd Focus (n=0)	4th Focus (n=0)	5th Focus (n=0)
1.5 - 3.0 µm	1st Focus (n=5)	2nd Focus (n=53)	3rd Focus (n=77)	4th Focus (n=81)	5th Focus (n=6)
3.0 - 4.5 µm	1st Focus (n=0)	2nd Focus (n=11)	3rd Focus (n=32)	4th Focus (n=106)	5th Focus (n=26)
	6th Focus (n=7)	7th Focus (n=3)	8th Focus (n=6)		
4.5 - 6.0 µm	1st Focus (n=0)	2nd Focus (n=0)	3rd Focus (n=0)	4th Focus (n=6)	5th Focus (n=3)
	6th Focus (n=10)	7th Focus (n=3)	8th Focus (n=4)	9th Focus (n=2)	

B

Cell Age	Populations of SBW25_*lacO*_pLICTRY Cells With Various Numbers of Foci When Grown in M9 0.4% Glycerol Media			
0.0 - 1.5 µm	1st Focus (n=0)	2nd Focus (n=0)	3rd Focus (n=0)	4th Focus (n=0)
1.5 - 3.0 µm	1st Focus (n=9)	2nd Focus (n=251)	3rd Focus (n=5)	4th Focus (n=3)
3.0 - 4.5 µm	1st Focus (n=0)	2nd Focus (n=81)	3rd Focus (n=9)	4th Focus (n=73)
4.5 - 6.0 µm	1st Focus (n=0)	2nd Focus (n=0)	3rd Focus (n=0)	4th Focus (n=7)

C

Cell Age	Populations of SBW25_*tetO*_pLICTRY Cells With Various Numbers of Foci When Grown in LB Media.				
0.0 - 1.5 µm	1st Focus (n=0)	2nd Focus (n=0)	3rd Focus (n=0)	4th Focus (n=0)	5th Focus (n=0)
1.5 - 3.0 µm	1st Focus (n=0)	2nd Focus (n=84) 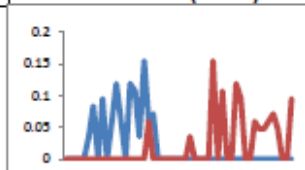	3rd Focus (n=96) 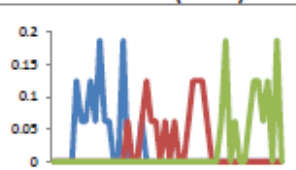	4th Focus (n=65) 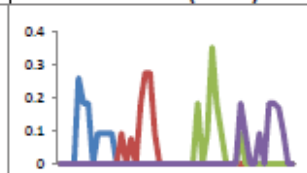	5th Focus (n=0)
3.0 - 4.5 µm	1st Focus (n=0) 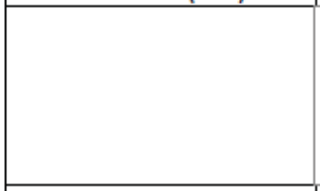	2nd Focus (n=36) 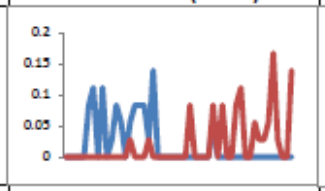	3rd Focus (n=72) 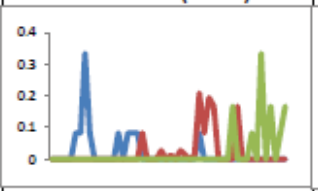	4th Focus (n=79) 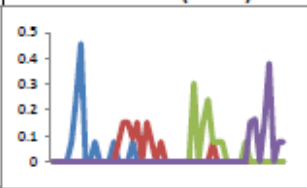	5th Focus (n=39) 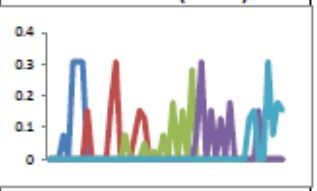
	6th Focus (n=2) 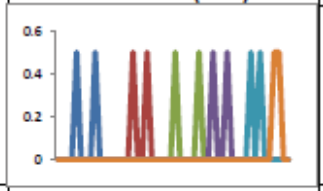				
4.5 - 6.0 µm	1st Focus (n=0)	2nd Focus (n=0)	3rd Focus (n=0)	4th Focus (n=0)	5th Focus (n=13) 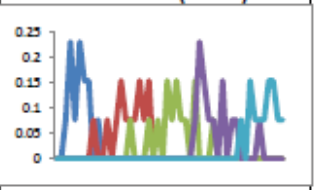
	6th Focus (n=4) 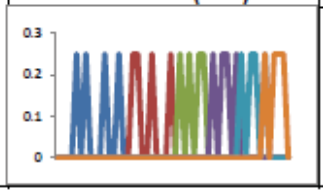				

1st Focus
2nd Focus
3rd Focus
4th Focus
5th Focus
6th Focus
7th Focus
8th Focus
9th Focus

6.0+ µm	1st Focus (n=0)	2nd Focus (n=0)	3rd Focus (n=0)	4th Focus (n=0)	5th Focus (n=0)
	6th Focus (n=0)	7th Focus (n=0)	8th Focus (n=1)		
			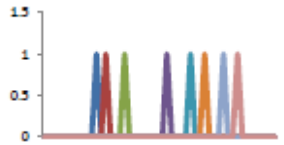		

D

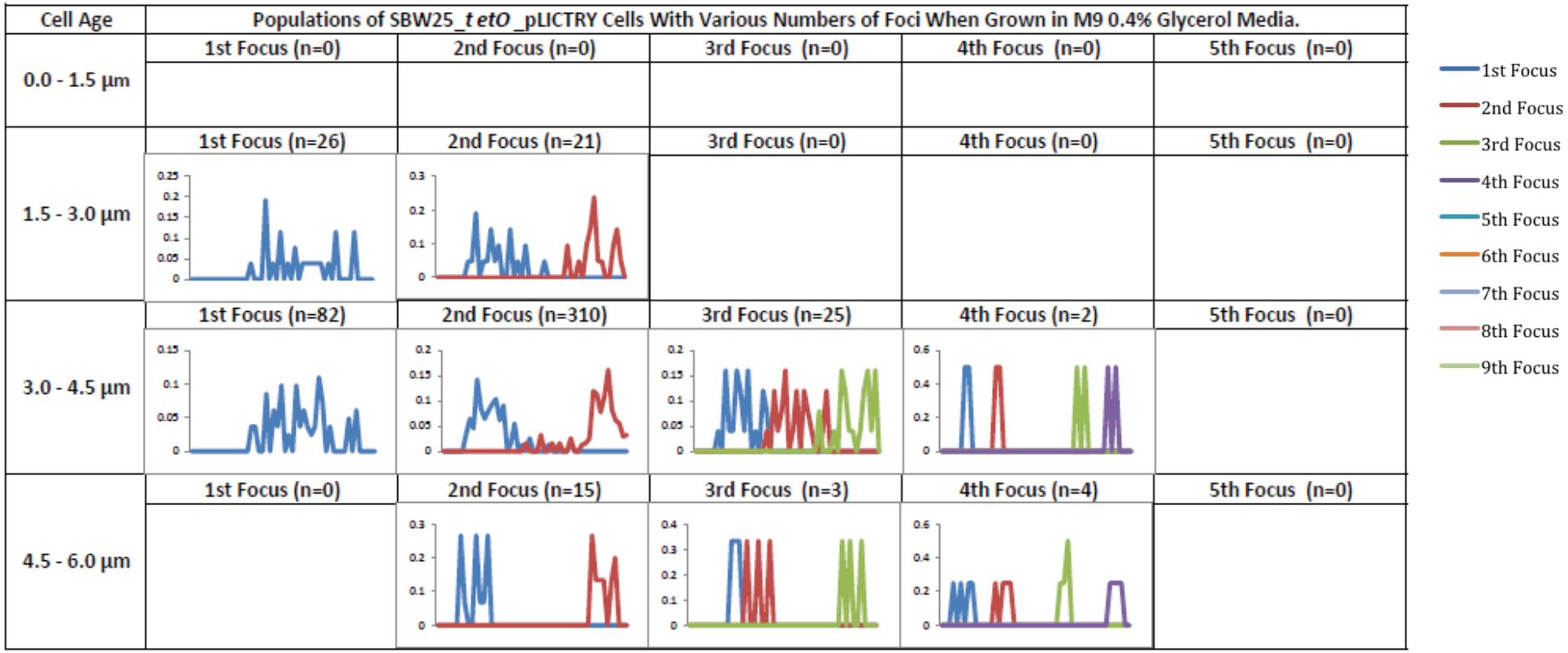

Figure 28: The above plots present the same data as from Figure 26, however instead of showing foci localizations inside individual cells, here we can see individual foci distributions of the whole population of SBW25_*lacO*_pLICTRY and SBW25_*tetO*_pLICTRY strains when grown to exponential phase in LB and M9 0.4% Glycerol media. The populations are divided into groups based on cell ages (*i.e.* cell lengths) and number of foci within the cells. (A). Shows data from the population of SBW25_*lacO*_pLICTRY cells when grown in LB media. (B). Shows data from the population of SBW25_*lacO*_pLICTRY cells when grown in M9 0.4% Glycerol media. (C). Shows data from the population of SBW25_*tetO*_pLICTRY cells when grown in LB media. (D). Shows data from the population of SBW25_*tetO*_pLICTRY cells when grown in M9 0.4% Glycerol media.

These plots show a clear distinction between the DNA replication and segregation dynamics of *P. fluorescens* SBW25, when cells are grown in nutrient-rich media as opposed to nutrient-poor media. While the scatter plots in Figure 26 show the distribution of foci inside individual cells, the charts shown in Figure 27 display the overlap in the overall range of cell lengths between the cell sub-populations consisting varying numbers of foci. The data displayed in Figure 26 is reorganized and portrayed differently in Figure 28, wherein instead of showing the foci distribution pattern inside of individual cells, foci distribution patterns of all the sub-populations consisting of varying numbers of foci are grouped by cell ages (i.e. cell lengths) and presented together. These plots are analyzed in the discussion section.

4.3 Discussion

Unlike the ParB-*parS* system, the LacI-*lacO* and TetR-*tetO* systems from Lau *et al.* (2003) [79] have worked very well with my model organism, *P. fluorescens* SBW25. Fluorescence microscopy has shown us that *P. fluorescens* SBW25 indeed performs multi-fork replication and can do so at much higher levels in a nutrient-rich environment than in a nutrient-poor environment. The foci are much bigger and brighter when the cells are grown in nutrient-poor media however, which may be a result of accumulation of the fluorescent fusion proteins as the growth rate of the cells is decreased in nutrient-poor environments.

It is unclear why the SBW25_*LacO*_pLICTRY and SBW25_*TetO*_pLICTRY restrict their growth rate in presence of antibiotic selection pressures, although it is unlikely that insertion of the genetic elements is the cause for this. This is because the elements appear to be stably maintained in the strains even in the absence of antibiotics, yet when antibiotics are removed from the environment, the growth rate impairment is cured. It is possible that the metabolic production costs for antibiotic resistance proteins is the source of this decrease in growth.

Even though both SBW25_*lacO*_pLICTRY and SBW25_*tetO*_pLICTRY strains were constructed using the same wild type *P. fluorescens* SBW25 strain and same methodology, there are some key differences observed between the two strains. Firstly, the average cell length of the SBW25_*tetO*_pLICTRY strain when grown in M9 0.4% glycerol media (~2.15 μm) is significantly shorter than the average cell length of the SBW25_*lacO*_pLICTRY strain (~2.91 μm) when grown under the same conditions. However in LB media, the cell lengths are quite similar. Furthermore, the average cell length of SBW25_*lacO*_pLICTRY cells appear to be unaffected by the nutrient availability in the medium, as in both nutrient-rich and nutrient-poor media, the cells maintained an overall average length of ~2.91 microns.

Secondly, the image analysis results (Figure 24) reveal that there is a lack of presence of single focus cells in the SBW25_*lacO*_pLICTRY strain, which, even when grown to stationary phase under nutrient-poor conditions, not only failed to display single focus cells but also presented many cells with 4 foci (Figure 25). This suggests that these cells are carrying out multi-fork DNA replication incessantly, even during stationary phase. This is not seen in SBW25_*tetO*_pLICTRY cells however, where single focus cells are abundant in stationary phase, and even form a significant proportion of the population during exponential phase in both LB and M9 0.4% Glycerol media.

Despite the key differences highlighted above, there are quite a few similarities between the two strains as well. Firstly, both strains appear to perform a higher number of DNA replication cycles simultaneously when growing in nutrient-rich media, in comparison with growth in nutrient-poor media (Figure 24, 26 and 28). In both cases, there is an apparent increase in the amount of asynchronous DNA replication initiation events when the cells are growing in nutrient-rich media in comparison to nutrient-poor media (Table 5). Secondly, as

seen from Figure 26, when multiple foci are present in cells grown in either media, the majority of foci appear to be distant from each other, implying the occurrence of rapid chromosome segregation. This is evident in both the mutant strains. Furthermore, as can be seen from the individual foci location distributions of the bacterial populations in Figure 28, it seems that generally the foci sites localize at certain 'hotspots' as the replication process continues and increases the number of foci within the cell. The locations of these hotspots are described below:

- In single focus cells, the foci generally seem to localize near the mid-cell region.
- In 2 foci cells, the generally foci seem to appear near opposite cell poles.
- In 3 foci cells, usually 2 foci are found at opposite cell poles, and a single focus is observed near mid-cell region.
- In 4 foci cells, two pairs of foci seem to appear on opposite cell halves.
- In 5 foci cells, the cells appear to distribute two pairs of foci on opposite cell halves and a single focus near mid-cell region.
- In cells with 6 foci or more, it is difficult to determine such a trend as the population sizes are too small.

The data from Figure 26A and C suggests that in both the mutant strains, SBW25_*tetO*_pLICTRY and SBW25_*lacO*_pLICTRY, when cells are grown in nutrient-rich media, the cells are typically born with an ongoing round of replication (2 foci present). These cells appear to be able to reach a maximum of ~ 8 – 9 foci and the average number of foci in both strains is ~ 3 – 4. Moreover, Figure 27 shows that the cell length and foci number appear to be decoupled in both strains, as we see a significant amount of overlap in cell length values between populations of cells with different numbers of foci. This may imply

that DNA replication initiation is not strictly controlled in this media, and essentially the cells are able to initiate new rounds of DNA replication at any length.

In M9 0.4% glycerol, there is an inconsistency between the two mutant strains (Figure 26B and D). While the SBW25_*lacO*_pLICTRY strain indicates that newborn cells are born with ongoing rounds of replication (2 foci present), even in nutrient-poor media; the SBW25_*tetO*_pLICTRY strain proposes that multi-fork replication does not occur in nutrient-poor media and usually the cells only maintain a single round of DNA replication for the duration of their cell cycle (*i.e.* sequential DNA replication). These results from the SBW25_*tetO*_pLICTRY strain are more in accordance with the results from a previous study conducted in 2013 by Vallet-Gelly and Boccard in *P. aeruginosa* (a closely related organism to *P fluorescens*). Vallet-Gelly and Boccard also found only sequential replication to be occurring in *P. aeruginosa* cells, when they were grown in nutrient-poor media [76]. Therefore, while the SBW25_*lacO*_pLICTRY cells are generally found to have either 2 or 4 foci in M9 0.4% glycerol media, the SBW25_*tetO*_pLICTRY cells are usually found to have only 1 or 2 foci (Figure 24E, G and 26B, D).

The data from Figure 27 also indicates that unlike the seemingly loosely controlled DNA replication initiation in nutrient-rich media, when either mutant strain is grown in nutrient-poor media, the cell length and foci numbers appear to be more closely correlated as there is significantly less overlap in cell length values between populations of cells with different numbers of foci. This may imply that DNA replication initiation is more controlled in this media, and that cells are only able to initiate new DNA replication cycles after they reach a certain length. This may also be true for cell division, as it appears that when SBW25_*lacO*_pLICTRY cells reach a length of ~ 4μm, and SBW25_*tetO*_pLICTRY cells reach a length of ~ 3 μm, the cells cannot continue growth any longer and divide into

newborn cells of lengths ~ 2 μm and ~ 1.5 μm respectively. This difference in lengths between the two strains is likely a result of the differing replication mechanisms being utilized.

Considering all of these aspects, three generalized cell cycle models for exponential cell growth in *P. fluorescens* SBW25 have been hypothesized – one for nutrient-rich media, where both the mutant strains appear to mostly agree with each other, and two for nutrient-poor media, where the mutant strains disagree with each other. These models are described in the concluding discussion (Chapter 5).

Chapter 5

Concluding Discussion

5.1 Objective of the Current Study

The primary aim of this study was to investigate the cell cycle of *P. fluorescens* SBW25, specifically the DNA replication process, in both nutrient-rich and nutrient-poor conditions. In order to do this, two strains of *P. fluorescens* SBW25 were constructed, in which the *oriC* regions of the genome were fluorescently labelled (one strain was incorporated with the LacI-*lacO* system, and the other the TetR-*tetO* system). Following this, rigorous fluorescent microscope examinations were carried out for each strain as they were growing in exponential growth in both nutrient-rich and nutrient-poor media; and individual cells from the resulting images were analyzed.

From the data collected, three speculative models were developed to explain how the DNA replication and segregation process occurs in these cells during fast growth in nutrient-rich conditions (1 model) and slow growth in nutrient-poor conditions (2 models). Since the results from our two constructed strains did not agree with each other completely when grown in nutrient-poor conditions, two potential models are hypothesized.

Overall, in a broader context, the results of this investigation provide insight into a new bacterial species that has not been studied yet regarding its cell cycle. The study results indicate that *P. fluorescens* SBW25 has the ability to carry out multi-fork replication, a trait that very few other species studied have displayed so far [55-57].

5.2 Summary of Results

All of my key results discussed in Chapter 4 are summarized and adapted into the three main models presented below. One model represents findings from both SBW25_*lacO*_pLICTRY and SBW25_*tetO*_pLICTRY strains to illustrate the *P. fluorescens* SBW25 cell cycle in nutrient-rich media; and the other two models separately represent the findings of SBW25_*lacO*_pLICTRY and SBW25_*tetO*_pLICTRY strains to illustrate *P. fluorescens* SBW25 cell cycle in nutrient-poor media.

5.2.1 Model for *P. fluorescens* SBW25 Growth in Nutrient-rich Media (from findings of both SBW25_*lacO*_pLICTRY and SBW25_*tetO*_pLICTRY strains)

In nutrient-rich media, during exponential growth, the cells typically appear to be born at an overall length of ~ 2 μm, with an already ongoing round of DNA replication occurring. At this stage, the two *oriC* sites present inside the cells are already somewhat distant from each other, localizing near the opposite cell poles. As these cells continue to grow and lengthen, they initiate new replication cycles. The newly generated *oriC* sites are swiftly separated by an active chromosome segregation mechanism (such as the ParABS system), which functions simultaneously with the DNA replication process. The new rounds of DNA replication cycles are likely initiated in a synchronous as well as an asynchronous fashion, possibly due to a stochastic influence by the replication initiator protein, DnaA. If the new DNA replication initiation occurs in a synchronous fashion, the resulting total of four *oriC* sites in the cell will be localized such that two pairs of *oriC* sites will be repositioned to each cell half. Alternatively, if the new DNA replication initiation occurs in an asynchronous fashion, the resulting total of 3 *oriC* sites in the cell will be localized such that two of the *oriC* sites will be confined near the opposite cell poles and the third (newest) *oriC* site will move near the mid-cell region.

Once the cells reach an overall length of ~ 4 µm, and have a minimum of three replication events occurring (*i.e.* 4 foci), they divide into two ~ 2 µm long daughter cells, each of which inherits a partially replicated chromosome along with a complete chromosome.

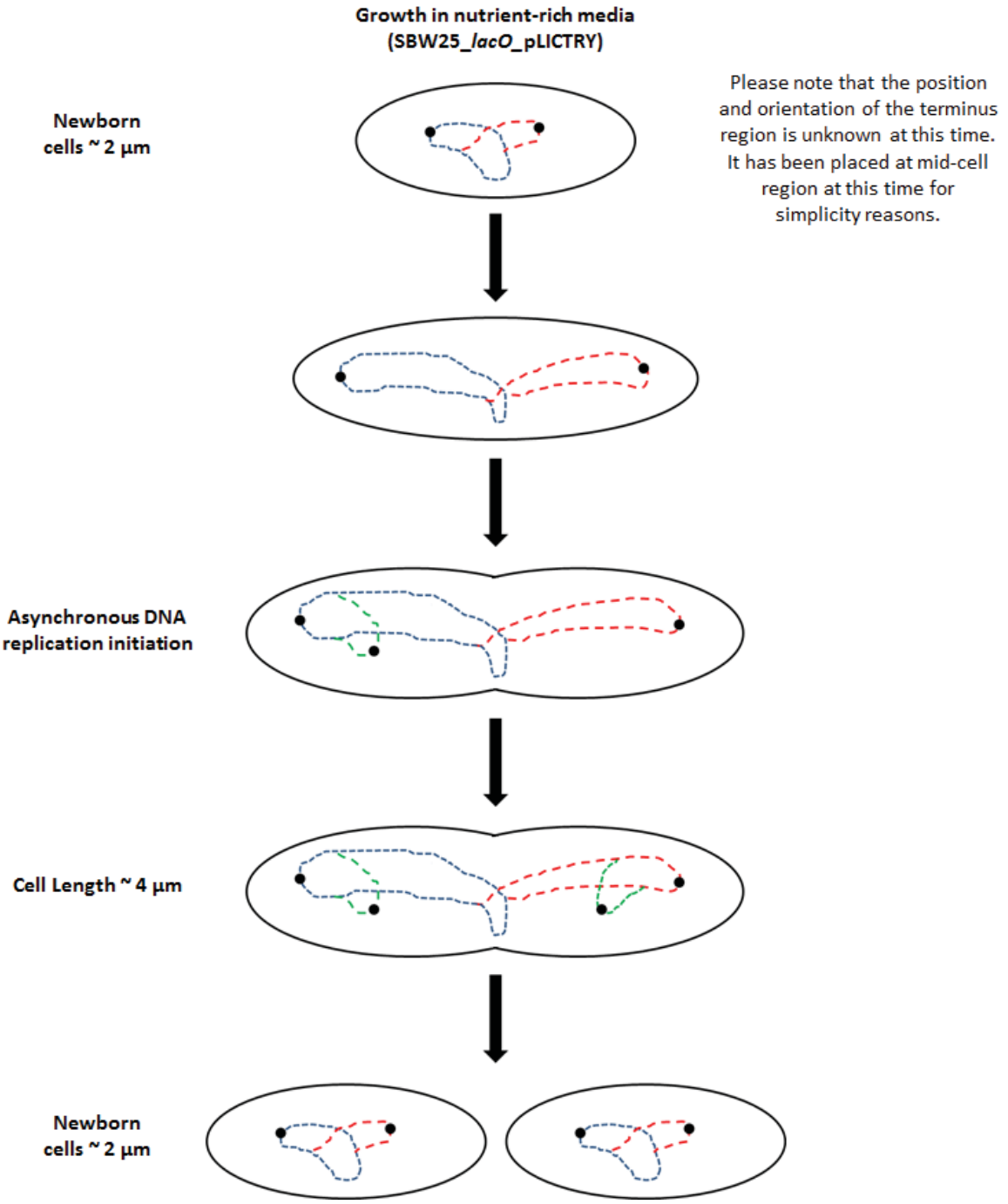

Figure 29: A schematic representation of the model hypothesized for the growth of *P. fluorescens* SBW25 in nutrient-rich conditions (from the findings of both SBW25_*lacO*_pLICTRY and SBW25_*tetO*_pLICTRY strains).

5.2.2 Model for *P. fluorescens* SBW25 Growth in Nutrient-poor Media (from findings of SBW25_*lacO*_pLICTRY strain)

In nutrient-poor media, during exponential growth, the cells generally appear to be born at an overall length of ~ 2μm, with an already ongoing round of DNA replication occurring. At this stage, the two *oriC* sites present inside the cells are already somewhat distant from each other, localizing near opposite cell poles. The cells then continue their growth until a length of ~ 3 μm is reached, at which point they are able to initiate two new cycles of DNA replication in a synchronous fashion. The newly generated *oriC* sites are quickly separated through an active chromosome segregation mechanism (such as the ParABS system), which functions in concurrence with the DNA replication process. This results in two pairs of *oriC* sites, each of which becomes localized in opposite cell halves. After further growth, when an overall length of ~ 4 μm is reached, the cells can no longer continue their growth and subsequently divide into two ~ 2 μm long daughter cells, each of which inherits a partially replicated chromosome along with a complete chromosome.

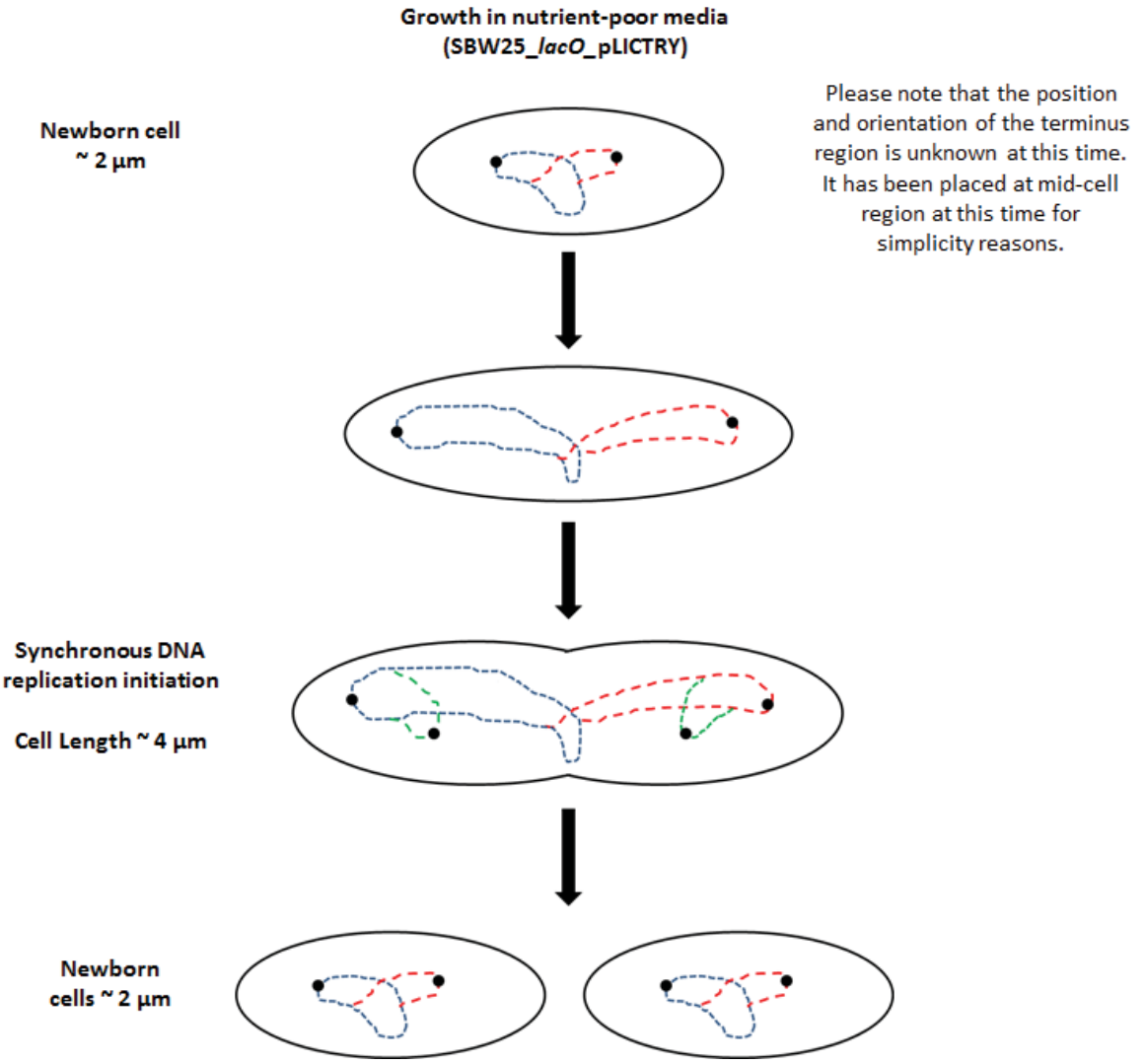

Figure 30: A schematic representation of the model hypothesized for the growth of *P. fluorescens* SBW25 in nutrient-poor conditions (from the findings of SBW25_*lacO*_pLICTRY strain).

5.2.3 Model for *P. fluorescens* SBW25 Growth in Nutrient-poor Media (from findings of SBW25_*tetO*_pLICTRY strain)

In nutrient-poor media, during exponential growth, the cells are born at an overall length of ~ 1.5 µm, comprising only a single copy of the chromosome. The *oriC* site in the cell at this stage is typically located near mid-cell region. The cells are able to immediately initiate a new round of DNA replication cycle, and the newly generated *oriC* sites are quickly separated from each other through an active chromosome segregation mechanism (such as the

ParABS system), which functions in parallel with the DNA replication process. As the cell lengthens and the replication process proceeds to completion in a sequential fashion, without initiation of any new DNA replication cycles, the *oriC* sites move further apart from each other, maintaining localization near the opposite cell poles. Once the cells reach an overall length of ~ 3 µm, they can no longer continue growing and subsequently divide into two ~ 1.5 µm long cells, each of which inherits a single copy of the replicated chromosome.

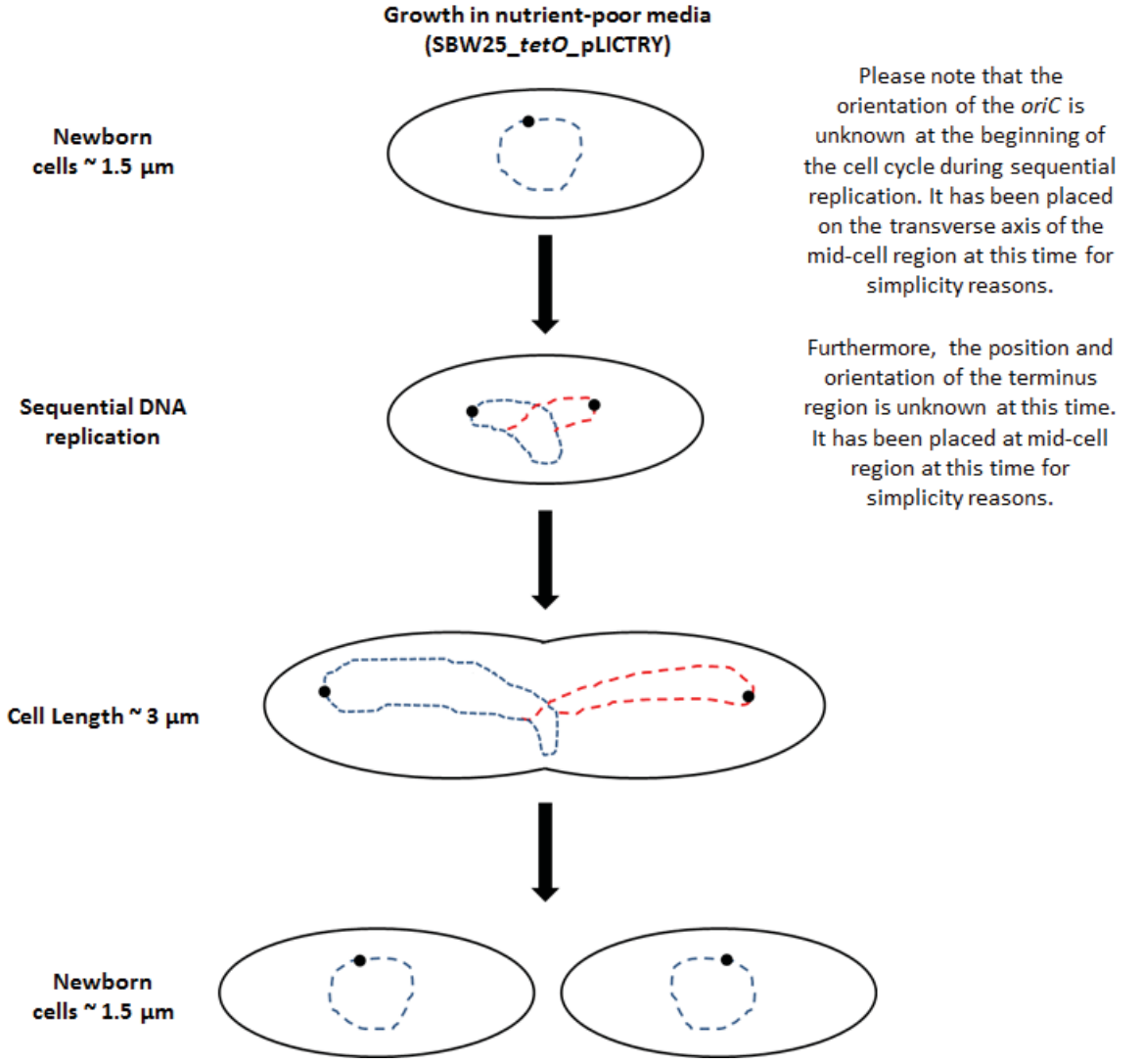

Figure 31: A schematic representation of the model hypothesized for the growth of *P. fluorescens* SBW25 in nutrient-poor conditions (from the findings of SBW25_*tetO*_pLICTRY strain).

5.2.4 Comparison between SBW25_*tetO*_pLICTRY and SBW25_*lacO*_pLICTRY Models in Nutrient-poor Media

While the SBW25_*tetO*_pLICTRY strain generally consisted of cells displaying only 1 or 2 *oriC* sites during exponential growth, the SBW25_*lacO*_pLICTRY strain was abundant with cells displaying 2 or 4 *oriC* sites (Figures 24E and G). Therefore, while the SBW25_*tetO*-_pLICTRY strain appears to be carrying out sequential DNA replication, the SBW25_*lacO*_pLICTRY strain appears to be carrying out multi-fork replication.

Although this difference raises doubts, the results from a past study in a closely related organism, *P. aeruginosa*, are consistent with the results from my SBW25_*tetO*_pLICTRY strain [76]. Because of this, and due to the fact that my SBW25_*lacO*_pLICTRY strain does not show cells with single *oriC* sites even during stationary phase (Figure 25), I feel more confident with the results obtained from the SBW25_*tetO*_pLICTRY strain. Possible explanations for why the SBW25_*lacO*_pLICTRY strain seems to always have 2 or 4 foci under the fluorescent microscope are discussed below:

5.2.4.1 Possible Explanations for SBW25_*lacO*_pLICTRY Cells Mostly Displaying 2 or 4 Foci

There are a few possible explanations for the SBW25_*lacO*_pLICTRY cells almost always displaying at least 2 foci:

1. It is possible that during insertion of the ~ 7 Kb *lacO* repetitive sequence into the *P. fluorescence* SBW25 genome using Tn7 transposons, the sequence was inserted into another random site as well as the target site. Sequence insertion techniques using transposons have not yet been perfected and random site insertions do happen [122]. If this is the case, then the LacI-CFP fusion proteins will be localizing at two regions

of the chromosome and thus extra foci will be displayed under the fluorescent microscope.

2. It is possible that due to some random mutation, the strain is overexpressing the DNA replication initiator protein, DnaA. In this case, the excess DnaA proteins may keep initiating new DNA replication cycles, thus resulting in several foci being displayed under the fluorescent microscope.
3. Since genomic regions rich in repetitive sequences are known to be prone to recombination [123], it is possible that a portion of the inserted *lacO* array was relocated to another region of the *P. fluorescens* SBW25 genome. Thus, the LacI-CFP fusion proteins would localize at two regions and extra foci would be displayed under the fluorescent microscope.

5.3 Future Directions

There is much potential for future work on this study to validate my results. A couple of key experiments I would have liked to do if I were to continue on this project are described below.

5.3.1 Fluorescent Microscopy

By increasing the number of operator arrays inserted in the genome by targeting key locations such as the terminus and various positions in the right and left arms of the chromosome, future studies could be able to carry out precise analysis of the *P. fluorescens* SBW25 cell cycle in various media and establish detailed models for the DNA replication and chromosome segregation processes.

5.3.2 Flow Cytometry

By utilizing flow cytometry techniques to conduct replication run-out experiments like those carried out by Skarstad et al. (1986) [48], complete distributions of cells with varying amounts of concurrent DNA replication cycles can be obtained from populations growing in various media. These experiments can be carried out on exponentially growing populations of wild type *P. fluorescens* SBW25 cells, which will have to be incubated with transcription inhibiting agents such as rifampicin, which is known to inhibit DNA replication initiation in *E. coli*; and cell division inhibiting agents such as chloramphenicol, which has also been tested on *E. coli*. The end result is that the treated cells cannot initiate new rounds of DNA replication and also cannot divide and pass on the replicated chromosomes to the offspring cells. Once the cells have been incubated long enough for all the pre-treatment replication cycles to be completed, these cells can then have their chromosomes stained with a dye and be analyzed under a flow cytometer and have their DNA content measured.

Abbreviations

Table 6: List of abbreviations

RNA	Ribonucleic acid	PCR	Polymerase chain reaction
DNA	Deoxyribonucleic acid	dNTP	Deoxynucleotide triphosphate
ssDNA	Single-stranded deoxyribonucleic acid	BSA	Bovine serum albumin
oriC	Origin of replication	DMSO	Dimethyl sulfoxide
oriI	*oriC* site of ChrI of *V. cholerae*	IPTG	Isopropyl-β-D-thiogalactopyranoside
oriII	*oriC* site of ChrII of *V. cholerae*	WT	Wild type
dif	Deletion induced filamentation	NT	No template
Tus	Terminus utilization substance	NP	No primers
RTP	Replication terminus protein	AT	Actual test
ORC	Origin recognition complex	OD	Optical density
CDK	Cyclin-dependent kinase	CFU	Colony forming unit
ADP	Adenosine diphosphate	GFP	Green fluorescent protein
ATP	Adenosine triphosphate	CFP	Cyan fluorescent protein
ChrI	Chromosome I of *V. cholerae*	YFP	Yellow fluorescent protein
ChrII	Chromosome II of *V. cholerae*	LB	Lysogeny broth

References

1. Whitman WB, Coleman DC, Wiebe WJ: **Prokaryotes: The unseen majority.** *Proc Natl Acad Sci U S A* 1998, **95:**6578–6583.

2. Rinke C, Schwientek P, Sczyrba1 A, Ivanova1 NN, Anderson IJ, Cheng J, Darling A, Malfatti S, Swan BK, Gies EA, et al: **Insights into the phylogeny and coding potential of microbial dark matter.** *Nature* 2013, **499:**431-437.

3. Martin W, Russell MJ: **On the origins of cells: a hypothesis for the evolutionary transitions from abiotic geochemistry to chemoautotrophic prokaryotes, and from prokaryotes to nucleated cells.** *Phil Trans R Soc* 2003, **358:**59-85.

4. de Bentzmann S, Plésiat P: **The *Pseudomonas aeruginosa* opportunistic pathogen and human infections.** *Environmental Microbiology* 2011, **13:**1655-1665.

5. Murray A, Hunt T: *The cell cycle: An introduction* New York: Oxford University Press; 1993.

6. Sapp J: **The Prokaryote-Eukaryote Dichotomy: Meanings and Mythology.** *Microbiol Mol Biol Rev* 2005, **69:**292-305.

7. Margolin W, Bernander R: **How Do Prokaryotic Cells Cycle?** *Current Biology* 2004, **14:**R768–R770.

8. Koch AL: **Biomass growth rate during the prokaryote cell cycle.** *Critical Reviews In Microbiology* 1993, **19:**17-42.

9. Dworkin M, Falkow S, Rosenberg E, Schleifer K, Stackebrandt E: *The Prokaryotes:* 3 edn: Springer; 2006.

10. Meselson M, Stahl F: **The Replication of DNA in *Escherichia coli*.** *Biology* 1958, **44:**671-682.

11. Cairns J: **The chromosome of *Escherichia coli*.** *Cold Spring Harbor Symp* 1961, **28:**43-46.

12. Gordon GS, Sitnikov D, Webb CD, Teleman A, Straight A, Losick R, Murray AW, Wright A: **Chromosome and low copy plasmid segregation in *E. coli*: visual evidence for distinct mechanisms.** *Cell* 1997, **90:**1113-1121.

13. Kuempel PL, Henson JM, Dircks L, Tecklenburg M, Lim DF: ***dif*, a *recA*-independent recombination site in the terminus region of the chromosome of *Escherichia coli*.** *New Biol* 1991, **3:**99-811.

14. Sclafani R, Holzen T: **Cell Cycle Regulation of DNA Replication.** *Annual Review Genetics* 2007, **41:**237-280.

15. Kitagawa R, Ozaki T, Moriya S, Ogawa T: **Negative control of replication initiation by a novel chromosomal locus exhibiting exceptional affinity for *Escherichia coli* DnaA protein.** *Genes & Development* 1998, **12:**3032-3043.

16. Neidhardt FC: *Escherichia coli and Salmonella typhimurium.* Washington DC: ACM Press; 1996.

17. Bramhill D, Kornberg A: **A model for initiation at origins of DNA replication.** *Cell* 1988, **54:**915-918.

18. Fuller RS, Kornberg A: **Purified DnaA protein in initiation of replication at the *Escherichia coli* chromosomal origin of replication.** *Proc Natl Acad Sci U S A* 1983, **80:**5817–5821.

19. Skarstad K, Boye E: **The initiator protein DnaA: Evolution, properties, and function.** *Biochim Biophys Acta* 1994, **1217:**111-130.

20. Messer W, Zakrzewska-Czerwinska C: ***Streptomyces* and *Escherichia coli*, model organisms for the analysis of the initiation of bacterial chromosome replication.** *Arch Immunol Ther Exp (Warsz)* 2002, **50**.

21. Ogasawara N, Yoshikawa H: **Genes and their organization in the replication origin region of the bacterial chromosome. .** *Mol Microbiol* 1992, **6:**629-634.

22. Willems H, Jager C, Baljer G: **Physical and genetic map of the obligate intracellular bacterium *Coxiella burnetii*.** *J Bacteriol* 1998, **180:**3816–3822.

23. Marczynski GT, Shapiro L: **Cell-cycle control of a cloned chromosomal origin of replication from *Caulobacter crescentus*.** *J Mol Biol* 1992, **226:**959-977.

24. Dingwall A, Shapiro L: **Rate, origin, and bidirectionality of *Caulobacter* chromosome replication as determined by pulsed-field gel electrophoresis.** *Proc Natl Acad Sci U S A* 1989, **86:**119–123.

25. Brassinga AK, Marczynski GT: **Replication intermediate analysis confirms that chromosomal replication origin initiates from an unusual intergenic region in *Caulobacter crescentus*.** *Nucleic Acids Res* 2001, **29:**4441–4451.

26. Mulugu S, Potnis A, Shamsuzzaman, Taylor J, Alexander K, Bastia D: **Mechanism of termination of DNA replication of *Escherichia coli* involves helicase–contrahelicase interaction.** *Proc Natl Acad Sci U S A* 2001, **98:**9569-9574.

27. Bastia D, Mohanty BK: *DNA Replication in Eukaryotic Cells.* Plainview, NY: Cold Spring Harbor Lab. Press; 1996.

28. Hill TM, Henson JM, Kuempel KL: **The terminus region of the *Escherichia coli* chromosome contains two separate loci that exhibit polar inhibition of replication.** *Proc Natl Acad Sci U S A* 1987, **84:**1754-1758.

29. Smith MT, Langley DB, Young PA, Wake RG: **The Minimal Sequence Needed to Define a Functional DNA Terminator in *Bacillus subtilis*.** *J Mol Biol* 1994, **241:**335-340.

30. Zechiedrich EL, Cozzarelli NR: **Roles of topoisomerase IV and DNA gyrask in DNA unlinking during replication in *Escherichia coli*** *Genes & Dev* 1995, **9:**2859-2869.

31. Campbell JL, Kleckner N: ***E. coli oriC* and the *dnaA* gene promoter are equestered from dam methyltransferase following the passage of the chromosomal eplication fork.** *Cell* 1990, **62:**967–979.

32. Lu M, Campbell JL, Boye E, Kleckner N: **SeqA: a negative modulator of eplication initiation in *E. coli*.** *Cell* 1994, **77:**413– 426.

33. von Freiesleben U, Rasmussen KV, Schaechter M: **SeqA limits DnaA ctivity in replication from *oriC* in *Escherichia coli*.** *Mol Microbiol* 1994, **14:**763-772.

34. Gadde S, Heald R: **Mechanisms and Molecules of the Mitotic Spindle.** *Current Biology* 2004, **14:**R768–R770.

35. Youngren B, Nielsen H, Jun S, Austin S: **The Multifork *Escherichia coli* chromosome is a self-duplicating and a self-segregating thermodynamic ring polymer.** *Genes Dev* 2014, **28:**71-84.

36. Jun S, Wright A: **Entropy as the driver of chromosome segregation.** *Nature Reviews Microbiology* 2010, **8:**600-6007.

37. Gerdes K, Møller-Jensen J, Bugge Jensen R: **Plasmid and chromosome partitioning: surprises from phylogeny.** *Mol Microbiol* 2000, **37**.

38. Kruse T, Blagoev B, Lobner-Olesen A, Wachi M, Sasaki K, Iwai N, Mann M, Gerdes K: **Actin homolog MreB and RNA polymerase interact and are both required for chromosome segregation in *Escherichia coli*.** *Genes Dev* 2006, **20:**113-124.

39. Balasubramanian MK, Bi E, Glotzer M: **Comparative Analysis of Cytokinesis in Budding Yeast, Fission Yeast and Animal Cells.** *Current Biology* 2004, **14:**R768–R770.

40. Huang KS, Durand-Heredia1 J, Janakiraman1 A: **FtsZ-ring stability: of bundles, tubules, crosslinks and curves.** *J Bacteriol* 2013, **195:**1859–1868.

41. Teather RM, Collins J, Donachie WD: **Quantal Behavior of a Diffusible Factor Which Initiates Septum Formation at Potential Division Sites in *Escherichia coli*.** *Journal of Bacteriology* 1974, **118:**407 – 413.

42. Erfei B, Lutkenhaus J: **Cell division inhibitors SulA and MinCD prevent formation of the FtsZ Ring.** *Journal of Bacteriology* 1993, **175:**1118 – 1125.

43. Edwards H, Errington J: **The *Bacillus subtilis* DivIVA Protein Targets the Division Septum and Controls the Site Specificity of Cell Division.** *Molecular Microbiology* 1997.

44. Bramkamp M, Emmins R, Weston L, Donovan C, Daniel R, Errington J: **A Novel Component of the Division-Site Selection System of *Bacillus subtilis* and a New Mode of Action for the Division Inhibitor MinCD.** *Molecular Microbiology* 2008, **70:**1556–1569.

45. Vicente M, Lowe J: **Ring, Helix, Sphere and Cylinder: the basic geometry of prokaryotic cell division.** *EMBO Reports 4* 2003, **4:**655–660.

46. Cooper S, Helmstetter CE: **Chromosome Replication and the Division Cycle of *Escherichia coli* B/r.** *Journal of Molecular Biology* 1968, **31:**619-644.

47. Nielsen HJ, Youngren B, Hansen FG, Austin S: **Dynamics of *Escherichia coli* Chromosome Segregation During Multifork Replication.** *Journal of Bacteriology* 2007, **189:**8660-8666.

48. Skarstad K, Boye E, Steen HB: **Timing of initiation of chromosome replication in individual *Escherichia coli* cells.** *The EMBO Journal* 1986, **5:**1711- 1717.

49. Zaritsky A, Wang P, Vischer NOE: **Instructive simulation of the bacterial cell division cycle.** *Microbiology* 2011, **157:**1876-1885.

50. Pritchard RH, Zaritsky A: **Effect of Thymine Concentration on the Replication Velocity of DNA in a Thymineless Mutant of *Escherichia coli*.** *Nature* 1970, **226:**126-131.

51. Quiñones-Soto S, Reams AR, Roth JR: **Pathways of Genetic Adaptation: Multistep Origin of Mutants Under Selection Without Induced Mutagenesis in *Salmonella enterica*.** *Genetics* 2012, **192:**987-999.

52. Niccum BA, Poteau R, Hamman GB, Varada JC, Dshalalow JH, Sinden RS: **On an Unbiased and Consistent Estimator for Mutation Rates.** *Journal of Theoretical Biology* 2012, **300:**360-367.

53. Schaechter M, Maalo O, Kjeldgaard NO: **Dependency on Medium and Temperature of Cell Size and Chemical Composition during Balanced Growth of *Salmonella typhimurium*.** *Journal of General Microbiology* 1958, **19:**592-606.

54. Cooper S: **Cell division and DNA replication following a shift to a richer medium.** *Journal of Molecular Biology* 1969, **43:**1-11.

55. Yoshikawa H, O'Sullivan A, Sueoka N: **Sequential Replication of *Bacillus subtilis* Chromosome, III. Regulation of Initiation.** *Genetics* 1964, **52**.

56. Maaloe O, Kjeldgaard NO: *Control of Macromolecular Synthesis.* NY and Amsterdam: W.A. Benjamin Inc.; 1966.

57. Skarstad K, Steen HB, Boye E: ***Escherichia coli* DNA Distributions Measured by Flow Cytometry and Compared with Theoretical Computer Simulations.** *Journal of Bacteriology* 1985, **163**.

58. Akerlund T, Nordstrom K, Bernander R: **Analysis of cell size and DNA content in exponentially growing and stationary-phase batch cultures of *Escherichia coli*.** *J Bacteriol* 1995, **177:**6791–6797.

59. Cooper S: **Regulation of DNA synthesis in bacteria: Analysis of the Bates/Kleckner licensing/initiation-mass model for cell-cycle control.** *Working Paper* 2006.

60. Mahaffy JM, Zyskind JW: **A Model for the Initiation of Replication in *Escherichia coli*.** *Journal of Theoretical Biology* 1989, **140:**453-477.

61. Grant MA, Saggioro C, Ferrari U, Bassett B, Sclavi B, Cosentino M, Lagomarsino: **DnaA and the Timing of Chromosome Replication in *Escherichia Coli* as a Function of Growth Rate.** *BMC Systems Biology* 2011, **5:**1-14.

62. Wang X, Rudner DZ: **Spatial organization of bacterial chromosomes.** *Current Opinion in Microbiology* 2014, **22:**66-72.

63. Stokke C, Waldminghaus T, Skarstad K: **Replication patterns and organization of replication forks in *Vibrio cholerae*.** *Microbiology* 2011, **157:**695-708.

64. Mohl DA, Easte JJ, Gober JW: **The chromosome partitioning protein, ParB, is required for cytokinesis in *Caulobacter crescentus*.** *Molecular Microbiology* 2001, **42:**741-755.

65. Skerker JM, Laub MT: **Cell-Cycle Progression and the Generation of Asymmetry in *Caulobacter Crescentus*.** *Nature Reviews: Microbiology* 2004, **2:**325-337.

66. Tobiason DM, Seifert HS: **The obligate human pathogen, *Neisseria gonorrhoeae*, is polyploid.** *PLoS Biol* 2006, **4:**e185.

67. O'Sullivan MA, Sueoka N: **Membrane Attachment of Replication Origins of a Multifork (Dichotomous) Chromosome in *Bacillus subtilis*.** *Journal of Molecular Biology* 1971, **69:**237-248.

68. Sharpe ME, Hauser PM, Sharpe RG, Errington J: ***Bacillus subtilis* Cell Cycle as Studied by Fluorescent Microscopy: Constancy of Cell Length at Initiation of DNA Replication and Evidence for Active Nucleoid Partitioning.** *Journal of Bacteriology* 1997, **180:**547 – 555.

69. Egan SE, Lobner-Olesen A, Walder MK: **Synchronous replication initiation of the two *Vibrio cholerae* chromosomes.** *Current Biology* 2004, **14:**R502.

70. Rasmussen T, Jensen RB, Skovgaard O: **The two chromosomes of *Vibrio cholerae* are initiated at different time points in the cell cycle.** *The EMBO Journal* 2007, **26:**3124–3131.

71. Kline KA, Sechman EV, Skaar EP, Seifert HS: **Recombination, repair, and replication in the pathogenic Neisseriae: The 3 R's of molecular genetics of two human-specific bacterial pathogens.** *Mol Microbiol* 2003, **50**.

72. Swanson J, Kraus SJ, Gotschlich EC: **Studies on gonococcus infection. I. Pili and zones of adhesion: Their relation to gonococcal growth patterns.** *J Exp Med* 1971, **134:**886–906.

73. Elmros T, Sandstrom G, Burman L: **Autolysis of *Neisseria gonorrhoeae*. Relation between mechanical stability and viability.** *Br J Vener Dis* 1976, **52:**246-249.

74. Dillard JP, Seifert HS: **A peptidoglycan hydrolase similar to bacteriophage endolysins acts as an autolysin in *Neisseria gonorrhoeae*.** *Mol Microbiol* 1997, **25**.

75. Marczynski GT: **Chromosome Methylation and Measurement of Faithful, Once and Only Once per Cell Cycle Chromosome Replication in *Caulobacter crescentus*.** *Journal of Bacteriology* 1999, **181:**1984 – 1993.

76. Vallet-Gely I, Boccard F: **Chromosomal Organization and Segregation in *Pseudomonas aeruginosa*.** *PLOS Genetics* 2013, **9:**e1003492.

77. Özen AI, Ussery DW: **Defining the Pseudomonas Genus: Where Do We Draw the Line with Azotobacter?** *Microbiological Ecology* 2012, **63:**239-248.

78. Rainey PB: **Adaptation of *Pseudomonas fluorescens* to the Plant Rhizosphere.** *Environmental Microbiology* 1999, **1:**243-257.

79. Lau IF, Filipe SR, Søballe B, Økstad O, Barre F, Sherratt DJ: **Spatial and Temporal Organization of Replicating *Escherichia coli* Chromosomes.** *Molecular Microbiology* 2003, **49:**731-743.

80. Haas D, Défago G: **Biological Control of Soil-Borne Pathogens by Fluorescent Pseudomonads** *Nature Reviews Microbiology* 2005**:**1-13.

81. Li Y, Austin S: **The P1 plasmid is segregated to daughter cells by a 'capture and ejection' mechanism coordinated with *Escherichia coli* cell division.** *Mol Microbiol* 2002, **46:**63-74.

82. Heeb S, Itoh Y, Nishijyo T, Schnider U, Keel C, J W, Walsh U, F.O. OG, Haas D: **Small, stable shuttle vectors based on the minimal pVS1 replicon for use in Gram-negative, plant-associated bacteria.** *Molecular Plant-Microbe Interactions* 2000, **13:**232-237.

83. Choi K, Schweizer HP: **mini-Tn7 insertion in bacteria with single attTn7 sites: example *Pseudomonas aeruginosa*.** *Nature Protocols* 2006, **1:**153-161.

84. Peters JE, Craig NL: **Tn7: Smarter Than we Thought.** *Nature Reviews Molecular Cell Biology* 2001, **2:**806-814.

85. Craig NL: **Transposon Tn7.** In *Transposable Elements. Volume* 204. Edited by Saedler H, Gierl A. Heidelberg: Springer Berlin 1996: 27-48

86. Schumacher MA: **Structural biology of plasmid partition: uncovering the molecular mechanisms of DNA segregation.** *Biochem J* 2008, **412:**1-18.

87. Ebersbach G, Gerdes K: **Plasmid segregation mechanism.** *Annu Rev Genet* 2005, **39:**453–479

88. Schumacher MA: **Structural biology of plasmid segregation proteins.** *Curr Opin Struct Biol* 2007, **17:**103-109.

89. Motallebi-Veshareh M, Rouch DA, Thomas CM: **A family of ATPases involved in active partitioning of diverse bacterial plasmids.** *Mol Microbiol* 1990, **4:**1455–1463.

90. Hayes F, Barill`a D: **The bacterial segrosome: a dynamic nucleoprotein machine for DNA trafficking and segregation.** *Nat Rev Microbiol* 2006, **4:**133-143.

91. Funnell BE: **Partition-mediated plasmid pairing.** *Plasmid* 2005, **53:**119-125.

92. Abeles AL, Friedman SA, Austin SJ: **Partition of unit-copy miniplasmids to daughter cells. III. The DNA sequence and functional organization of the P1 partition region.** *J Mol Biol* 1985, **185:**261-272.

93. Ogura T, Hiraga S: **Partition mechanism of F plasmid: two plasmid gene-encoded products and a *cis*-acting region are involved in partition.** *Cell* 1983, **2:**351-360.

94. Youngren B, Austin S: **Altered ParA partition proteins of plasmid P1 act via the partition site to block plasmid propagation.** *Mol Microbiol* 1997, **25:**1023–1030

95. Dam M, Gerdes K: **Partitioning of plasmid R1: ten direct repeats flanking the parA promoter constitute a centromere-like partition site *parC* that expresses incompatibility.** *J Mol Biol* 1994, **236:**1289-1298.

96. Austin S, Abeles A: **Partition of unit-copy miniplasmids to daughter cells. I. P1 and F miniplasmids contain discrete, interchangeable sequences sufficient to promote equipartition.** *J Mol Biol* 1983, **169:**353-372.

97. Austin S, Abeles A: **Partition of unit-copy miniplasmids to daughter cells. II. The partition region of miniplasmid P1 encodes an essential protein and a centromere-like site at which it acts.** *J Mol Biol* 1983, **169:**373-387.

98. Gerdes K, Howard M, Szardenings F: **Pushing and Pulling in Prokaryotic DNA Segregation.** *Cell* 2010.

99. Surtees JA, Funnell BE: **Plasmid and chromosome traffic control: how ParA and ParB drive partition.** *Curr Top Dev Biol* 2003, **56:**145-180.

100. Hayes F, Barill`a D: **Assembling the bacterial segrosome.** *Trends Biochem Sci* 2006, **31:**247-250.

101. Jensen RB, Lurz R, Gerdes K: **Mechanism of DNA segregation in prokaryotes: replicon pairing by *parC* of plasmid R1.** *Proc Natl Acad Sci USA* 1998, **95:**8550-8555.

102. Ireton K, Gunther NW, Grossman AD: **Spo0J is required for normal chromosome segregation as well as the initiation of sporulation in *Bacillus subtilis*.** *J Bacteriol* 1994, **176:**5320-5329.

103. Bartosik AA, Lasocki K, Mierzejewska J, Thomas CM, Jagura-Burdzy G: **ParB of *Pseudomonas aeruginosa* : interactions with its partner ParA and its target *parS* and specific effects on bacterial growth.** *J Bacteriol* 2004, **186:**6983–6998

104. Lasocki K, Bartoski AA, Mierzejewska J, Thomas CM, Jagura-Burdzy G: **Deletion of the *parA* (soj) homologue in *Pseudomonas aeruginosa* causes ParB instability and affects growth rate, chromosome segregation and motility.** *J Bacteriol* 2007, **189:**5762–5772.

105. Lin DC, Grossman AD: **Identification and characterization of a bacterial chromosome partitioning site.** *Cell* 1998, **92:**675-685.

106. Yamaichi Y, Fogel MA, Waldor MK: **par genes and the pathology of chromosome loss in *Vibrio cholerae*.** *Proc Natl Acad Sci USA* 2007, **104:**630-635.

107. Saint-Dic D, Frushour BP, Kehrl JH, Kahng LS: **A ParA homolog selectively influences positioning of the large chromosome origin in *Vibrio cholerae*.** *J Bacteriol* 2006, **188:**5626-5231.

108. Mohl DA, Gober JW: **Cell cycle-dependent polar localization of chromosome partitioning proteins in *Caulobacter crescentus*.** *Cell* 1997, **88:**675-684.

109. Figge RM, Easter J, J. , Gober JW: **Productive interaction between the chromosome partitioning proteins, ParA and ParB, is required for the progression of the cell cycle in *Caulobacter crescentus*.** *Mol Microbiol* 2003, **47:**1225–1237.

110. Meyer JM, Hornsperger JM: **Role of Pyoverdine, the Iron-binding Fluorescent Pigment of *Pseudomonas fluorescens*, in Iron Transport.** *Journal of General Microbiology* 1978, **107:**329-331.

111. Ravel J, Cornelis P: **Genomics of pyoverdine-mediated iron uptake in pseudomonads.** *Trends in Microbiology* 2003, **11:**195-200.

112. Cox CD, Adams P: **Siderophore Activity of Pyoverdin for *Pseudomonas aeruginosa*.** *Infection and Immunity* 1985, **48:**130-138.

113. StringDatabase: **Search Tool for the Retrieval of Interacting Genes/Proteins - String 10.** 2015.

114. Straight AF, Belmont AS, Robinett CC, Murray AW: **GFP tagging of budding yeast chromosomes reveals that protein–protein interactions can mediate sister chromatid cohesion.** *Current Biology* 1996, **6:**1599-1608.

115. Michaelis C, Ciosk R, Nasmyth K: **Cohesins: Chromosomal Proteins that Prevent Premature Separation of Sister Chromatids.** *Cell* 1997, **91**.

116. Robinett cC, Straight A, Li G, Willhelm C, Sudlow G, Murray A, Belmont AS: ***In Vivo* Localization of DNA Sequences and Visualization of Large-Scale Chromatin Organization Using Lac Operator/Repressor Recognition.** *The Journal of Cell Biology* 1996, **135:**1685-1700.

117. Kato N, Lam E: **Detection of chromosomes tagged with green fluorescent protein in live *Arabidopsis thaliana* plants.** *Genome Biology* 2001, **2:**0045.0041-0045.0010.

118. Matzke AJM, van der Winden J, Matzke M: **Tetracycline operator/repressor system to visualize fluorescence-tagged T-DNAs in interphase nuclei of *Arabidopsis*.** *Plant Molecular Biology Reporter* 2012, **21:**9-19.

119. Newell CA, Gray JC: **Binding of lac repressor-GFP fusion protein to lac operator sites inserted in the tobacco chloroplast genome examined by chromatin immunoprecipitation.** *Nucleic Acids Res* 2010, **38:**13.

120. Dworkin J, Losick R: **Does RNA polymerase help drive chromosome segregation in bacteria?** *PNAS* 2002, **99:**14089-14094.

121. Kusiak M, Gapczyn´ska A, Płochocka D, Thomas CM, Jagura-Burdzy G: **Binding and Spreading of ParB on DNA Determine Its Biological Function in *Pseudomonas aeruginosa*.** *Journal of Bacteriology* 2011, **193:**3342-3355.

122. Green B, Bouchier C, Fairhead C, Craig NL, Cormack BP: **Insertion site preference of Mu, Tn5, and Tn7 transposons.** *Mob DNA* 2012, **3**.

123. Aras RA, Kang J, Tschumi AI, Harasaki Y, Blaser MJ: **Extensive repetitive DNA facilitates prokaryotic genome plasticity.** *Proc Natl Acad Sci U S A* 2003, **100:**13579–13584.